SLAC–PUB–4947
March 1989
(M)

EXCLUSIVE PROCESSES IN QUANTUM CHROMODYNAMICS*

STANLEY J. BRODSKY

Stanford Linear Accelerator Center
Stanford University, Stanford, California 94309

and

G. PETER LEPAGE

Laboratory of Nuclear Studies
Cornell University, Ithaca, New York 14853

CONTRIBUTION TO "PERTURBATIVE QUANTUM CHROMODYNAMICS"
Edited by A. H. Mueller
To be published by World Scientific Publishing Co.

* Work supported in part by the Department of Energy under contract number DE-AC03-76SF00515 and the National Science Foundation

1. INTRODUCTION

What is a hadron?

In practice, the answer to this question depends upon the energy scale of interest. At the atomic scale a hadron can be treated as an elementary point-like particle. The proton's electromagnetic interactions, for example, are well described by the simple Hamiltonian for a point-like particle:

$$H = \frac{(\vec{p} - e\vec{A})^2}{2M} + e\phi \tag{1.1}$$

This Hamiltonian describes a wide range of low-energy phenomena—*e.g.*proton-electron elastic scattering ($ep \to ep$), Compton scattering of protons ($\gamma p \to \gamma p$), atomic structure...—and it can be made arbitrarily accurate by adding interactions involving the magnetic moment, charge radius, *etc.* of the proton.

The description of the proton becomes much more complicated as the energy is increased up to the strong interaction scale (~ 1 GeV). In proton-electron elastic scattering, for example, one must introduce phenomenological form factors $F(Q^2)$ to correct the predictions from the point-like theory: in effect, $T(ep) = F(Q^2)\, T(ep)_{\text{point-like}}$ where Q is the momentum transfer and

$$F(Q^2) \sim \left(\frac{\lambda^2}{Q^2 + \lambda^2}\right)^2 . \tag{1.2}$$

One might try to modify the proton-photon interaction in the point-like Hamiltonian to reproduce the phenomenological form factors, but the resulting interaction would be very complicated and nonlocal. Furthermore such a modification would not suffice to account for the changes in the Compton amplitude of the proton at high energies. In fact, new terms would have to be added to the Hamiltonian for every process imaginable, resulting in a horrendously complicated theory with little predictive power.

The tremendous complexity of the high-energy phenomenology of hadrons stalled the development of strong interaction theory for a couple of decades. The breakthrough to a fundamental description came with the realization that the rich structure evident in the data was a consequence of the fact that hadrons are themselves composite particles. The constituents, the quarks and gluons, are again described by a very simple theory, Quantum Chromodynamics (QCD).[1] The complexity of the strong interactions comes not from the fundamental interactions, but rather from the structure of the hadrons. The key to the properties of the form factors and other aspects of the phenomenology of the proton thus lies in an understanding of the wavefunctions describing the proton in terms of its quark and gluon constituents.

In this article we shall discuss the relationship between the high-energy behavior of wide-angle exclusive scattering processes and the underlying structure of hadrons. Exclusive processes are those in which all of the final state particles are observed: *e.g.* $ep \to ep$, $\gamma p \to \gamma p$, $pp \to p\bar{p}$.... As we shall demonstrate, the highly varied behavior exhibited by such processes at large momentum transfer be understood in terms of simple perturbative interactions between hadronic constituents.[2,3] Large momentum transfer exclusive processes are sensitive to coherent hard scattering quark-gluon amplitudes and the quark and gluon composition of hadrons themselves. The key result which separates the hard scattering amplitude from the bound state dynamics is a factorization formula:[4,2] To leading order in $1/Q$ a hard exclusive scattering amplitude in QCD has the form

$$\mathcal{M} = \int_0^1 T_H(x_j, Q) \prod_{H_i} \phi_{H_i}(x_j, Q)[dx] \ . \tag{3}$$

Here T_H is the hard-scattering probability amplitude to scatter quarks with fractional momenta $0 < x_j < 1$ collinear with the incident hadrons to fractional momenta collinear to the final hadron directions. The distribution amplitude ϕ_{H_i} is the process-independent probability amplitude to find quarks in the wavefunction of hadron H_i collinear up to the scale Q, and

$$[dx] = \prod_{j=1}^{n_i} dx_j \delta\left(1 - \sum_{k=1}^{n_i} x_k\right) \tag{4}$$

Remarkably, this factorization is gauge invariant and only requires that the momentum transfers in T_H be large compared to the intrinsic mass scales of QCD. Since the distribution amplitude and the hard scattering amplitude are defined without reference to the perturbation theory, the factorization is valid to leading order in $1/Q$, independent of the convergence of perturbative expansions.

Factorization at large momentum transfer leads immediately to a number of important phenomenological consequences including dimensional counting rules,[5] hadron helicity conservation,[6] and a novel phenomenon[7] called "color transparency", which follows from the predicted absence of initial and final state interactions at high momentum transfer. In some cases, the perturbation expansion may be poorly convergent, so that the normalization predicted in lowest order perturbative QCD may easily be wrong by factors of two or more. Despite the possible lack of convergence of perturbation theory, the predictions of the spin, angular, and energy structure of the amplitudes may still be valid predictions of the complete theory.

This article falls into two large parts. In the first part, we introduce the general perturbative theory of high-energy wide-angle exclusive processes. Our discussion begins in Section 2 with a discussion of hadronic form factors for mesons composed of heavy quarks. This simple analysis, based upon nonrelativistic Schrödinger theory, illustrates many of the key ideas in the relativistic analysis that follows. In Section 3 we introduce a formalism for describing hadrons in terms of their constituents, and discuss general properties of the hadronic wavefunctions that arise in this formalism. In Section 4 we give a detailed description of the perturbative analysis of wide-angle exclusive scattering.

In the second part of the article we present a survey of the extensive phenomenology of these processes. In Sections 5 and 6 we review the general predictions of QCD for exclusive reactions and the methods used to calculate the hard scattering amplitude. Various applications to electromagnetic form factors, electron-positron annihilation processes and exclusive charmonium decays are also discussed. One of the most important testing grounds for exclusive reactions in QCD are the photon-photon annihilation reactions. These reactions and related Compton processes are discussed in Section 7.

In Section 8, the QCD analysis is extended to nuclear reactions. The reduced amplitude formalism allows an extension of the QCD predictions to exclusive reactions involving light nuclei. Quasi-elastic scattering processes inside of nuclei allow one to filter hard and soft contributions to exclusive processes and to study color transparency.

The most difficult challenges to the perturbative QCD description of exclusive reactions are the data on spin-spin correlations in proton scattering. We review this area and a possible explanation for the anomalies in the spin correlations and color transparency test in Section 9. General conclusions on the status of exclusive reactions are given in Section 10.

The appendices provide a guide to the main features of baryon form factor and evolution equations; a review of light-cone quantization and perturbation theory; and a discussion of a possible method[8] to calculate the hadronic wavefunctions by directly diagonalizing the Hamiltonian in QCD.

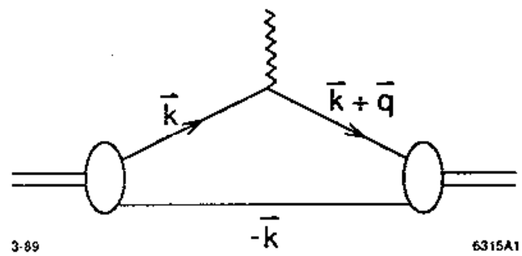

Figure 1. Nonrelativistic form factor for a heavy-quark meson.

2. NONRELATIVISTIC FORM FACTORS FOR HEAVY-QUARK MESONS

The simplest hadronic form factor is the electromagnetic form factor of a heavy-quark meson such as the Υ. In this section we show how perturbative QCD can be used to analyze such a form factor for momentum transfers that are large compared with the momentum internal to the meson, but small compared with the meson's mass. The analysis for relativistic momentum transfers is presented in subsequent sections.

Heavy-quark mesons are the simplest hadrons to analyze insofar as they are well described by a nonrelativistic quark-antiquark wavefunction. The amplitude that describes the elastic scattering of such a meson off a virtual photon is, by definition of the form factor, the amplitude for scattering a point-like particle multiplied by the electromagnetic form factor. The form factor is given by a standard formula from nonrelativistic quantum mechanics (see Fig. 1):

$$F(\vec{q}^{\,2}) = \int \frac{d^3k}{(2\pi)^3}\, \psi^*(\vec{k} + \vec{q}/2)\, \psi(\vec{k}). \tag{5}$$

(Note that the wavefunction's argument is 1/2 of the relative momentum between the quark and antiquark.) At first sight it seems that we require full knowledge of the meson wavefunction in order to proceed, but in fact we need know very little about the wavefunction if $\vec{q}^{\,2}$ is sufficiently large. To see why we must determine which regions of k-space dominate the integral in Eq. (5) when $\vec{q}^{\,2}$ is large.

When $\vec{q}^{\,2} \approx 0$ the integral in Eq. (5) is just the normalization integral for the wavefunction, and $F(\vec{q}^{\,2}) \approx 1$—the meson looks like a point-like particle to long-wavelength probes. As $\vec{q}^{\,2}$ becomes large, large momentum flows through one or the other or both of the wavefunctions in Eq. (5). Since nonrelativistic wavefunctions are strongly peaked at low momentum, the form factor is then suppressed. The dominant region of k-space is that which minimizes the suppression due to stressed wavefunctions. There are three regions that might dominate:

1) $|\vec{k}\,| \ll |\vec{q}\,|$, where $\psi^*(\vec{k}+\vec{q}/2)$ is small but $\psi(\vec{k}\,)$ is large;
2) $|\vec{k}+\vec{q}/2| \ll |\vec{q}\,|$, where $\psi(\vec{k}\,)$ is small but $\psi^*(\vec{k}+\vec{q}/2)$ is large;
3) $|\vec{k}+\vec{q}/2| \approx |\vec{k}\,| \approx |\vec{q}/4|$, where both $\psi(\vec{k}\,)$ and $\psi^*(\vec{k}+\vec{q}/2)$ are small, but not as small as the stressed wavefunction in either of the other two regions.

The q-dependence of the contributions to $F(\vec{q}^{\,2})$ from each of these regions is readily related to the high-momentum behavior of the wavefunction. In region 1), $\vec{k}$ can be neglected relative to $\vec{q}/2$ in the first wavefunction and so the form factor has q-dependence

$$F(\vec{q}^{\,2}) \sim \psi^*(\vec{q}/2). \tag{6}$$

The contribution from region 2) is essentially identical, as is clear if one makes the variable change $\vec{k} \to \vec{k}' \equiv \vec{k}+\vec{q}/2$. In region 3), the phase space contributes a factor of q^3 while each wavefunction goes like $\psi(\vec{q}/4)$ so that

$$F(\vec{q}^{\,2}) \sim q^3|\psi(\vec{q}/4)|^2. \tag{7}$$

The dominant region is clearly a function of the high-momentum behavior of the wavefunction.

In fact wavefunctions for heavy-quark mesons, like those for QED atoms, fall off as inverse powers of the momentum when it becomes large. As we show below, the ground state wavefunction falls off like $1/q^4$ up to factors of $\log(q^2)$. Then the form factor is dominated by regions 1) and 2) for large (nonrelativistic) $\vec{q}^{\,2}$, and falls off as $\psi(\vec{q}/2) \sim (1/\vec{q}^{\,2})^2$. The contribution from region 3) is suppressed by an additional factor of $1/|\vec{q}\,|$, and so can be neglected when $\vec{q}^{\,2}$ is sufficiently large. Note that this behavior is characteristic of wavefunctions that vanish as powers of the momentum. With a Gaussian wavefunction, for example, region 3) dominates and the form factor is exponentially damped for high momentum transfers.

Neglecting $\vec{k}$ relative to $\vec{q}/2$, the contribution to $F(\vec{q}^{\,2})$ coming from region 1) has the simple form

$$\psi^*(\vec{q}/2) \int \frac{d^3k}{(2\pi)^3}\, \psi(\vec{k}\,) \;=\; \psi^*(\vec{q}/2)\, \psi(\vec{r}=0) \tag{8}$$

where $\psi(\vec{r}=0)$ is the wavefunction evaluated at the origin (in coordinate space). We can further simplify this equation using the Schrödinger equation for $\psi(\vec{q}/2)$ (Fig. 2):

$$\psi(\vec{q}/2) = \left[\varepsilon - \frac{(\vec{q}/2)^2}{2M_r}\right]^{-1} \int \frac{d^3k}{(2\pi)^3}\, V(\vec{k} - \vec{q}/2)\, \psi(\vec{k}\,) \tag{9}$$

where ε is the nonrelativistic binding energy, $M_r = M_Q/2$ is the reduced mass of the quark and antiquark, and V is the interaction potential between them. The

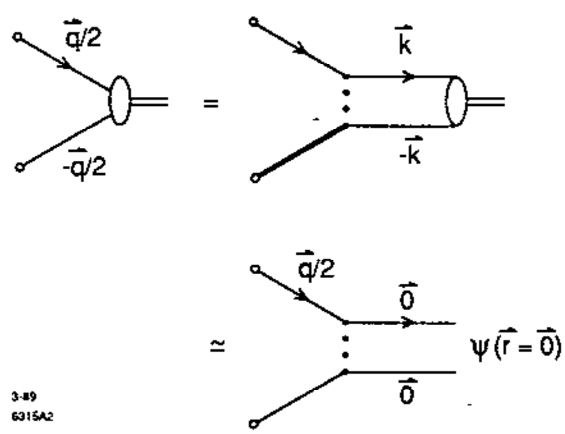

Figure 2. Momentum-space Schrödinger equation for the meson wavefunction.

potential $V(\vec{q})$ can be computed using perturbation theory when the momentum transfer $\vec{q}$ is large; to leading order it is just the Coulomb interaction modified by a running coupling constant:

$$V(\vec{q}) = -\frac{4\pi\, \alpha_s(\vec{q}^{\,2})\, C_F}{\vec{q}^{\,2}}. \tag{10}$$

Here $C_F = 4/3$ is the value of the Casimir operator for the fundamental representation of SU3 (*i.e.* the quark's representation), and

$$\alpha_s(Q^2) = \frac{4\pi}{\beta_0 \log(Q^2/\Lambda_{QCD}^2)}$$

is the running coupling constant of QCD, with scale parameter $\Lambda_{QCD} \sim 200$ MeV, and $\beta_0 = 11 - 2n_f/3$ where n_f is the number of active quark flavors ($n_f = 4$ for the Υ). Given this behavior for V we can show that the region $|\vec{k}| \ll |\vec{q}/2|$ dominates the integral in Eq. (9) by using arguments similar to those just applied to the form factor (Eq. (5)). Thus when $\vec{q}$ is large Eq. (9) becomes

$$\psi(\vec{q}/2) \approx \left[-\frac{(\vec{q}/2)^2}{2M_r}\right]^{-1} V(-\vec{q}/2)\,\psi(\vec{r}=0), \tag{11}$$

and the form factor takes the form

$$\begin{aligned} F(\vec{q}^{\,2}) &\approx \psi^*(\vec{r}=0)\left\{V(-\vec{q}/2)\frac{1}{-(\vec{q}/2)^2/2M_r} + \frac{1}{-(\vec{q}/2)^2/2M_r}V(-\vec{q}/2)\right\}\psi(\vec{r}=0) \\ &\approx \frac{128\pi\,\alpha_s(\vec{q}^{\,2}/4)\,M_Q C_F}{(\vec{q}^{\,2})^2}\,|\psi(\vec{r}=0)|^2 \end{aligned} \tag{12}$$

where we have now included the contributions from both regions (1) and (2). So all we really need to know about the meson is its wavefunction evaluated at the origin. The high-$\vec{q}^{\,2}$ form factor is completely determined by perturbation theory up to an overall multiplicative constant!

Equation (12) has a simple, intuitive interpretation that generalizes easily to the relativistic case and to other processes. The quantity

$$\begin{aligned} T_H(\vec{q}^{\,2}) &\equiv V(-\vec{q}/2)\frac{1}{-(\vec{q}/2)^2/2M_r} + \frac{1}{-(\vec{q}/2)^2/2M_r}V(-\vec{q}/2) \\ &\approx \frac{128\pi\,\alpha_s(\vec{q}^{\,2}/4)\,M_Q C_F}{(\vec{q}^{\,2})^2} \end{aligned} \tag{13}$$

that appears in the first expression of Eq. (12) is just the nonrelativistic meson form factor but with each of the initial and final state mesons replaced by an on-shell quark-antiquark pair. The quark and antiquark share the meson's three-momentum equally. Our analysis shows that momenta internal to the mesons can be neglected relative to $\vec{q}$ in this "hard-scattering amplitude"—*i.e.* that T_H is roughly independent of the relative momenta of the quark and antiquark when $\vec{q}$ is large. In coordinate space this means that the separation between the quark and antiquark in this process ($\sim 1/|\vec{q}\,|$) is much smaller than the size of the mesons. Thus Eq. (12) for the asymptotic form factor can be recast in the highly suggestive form (Fig. 3)

$$F(\vec{q}^{\,2}) = \psi^*(\vec{r}=0)\, T_H(\vec{q}^{\,2})\, \psi(\vec{r}=0). \tag{14}$$

where $\psi(\vec{r}=0)$ is the amplitude for finding the quark and antiquark on top of each other in the initial meson, T_H is the amplitude for scattering the quark-antiquark pair from the initial direction to the final direction, and $\psi^*(\vec{r}=0)$ is the amplitude for transforming the resulting quark-antiquark pair into the final meson.

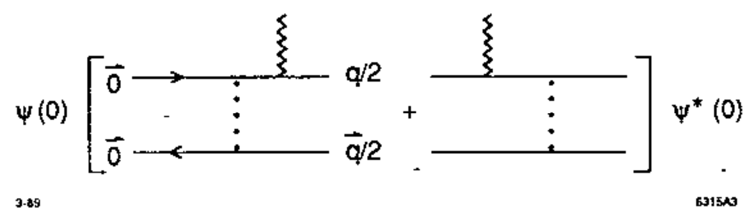

Figure 3. The asymptotic form factor in terms of the hard scattering amplitude T_H and the meson's wavefunction at the origin $\psi(\vec{r}=0)$.

Notice that we are justified in using perturbation theory to compute T_H only because the hard-scattering subprocess occurs over short distances. This highlights an important distinction between the perturbative analysis of form factors and that of other processes like deep inelastic scattering. Perturbative QCD is reliable only for phenomena that occur over short distances (or near the light cone). In processes like deep inelastic scattering the short distances arise for largely kinematical reasons: the cross section for deep inelastic scattering is given by a matrix element of two currents separated by $z^2 \sim 1/Q^2$. By contrast, we find short distances in our form factor analysis only by looking inside the process. Short distances arise as a result of the properties of the hard-scattering amplitude T_H—*i.e.* as a result of the dynamics of the theory. As a consequence the validity of a perturbative analysis of form factors is perhaps not as well established as it is for, say, deep inelastic scattering. By the same token the analysis is perhaps more interesting because of the critical role played by the dynamics and by hadron structure.

Finally we should comment briefly upon the principal limitation of our perturbative analysis: it is valid only over a limited range of momentum transfer. It is clear from our analysis that $\vec{q}/2$ must be larger than the root-mean-square momentum in the wavefunction. This is evident from the form factor for ground-state positronium, which can be computed analytically:

$$F_{\mathrm{Ps}}(\vec{q}^{\,2}) = \left(\frac{16\gamma^2}{\vec{q}^{\,2} + 16\gamma^2}\right)^2 \tag{15}$$

where $\gamma \equiv \alpha m_e/2$ is the rms momentum. Here $\vec{q}$ must be of order 4 times the rms momentum before the form factor begins to fall off like the asymptotic form factor. In the QCD case $\vec{q}/2$ must also be sufficiently large that the perturbative part of $V(\vec{q}/2)$ dominates the nonperturbative part. At the high end, $\vec{q}$ is limited by the fact that our analysis is nonrelativistic. Also radiative corrections to the form factor (Eq. (5)) and to the quark potential (Eq. (10)) contribute corrections of order $\vec{q}^{\,2}/M_Q^2$ that become important for relativistic $\vec{q}$. These limitations make it unlikely that our results can be used for the Ψ or even for the Υ; neither meson is sufficiently nonrelativistic. So we must develop a relativistic analysis if we are to treat these mesons or, more generally, light-quark hadrons properly.

3. HADRONIC WAVEFUNCTIONS

The relativistic analysis of hadronic form factors and other large-$p_\perp$ processes is conceptually similar to the nonrelativistic analysis. The only significant difference is in the formalism used to describe hadronic structure in terms of its constituents. To proceed we require a relativistic formulation of the bound state problem.

The conventional formalism for relativistic bound states is the Bethe-Salpeter formalism. In this formalism a meson is described by a covariant wavefunction

$$\Psi^{BS}(k_1, k_2) = \left\langle 0 \,|\, T\psi(k_1)\overline{\psi}(k_2) \,|\, M \right\rangle \tag{16}$$

that depends upon the four momenta of its quark and antiquark constituents. Although formally correct, this formalism is of little use in the description of such simple systems. The problem is that the couplings between different channels—*e.g.* between quark-antiquark and quark-antiquark-gluon channels—is usually large in highly relativistic systems, and the energy available is more than ample for particle creation. Thus the physics of such systems tends to depend upon the interplay between a large number of channels. A meson for example is a superposition of states involving a quark-antiquark pair, a quark-antiquark pair plus a gluon, a quark-antiquark pair plus two gluons, two quark-antiquark pairs, and so on. In the Bethe-Salpeter formalism this interplay between channels is implicit since the meson is described entirely by a quark-antiquark wavefunction. Reference to all other channels is buried inside the potential and irreducible scattering amplitudes used in analyzing hadronic processes, and as a result these potentials and scattering amplitudes become largely intractable. Even in situations where a single channel dominates, the formalism is still quite complicated and very nonintuitive. For example the Bethe-Salpeter wavefunction has no simple probabilistic interpretation analogous to that for nonrelativistic wavefunctions. Because of such complexity the Bethe-Salpeter formalism has been largely abandoned, even in state-of-the-art calculations pertaining to such highly nonrelativistic systems as positronium or the hydrogen atom.

Intuitively one would like to describe hadrons in terms of a series of wavefunctions, one for each channel, just as one would in nonrelativistic quantum mechanics: *e.g.*

$$|\pi\rangle = \sum_{q\bar{q}} |q\bar{q}\rangle\, \psi_{q\bar{q}/\pi} + \sum_{q\bar{q}g} |q\bar{q}g\rangle\, \psi_{q\bar{q}g/\pi} + \cdots . \tag{17}$$

Formally this can be done by quantizing QCD at a particular time, say $t = 0$, and using the creation and annihilation operators from the fields to define the basis states for such a "Fock-state" representation. The problem with this approach is that the zero-particle state in this basis is not an eigenstate of the Hamiltonian. An interaction term in the Hamiltonian like $g\overline{\psi}\gamma_\mu A^\mu \psi$ contains contributions such as $b^\dagger a^\dagger d^\dagger$ that create particles from the zero-particle state. As a result not all of the bare quanta in an hadronic Fock state need be associated with the hadron: some may be disconnected and possibly quite remote elements of the vacuum (Fig. 4). This greatly complicates the interpretation of the hadronic wavefunctions. Also Lorentz transformations are very complicated in this formalism; boost operators tend to create all sorts of additional quanta. This is because the quantization surface $t = 0$ is not invariant under boosts, and thus boosting a state inevitably involves the dynamical evolution (in t) of parts of that state. This is a serious problem for our analysis of large-$p_\perp$ processes since the initial and final state hadrons necessarily have very different momenta.

Fortunately there is a convenient and intuitive formalism, originally due to Dirac,[9] that avoids these problems. This is based upon the "light-cone quantization" of QCD, where the theory is quantized at a particular value of light-cone time $\tau \equiv t + z$ rather than at a particular time t. In this formalism the

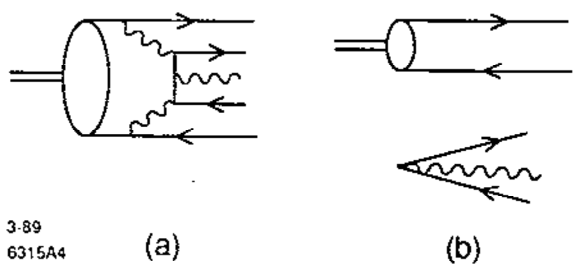

Figure 4. Perturbative contributions to the pion's $q\bar{q}q\bar{q}g$ wavefunction. Contributions of type b) correspond to creation of a $q\bar{q}g$ from the vacuum, and have nothing to do with the hadron. These latter contributions do not arise in light-cone quantization.

hadronic wavefunctions describe the hadron's composition at a particular τ, and the temporal evolution of the state is generated by the light-cone Hamiltonian: $H_{LC} \equiv P^- \equiv P^0 - P^3$, conjugate to τ. Remarkably a simple kinematical argument shows that the zero-particle state in the light-cone Fock basis is an *exact* eigenstate of the full Hamiltonian H_{LC}. Therefore all bare quanta in an hadronic Fock state are part of the hadron. Furthermore Lorentz boosts are greatly simplified in this framework since the quantization surface $\tau = 0$ is invariant under longitudinal boosts. It is also convenient to use τ-ordered light-cone perturbation theory (LCPTh), in place of covariant perturbation theory, for much of our analysis of exclusive processes. LCPTh provides the natural perturbative framework for computing amplitudes in terms of the light-cone wavefunctions that describe hadrons, the resulting formalism being conceptually very similar to ordinary time-dependent perturbation theory in nonrelativistic quantum mechanics. LCPTh is also very convenient for analyzing other light-cone dominated processes, such as deep inelastic scattering. Unlike t-ordered perturbation theory, τ-ordered perturbation theory does not suffer from an explosion in the number of diagrams relative to covariant perturbation theory.

The advantages of light-cone quantization do not come for free. The quantization surface $\tau = 0$ is not invariant under arbitrary rotations or even under parity inversions. As a consequence the operators that generate these transformations are as complicated as the light-cone Hamiltonian, making it difficult, for example, to specify the spin of a particular hadronic state. However the simplicity of the vacuum and of boosts is more important for our applications than is rotation symmetry.

Light-cone quantization and perturbation theory are briefly reviewed for QCD in Appendix III. In the following sections we describe the Fock state basis and wavefunctions in greater detail, emphasizing those features important to our analysis of form factors.

3.1. Definitions

It is convenient when quantizing on the light-cone to rewrite four-vectors in terms of their +, −, and ⊥ components:

$$\begin{aligned} P^+ &\equiv P^0 + P^3 \\ P^- &\equiv P^0 - P^3 \\ \overrightarrow{P}_\perp &\equiv (P^1, P^2). \end{aligned} \tag{18}$$

These components transform very simply under boosts along the z-direction: $P^\pm \rightarrow \exp(\pm\alpha)\, P^\pm$ and $\overrightarrow{P}_\perp \rightarrow \overrightarrow{P}_\perp$. In this notation dot-products have the form

$$P \cdot P = P^+P^- - \overrightarrow{P}_\perp^{\,2} \qquad P \cdot q = \frac{P^+q^- + P^-q^+}{2} - \overrightarrow{P}_\perp \cdot \vec{q}_\perp. \tag{19}$$

If $\tau \equiv x^+ \equiv t + z$ is to play the role of time in our light-cone formalism then P^-, the momentum conjugate to τ, plays the role of the Hamiltonian, and $\underline{P} = (P^+, \overrightarrow{P}_\perp)$ is the three-momentum that specifies the state of a particle. The light-cone energy of a noninteracting particle with mass M is just

$$P^- = \frac{\overrightarrow{P}_\perp^{\,2} + M^2}{P^+}, \tag{20}$$

and the particle's phase space is given by

$$\frac{d^4P}{(2\pi)^4}\, 2\pi\, \delta^+(P^2 - M^2) \;=\; \frac{dP^+\, d^2\overrightarrow{P}_\perp}{2P^+\,(2\pi)^3}. \tag{21}$$

Thus a properly normalized momentum eigenstate satisfies

$$\langle \underline{P} | \underline{P}' \rangle = 2P^+(2\pi)^3\, \delta^3(\underline{P} - \underline{P}'). \tag{22}$$

Note that the longitudinal momentum P^+ for a particle is always positive.

To quantize QCD on the light-cone one defines commutators for the independent fields at a particular light-cone time τ. (See Appendix III). Particle creation and annihilation operators are obtained by Fourier transforming the unrenormalized field operators. These create and destroy bare quarks and gluons that have specific three-momenta and helicities. Using the creation and annihilation operators we can define a set of basis states for the quantum theory:

$$
\begin{aligned}
&|0\rangle \\
&|q\bar{q} : \underline{k}_i \lambda_i\rangle = b^\dagger(\underline{k}_1 \lambda_1)\, d^\dagger(\underline{k}_2 \lambda_2)\; |0\rangle \\
&|q\bar{q}g : \underline{k}_i \lambda_i\rangle = b^\dagger(\underline{k}_1 \lambda_1)\, d^\dagger(\underline{k}_2 \lambda_2)\, a^\dagger(\underline{k}_3 \lambda_3)\; |0\rangle \\
&\vdots
\end{aligned}
\tag{23}
$$

where $b^\dagger$, $d^\dagger$ and $a^\dagger$ create bare quarks, antiquarks and gluons having three-momenta $\underline{k}_i$ and helicities λ_i. Of course these "Fock states" are generally not eigenstates of the full Hamiltonian H_{LC}. However the zero-particle state is the only one with zero total P^+, since all quanta must have positive k^+, and thus this state cannot mix with the other states in the basis. It is an exact eigenstate of H_{LC}.#1 Although they do not diagonalize the Hamiltonian, the Fock states form a very useful basis for studying the physical states of the theory. For example, a pion with momentum $\underline{P} = (P^+, \overrightarrow{P}_\perp)$ is described by state

$$
|\pi : \underline{P}\rangle = \sum_{n,\lambda_i} \int \overline{\prod_i} \frac{dx_i d^2\vec{k}_{\perp i}}{\sqrt{x_i}16\pi^3} \left| n : x_i P^+, x_i \overrightarrow{P}_\perp + \vec{k}_{\perp i}, \lambda_i \right\rangle \psi_{n/\pi}(x_i, \vec{k}_{\perp i}, \lambda_i)
\tag{24}
$$

#1 The restriction $k^+ > 0$ is a key difference between light-cone quantization and ordinary equal-time quantization. In equal-time quantization the state of a parton is specified by its ordinary three-momentum $\vec{k} = (k^1, k^2, k^3)$. Since each component of $\vec{k}$ can be either positive or negative, it is easy to make zero-momentum Fock states that contain particles, and these will mix with the zero-particle state to build up the ground state. In light-cone quantization each of the particles forming a zero-momentum state must have vanishingly small k^+. Such a configuration represents a point of measure zero in the phase space, and therefore such states can usually be neglected. Actually some care must be taken here since there are operators in the theory that are singular at $k^+ = 0$—*e.g.* the kinetic energy $(\vec{k}_\perp^2 + M^2)/k^+$. In certain circumstances states containing $k^+ \to 0$ quanta can significantly alter the ground state of the theory. One such circumstance is when there is spontaneous symmetry breaking. However such effects play little role in the sort analysis we deal with in this article, since we are concerned with high-energy, short-distance phenomena. Note also that the space of states that play a role in the vacuum structure is much smaller for light-cone quantization than for equal-time quantization; the state of each parton is specified by a two-momentum rather than a three-momentum since $k^+ = 0$. This suggests that vacuum structure may be far simpler to analyze using the light-cone formulation.

where the sum is over all Fock states and helicities, and where

$$\overline{\prod_i} dx_i \equiv \prod_i dx_i \, \delta\left(1 - \sum_j x_j\right)$$
$$\overline{\prod_i} d^2\vec{k}_{\perp i} \equiv \prod_i d^2\vec{k}_{\perp i} \, 16\pi^3 \, \delta^2\left(\sum_j \vec{k}_{\perp j}\right). \tag{25}$$

The wavefunction $\psi_{n/\pi}(x_i, \vec{k}_{\perp i}, \lambda_i)$ is the amplitude for finding partons with momenta $(x_i P^+, x_i \overrightarrow{P}_\perp + \vec{k}_{\perp i})$ in the pion. It does not depend upon the pion's momentum. This special feature of light-cone wavefunctions is not too surprising since x_i is the longitudinal momentum fraction carried by the i^{th}-parton $(0 \leq x_i \leq 1)$, and $\vec{k}_{\perp i}$ its momentum "transverse" to the direction of the meson. Both of these are frame independent quantities.

Throughout our analysis we employ the light-cone gauge, $\eta \cdot A = A^+ = 0$, for the gluon field. The use of this gauge results in well known simplifications in the perturbative analysis of light-cone dominated processes such as high-momentum hadronic form factors. Furthermore it is indispensable if one desires a simple, intuitive Fock-state basis, for there are neither negative-norm gauge boson states nor ghost states in $A^+ = 0$ gauge. Thus each term in the normalization condition

$$\sum_{n,\lambda_i} \int \overline{\prod_i} \frac{dx_i d^2\vec{k}_{\perp i}}{16\pi^3} \left|\psi_{n/\pi}(x_i, \vec{k}_{\perp i}, \lambda_i)\right|^2 = 1 \tag{26}$$

is positive. This equation follows immediately from the normalization condition for the full pion-state.

3.2. Light-Cone Bound-State Equations

Any hadron state, such as $|\pi\rangle$ for the pion, must be an eigenstate of the light-cone Hamiltonian. Consequently, when working in the frame where $\underline{P}_\pi = (1, 0)$ and $P_\pi^- = M_\pi^2$, the state $|\pi\rangle$ satisfies an equation

$$\left(M_\pi^2 - H_{LC}\right)|\pi\rangle = 0. \tag{27}$$

Projecting this onto the various Fock states $\langle q\overline{q}|$, $\langle q\overline{q}g| \ldots$ results in an infinite number of coupled integral eigenvalue equations,

$$\left(M_\pi^2 - \sum_i \frac{\vec{k}_{\perp i}^2 + m_i^2}{x_i}\right)\begin{bmatrix}\psi_{q\bar{q}/\pi}\\ \psi_{q\bar{q}g/\pi}\\ \vdots\end{bmatrix} = \begin{bmatrix}\langle q\bar{q}|\,V\,|q\bar{q}\rangle & \langle q\bar{q}|\,V\,|q\bar{q}g\rangle & \cdots\\ \langle q\bar{q}g|\,V\,|q\bar{q}\rangle & \langle q\bar{q}g|\,V\,|q\bar{q}g\rangle & \cdots\\ \vdots & \vdots & \ddots\end{bmatrix}\begin{bmatrix}\psi_{q\bar{q}/\pi}\\ \psi_{q\bar{q}g/\pi}\\ \vdots\end{bmatrix} \tag{28}$$

where V is the interaction part of H_{LC}. Diagrammatically, V involves completely irreducible interactions—*i.e.* diagrams having no internal propagators—coupling Fock states (Fig. 5). These equations determine the hadronic spectrum and

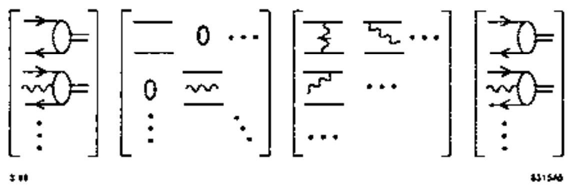

Figure 5. Coupled eigenvalue equations for the light-cone wavefunctions of a pion.

wave functions. Although the potential is essentially trivial, the many channels required to describe an hadronic state make these equations very difficult to solve. Nevertheless the first attempts at a direct solution have been made.

The bulk of the probability for a nonrelativistic system is in a single Fock state—*e.g.* $|e\bar{e}\rangle$ for positronium, or $|b\bar{b}\rangle$ for the Υ meson. For such systems it is useful to replace the full set of multi-channel eigenvalue equations by a single equation for the dominant wavefunction. To see how this can be done, note that the bound state equation, say for positronium, can be rewritten as two equations using the projection operator $\mathcal{P}$ onto the subspace spanned by $e\bar{e}$ states, and its complement $\mathcal{Q} \equiv 1 - \mathcal{P}$:

$$\begin{aligned} H_{\mathcal{PP}}\,|\mathrm{Ps}\rangle_{\mathcal{P}} + H_{\mathcal{PQ}}\,|\mathrm{Ps}\rangle_{\mathcal{Q}} &= M^2\,|\mathrm{Ps}\rangle_{\mathcal{P}} \\ H_{\mathcal{QP}}\,|\mathrm{Ps}\rangle_{\mathcal{P}} + H_{\mathcal{QQ}}\,|\mathrm{Ps}\rangle_{\mathcal{Q}} &= M^2\,|\mathrm{Ps}\rangle_{\mathcal{Q}} \end{aligned} \tag{29}$$

where $H_{\mathcal{PQ}} \equiv \mathcal{P}H\mathcal{Q}\ldots$, and $|\mathrm{Ps}\rangle_{\mathcal{P}} \equiv \mathcal{P}\,|\mathrm{Ps}\rangle\ldots$. Solving the second of these equations for $|\mathrm{Ps}\rangle_{\mathcal{Q}}$ and substituting the result into the first equation, we obtain a single equation for the $e\bar{e}$ or valence part of the positronium state:

$$H_{\text{eff}}\,|\mathrm{Ps}\rangle_{\mathcal{P}} = M^2\,|\mathrm{Ps}\rangle_{\mathcal{P}} \tag{30}$$

where the effective $e\bar{e}$ Hamiltonian is

$$H_{\text{eff}} = H_{\mathcal{PP}} + H_{\mathcal{PQ}} \frac{1}{M^2 - H_{\mathcal{QQ}}} H_{\mathcal{QP}}. \tag{31}$$

The second term of H_{eff} includes all effects from nonvalence Fock states; in light-cone perturbation theory it is given by the sum of all diagrams for $e\bar{e} \to e\bar{e}$ having no $e\bar{e}$ intermediate states (*i.e.* it is "$e\bar{e}$-irreducible"). Thus we have (Fig. 6)

$$\left(M^2 - \frac{\vec{k}_\perp{}^2 + m_e^2}{x(1-x)}\right) \psi_{e\bar{e}}(x, \vec{k}_\perp) = \int_0^1 dy \int \frac{d^2\vec{l}_\perp}{16\pi^3}\, V_{\text{eff}}(x, \vec{k}_\perp; y, \vec{l}_\perp; M^2)\, \psi_{e\bar{e}}(y, \vec{l}_\perp). \tag{32}$$

where V_{eff} is given by

$$V_{\text{eff}} = \frac{T_{\text{irr}}(e\bar{e} \to e\bar{e})}{[x(1-x)y(1-y)]^{1/2}} \tag{33}$$

and $T_{\text{irr}}(e\bar{e} \to e\bar{e})$ is the $e\bar{e}$-irreducible amplitude for elastic $e\bar{e}$ scattering. The helicity dependence is implicit in this equation.

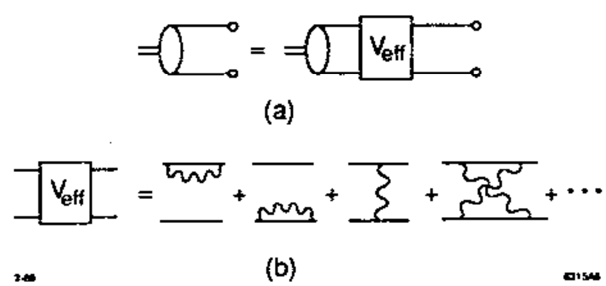

Figure 6. a) Bound state equation for the $e\bar{e}$ wavefunction of positronium. b) The $e\bar{e}$-irreducible potential.

One might wonder whether or not this simple equation is also useful for relativistic states like light-quark hadrons. For positronium the effective potential, $V_{\text{eff}} \approx V_{\text{Coulomb}}$, is little modified by nonvalence Fock states and so this reduction to a valence equation is well warranted. However nonvalence states are most likely quite important for a light-quark hadron, and therefore V_{eff} cannot help but be very complex in this case. For example, retardation effects must become significant when non-valence states become important, as is evident from the normalization condition for the valence wavefunction:

$$\sum_{\lambda_i} \int \prod_i \frac{dx_i d^2\vec{k}_{\perp i}}{16\pi^3} |\psi_{\text{val}}(x_i, \vec{k}_{\perp i}, \lambda_i)|^2 = 1 - \langle\psi_{\text{val}}| \frac{\partial V_{\text{eff}}}{\partial M^2} |\psi_{\text{val}}\rangle \tag{34}$$

—the expectation value of $\partial V_{\text{eff}}/\partial M^2$, a measure of the retardation, equals the probability carried by nonvalence Fock states. So usually one is forced to use the full coupled-channel equations when analyzing ordinary hadrons. However, as we shall see, the valence state plays a special role in high-momentum form factors, and so the valence-state equation will be useful in our analysis.

3.3. General Properties of Light-Cone Wavefunctions

One major advantage of the Fock-state description of a hadron is that much intuition exists about the behavior of bound state wavefunctions. So, while the task of solving Eq. (28) remains formidable, there is nevertheless much we can say about the hadronic wavefunctions. An important feature that is immediately evident from Eq. (28) is that all wavefunctions have the general form

$$\psi_n(x_i, \vec{k}_{\perp i}, \lambda_i) = \frac{1}{M^2 - \sum_i (\vec{k}_{\perp i}^2 + m_i^2)/x_i} (V\Psi). \tag{35}$$

Consequently ψ_n tends to vanish when

$$\mathcal{E} \equiv M^2 - \sum_i \frac{\vec{k}_{\perp i}^2 + m_i^2}{x_i} \rightarrow -\infty. \tag{36}$$

This is intuitively plausible. In the Fock state expansion we think of the bare quanta as being on mass shell but off (light-cone) energy shell: *i.e.* each parton comprising a state with $\underline{P} = (P^+, \overrightarrow{P}_\perp)$ has

$$k_i^- = \frac{(x_i \overrightarrow{P}_\perp + \vec{k}_{\perp i})^2 + m_i^2}{x_i P^+} \implies k_i^2 = m_i^2, \tag{37}$$

but the sum over all k_i^- is not equal to P^-. In fact the difference is just

$$P^- - \sum_i k_i^- = \frac{\overrightarrow{P}_\perp^2 + M^2}{P^+} - \left(\sum_i \frac{\vec{k}_{\perp i}^2 + m_i^2}{x_i P^+} + \frac{\overrightarrow{P}_\perp^2}{P^+} \right) = \frac{\mathcal{E}}{P^+}. \tag{38}$$

Parameter $\mathcal{E}$ is a boost-invariant measure of how far off energy shell a Fock state is. Thus Eq. (35) implies that a physical particle has little probability of being in a Fock state far off shell. In general $\mathcal{E}$ is large when $\vec{k}_{\perp i}^2$ or x_i is small—*i.e.* the wavefunction should vanish as $\vec{k}_{\perp i}^2 \to \infty$ or $x_i \to 0$. Formally such constraints appear as boundary conditions on the wavefunctions and are important if the Hamiltonian is to be well defined (*e.g.* self-adjoint). These are subtle issues that we will not discuss here. Suffice it to note that all wavefunctions must satisfy the conditions

$$\begin{aligned} \vec{k}_{\perp i}^2\ \psi_n(s_i, \vec{k}_{\perp i}, \lambda_i) &\to 0 \quad \text{as } \vec{k}_{\perp i}^2 \to \infty \\ \psi_n(x_i, \vec{k}_{\perp i}, \lambda_i) &\to 0 \quad \text{as } x_i \to 0. \end{aligned} \tag{39}$$

if the free-particle Hamiltonian is to have a finite expectation value.

Perturbation theory is a useful source of intuition concerning wavefunctions and Fock-state expansions. The electron's Fock-state expansion, for example, can be computed perturbatively. To lowest and first order there are only electron and electron-photon components in the physical electron state: *e.g.* an electron with momentum $\underline{P} = (1, 0)$ and positive helicity is described by

$$\begin{aligned} \left|\text{physical } e_\uparrow\right\rangle = \left|e_\uparrow\right\rangle \sqrt{Z_2} + \\ \int \frac{dx\, d^2\vec{k}_\perp}{16\pi^3\,(x(1-x))^{1/2}} \left\{ \left|e_\uparrow\gamma_\uparrow : x, \vec{k}_\perp\right\rangle \psi_{e_\uparrow\gamma_\uparrow/e_\uparrow}(x, \vec{k}_\perp) + \right. \\ \left. \left|e_\uparrow\gamma_\downarrow : x, \vec{k}_\perp\right\rangle \psi_{e_\uparrow\gamma_\downarrow/e_\uparrow}(x, \vec{k}_\perp) + \cdots \right\} \end{aligned} \tag{40}$$

where the electron in $\left|e\gamma : x, \vec{k}_\perp\right\rangle$ has momentum $\underline{k}_e = (x, \vec{k}_\perp)$ and the photon has momentum $\underline{k}_\gamma = (1-x, -\vec{k}_\perp)$. The $e\gamma$-component of this state is readily computed from the light-cone Hamiltonian using ordinary first-order Rayleigh-Schrödinger perturbation theory. Schematically this term is given by the expression

$$\sum_{e\gamma} \frac{|e\gamma\rangle\, \langle e\gamma|\, V\, |e\rangle}{m_e^2 - P_{e\gamma}^-} \tag{41}$$

which is identical in form to the LCPTh amplitude for the diagram in Fig. 7. Thus the $e\gamma$-wavefunctions follow directly from LCPTh: *e.g.*

$$\psi_{e_\uparrow\gamma_\uparrow/e_\uparrow}(x, \vec{k}_\perp) = \frac{e\, \overline{u}_\uparrow(\underline{k}_e)\, \varepsilon_\uparrow^*(\underline{k}_\gamma) \cdot \gamma\, u_\uparrow(\underline{P})}{m_e^2 - (\vec{k}_\perp^2 + x\, m_e^2)/x(1-x)} = \frac{-e\,(k_1 - i\,k_2)}{\vec{k}_\perp^2 + x^2 m_e^2}. \tag{42}$$

Having computed these wavefunctions, the renormalization constant Z_2 is fixed by the normalization condition for the full electron state; obviously Z_2 is the probability for finding a bare electron in a physical electron. The wavefunctions for an elementary particle like the electron can be used in much the same way as the wavefunctions for a composite particle; given the wavefunctions, there is little distinction between composite and elementary particles in this formalism. Notice that the $e\gamma$-wavefunctions do not satisfy the boundary conditions discussed above, and as a result Z_2 is not finite. This is of course just the usual ultraviolet divergence in QED. As we discuss in the next section, neither of these boundary conditions is generally satisfied in the absence of ultraviolet ($\vec{k}_\perp \to \infty$) and infrared ($x \to 0$) regulators.

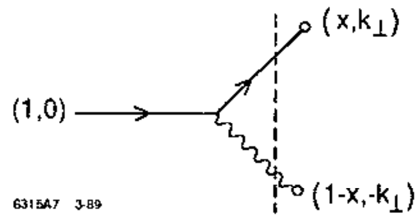

Figure 7. LCPTh amplitude corresponding to the $e\gamma$-wavefunction for a physical electron.

More generally perturbation theory can be used to compute the high-momentum behavior of light-cone wavefunctions. The basic ansatz of perturbative QCD is that the short distance behavior of the theory is perturbative; only perturbative interactions are sufficiently singular to contribute at short distances. Consequently wavefunctions behave in much the same way as perturbative amplitudes (in LCPTh) when $\vec{k}_\perp \to \infty$.[#2] This is evident from our analysis of the non-relativistic wavefunction for heavy-quark mesons: the large-$\vec{q}$ dependence of the wavefunction is obtained by replacing the meson with an on-shell quark-antiquark pair and computing in perturbation theory. A similar analysis in the relativistic case shows that the pion's $q\overline{q}$ wavefunction falls off roughly as $1/\vec{k}_\perp^2$ when $\vec{k}_\perp^2 \to \infty$, just like the LCPTh amplitude for $q\overline{q} \to q^*\overline{q}^*$ that is shown in Fig. 8a. Similarly one expects the $q\overline{q}g$ wavefunction to fall like the perturbative amplitude in Fig. 8b—*i.e.* $\psi_{q\overline{q}g} \sim 1/|\vec{k}_\perp|$ as $|\vec{k}_\perp| \to \infty$.

In addition to determining the large-$\vec{k}_\perp$ behavior of wavefunctions, perturbation theory also serves as a guide to modelling such things as the helicity dependence of wavefunctions. Normally one can say little about the angular-momentum

#2 This connection can be made precise using the operator product expansion, as we illustrate in later sections.

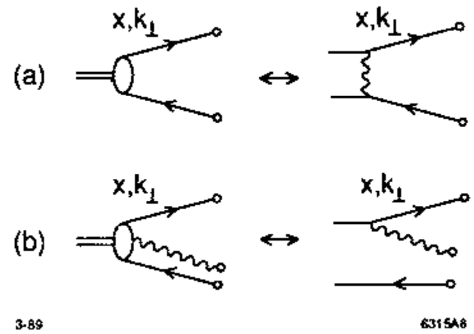

Figure 8. LCPTh diagrams having behavior similar to that of wavefunctions for $\vec{k}_\perp$ large.

content of a model wavefunction, since the angular momentum operators are very complicated in light-cone quantization. However perturbation theory can be used to produce examples of wavefunctions having particular spin quantum numbers, and these can be used to motivate non-perturbative models. For example, to see what a pion's $q\overline{q}$ wavefunction might look like, we can treat the pion as an elementary particle that couples to the quarks through elementary couplings like $\overline{\psi}\,\gamma_5\,\vec{\pi}\cdot\vec{\tau}\,\psi$ or $\overline{\psi}\,\gamma_5\gamma\cdot\partial\vec{\pi}\cdot\vec{\tau}\,\psi$. The wavefunction can then be computed perturbatively in much the same way we compute $\psi_{e\gamma/e}$ above. This wavefunction has the correct quantum numbers in the limit where the quark-antiquark interactions are negligible, and so it can serve as the starting point for the design of empirical wavefunctions to model the pion. Note that such a wavefunction is more singular at large momenta than the pion's true wavefunction; this is the essential difference between an elementary particle and a composite particle.

Further intuition about wavefunctions comes from the physics of nonrelativistic bound states. In the rest frame, where $P^+ = P^- = M$ and $\overrightarrow{P}_\perp = 0$, time t and light-cone time $\tau = t + z/c$ are almost identical for a nonrelativistic system since the speed of light c is effectively infinite. Consequently the usual Schrödinger wavefunction defined at a particular t should be almost the same as the light-cone wavefunction defined at $\tau \approx t$. To make the connection notice that the $i^{\rm th}$ constituent has longitudinal momentum

$$k_i^+ = x_i M = k_i^0 + k_i^3 \approx m_i + \mathcal{O}(m_i v^2) + k_i^3 \tag{43}$$

where the constituent's energy k_i^0 is just its mass m_i plus small corrections (due to kinetic and potential energies) of $\mathcal{O}(m_i v^2) \ll k_i^3 \sim m_i v$. Thus the quantity $x_i M -$

m_i is effectively equal to k_i^3, and a Schrödinger wavefunction can be converted to a light-cone wavefunction simply by the replacement: $k_i^3 \to x_i M - m_i$. This is also evident when we note that all energy denominators have the form

$$M^2 - \sum_i \frac{\vec{k}_{\perp i}^2 + m_i^2}{x_i} \approx 2M \left\{ E_{NR} - \sum_i \frac{\vec{k}_{\perp i}^2 + (x_i M - m_i)^2}{2m_i} \right\} \tag{44}$$

when $|x_i M - m_i| \ll m_i$. This correspondence indicates that nonrelativistic light-cone wavefunctions are sharply peaked at

$$x_i = \frac{m_i}{M} \qquad \vec{k}_{\perp i} = 0, \tag{45}$$

just as Schrödinger wavefunctions are peaked at low $\vec{k}_i$ ($\ll m_i$). This is well illustrated by the wavefunction for ground state positronium (or hydrogen) which is given by

$$\psi(x_e, \vec{k}_\perp) \approx \left(\frac{2M\gamma^3}{\pi}\right)^{1/2} \frac{8\pi\gamma}{\left(\vec{k}_\perp^2 + (x_e M - m_e)^2 + \gamma^2\right)^2}. \tag{46}$$

when $\vec{k}_\perp^2$, $(x_e M - m_e)^2 \ll m_e^2$. Here $\gamma \equiv \alpha m_r$ where m_r is the reduced mass.

3.4. Renormalization

As we discuss in earlier sections, perturbation theory indicates that hadronic wavefunctions do not fall off sufficiently quickly as $\vec{k}_\perp^2 \to \infty$. This leads to infinities in the unitarity sum (Eq. (26)), energy expectation values, and in the wavefunctions themselves. Of course this is not unexpected given that the wavefunctions and the theory are as yet unrenormalized. To make the theory finite we must truncate the Fock space by in effect discarding all Fock states with light-cone energy $|\mathcal{E}| > \Lambda^2$. This ultraviolet cutoff can be introduced by using Pauli-Villars and related regulators or, equivalently, dimensional regularization. These regulators preserve the Poincaré and gauge symmetries of the theory. For our purposes, however, it is simpler and more intuitive to simply truncate the Fock space, excluding all states with $|\mathcal{E}|$ or $\vec{k}_\perp^2$ greater than some Λ^2. This procedure causes no problems in "leading-log" analyses of the sort we are concerned with here. The end result is that all loop integrations in LCPTh are finite, and the wavefunctions all vanish at large $\vec{k}_\perp$.

Usually one takes $\Lambda \to \infty$ when computing. However the key physical characteristic of renormalizable theories is that this cutoff has no effect on the results for any process provided only that Λ is much larger than all mass scales, energies, and so on relevant to the process of interest. So we can compute with finite Λ. This is not to say that states with $|\mathcal{E}| > \Lambda^2$ are unimportant—the existence of ultraviolet divergences is dramatic evidence to the contrary. Rather it means that all low-energy effects due to these very high-energy states can be accounted for by redefining the coupling constants, masses, *etc.* appearing in the effective Lagrangian (or Hamiltonian) for the truncated theory—*e.g.*

$$\mathcal{L}^{(\Lambda)} = \overline{\psi}(i\partial\cdot\gamma - g(\Lambda)A\cdot\gamma - m(\Lambda))\psi + 1/4F^2 + \mathcal{O}\left(\frac{\overline{\psi}\sigma\cdot F\psi}{\Lambda} + \cdots\right). \quad (47)$$

These bare parameters vary with Λ in the usual way, as more or less of the high-energy Fock space is absorbed:

$$\Lambda\frac{d}{d\Lambda}\alpha_s(\Lambda^2) = \beta\left(\alpha_s(\Lambda^2), \frac{m(\Lambda)}{\Lambda}\right) \quad (48)$$

$$\vdots$$

In general nonrenormalizable interactions appear as well, but these are suppressed by powers of $1/\Lambda$, as is suggested by simple dimensional arguments. Also the effective Lagrangian can change radically as Λ passes thresholds for new heavy quarks, or say for observing quark substructure (if there is any).

Working with a finite cutoff, the couplings, masses, and wavefunctions of the theory are both well defined and well behaved. Furthermore they have a simple interpretation. The bare parameters—$g(\Lambda)$, $m(\Lambda)\ldots$—are the effective couplings and masses of the theory at energies of order Λ (*i.e.* at distances of $\sim 1/\Lambda$). Indeed as we shall see, a process or quantity in which only a single scale Q is relevant is most naturally expressed in terms of the couplings, masses, wavefunctions, *etc.* of the theory with cutoff $\Lambda \sim Q$. Of course one must compute with $\Lambda \gg Q$, but the dominant effect of vertex and self-energy corrections is to replace $g(\Lambda)$, $m(\Lambda)$, $\psi^{(\Lambda)}\ldots$ by $g(Q)$, $m(Q)$, $\psi^{(Q)}\ldots$. Thus as Q is increased, ever finer structure is unveiled in the wavefunctions and in the theory.

The wavefunction $\psi_n^{(\Lambda)}(x_i, \vec{k}_{\perp i}, \lambda_i)$ has a multiplicative dependence upon Λ when x_i and $\vec{k}_{\perp i}$ are held fixed, and when $\vec{k}_{\perp i}^2 \ll \Lambda^2$:

$$\psi_n^{(\Lambda)}(x_i, \vec{k}_{\perp i}, \lambda_i) = \prod_j \left(\frac{Z_j^{(\Lambda)}}{Z_j^{(\Lambda_0)}}\right)^{1/2} \psi_n^{(\Lambda_0)}(x_i, \vec{k}_{\perp i}, \lambda_i) \quad (49)$$

where $Z_j^{(\Lambda)}$ is the usual wavefunction renormalization constant for the j^{th} parton. This formula is easily understood by recalling that $Z_j^{(\Lambda)}$ is the probability for finding a "bare" parton in a "dressed" parton. Also it follows that $0 \leq Z_j^{(\Lambda)} \leq 1$. Furthermore, $Z_j^{(\Lambda)}$ generally decreases with increasing Λ since the effective phase space, and therefore the probability, for the multi-parton Fock states in a dressed parton increases with Λ. Although the probability shifts from Fock state to Fock state with varying Λ, the total probability is always conserved:

$$\sum_{n,\lambda_i} \int \overline{\prod_i} \frac{dx_i d^2\vec{k}_{\perp i}}{16\pi^3} |\psi_n^{(\Lambda)}(x_i, \vec{k}_{\perp i}, \lambda_i)|^2 = 1 + \mathcal{O}\left(\frac{m}{\Lambda}\right). \tag{50}$$

One final modification of theory is required. The polarization sum for a gluon is singular as the gluon's longitudinal momentum k^+ vanishes:

$$\sum_\lambda \varepsilon_\mu(\underline{k}, \lambda)\, \varepsilon_\nu^*(\underline{k}, \lambda) = -g_{\mu\nu} + \frac{\eta_\mu k_\nu + \eta_\nu k_\mu}{k^+}. \tag{51}$$

As a result wavefunctions for states with gluons diverge as $k_g^+ \to 0$, again contrary to the boundary conditions Eq. (39). This singularity is to some extent an artifact of light-cone gauge. For our purposes it can be regulated by making the replacement:

$$\left(\frac{1}{k^+}\right)^n \to \frac{1}{2}\left\{\frac{1}{(k^+ + i\delta)^n} + \frac{1}{(k^+ - i\delta)^n}\right\}. \tag{52}$$

Physical amplitudes or cross sections are independent of δ provided it is sufficiently small. This implies that gluons decouple when $k_g^+ \leq \delta$ for some small δ. Thus we can use this regulator with a small but non-zero δ to obtain wavefunctions that are well behaved when gluons have vanishingly small longitudinal momenta. Typically the cutoff point must be $\delta \leq \langle k_\perp \rangle / Q$, where $\langle k_\perp \rangle$ is some average of the gluon's $\vec{k}_\perp$, and Q is the momentum scale of the probe. Therefore as Q increases, so does the number of "wee" gluons. Notice finally that $\langle k_\perp \rangle$ can never vanish for physical states since very long wavelength gluons cannot couple to a color-singlet state. Thus, with finite δ and Λ cutoffs, all Fock-state wavefunctions are well behaved, both as $x_i \to 0$ and $\vec{k}_{\perp i} \to \infty$.

3.5. Calculating

In principle the hadronic wavefunctions determine all properties of a hadron. Here we illustrate the relation between the wavefunctions and measurable quantities by briefly examining a number of processes. These examples also demonstrate the calculational rule for using wavefunctions: *i.e.* an amplitude involving wavefunction $\psi_n^{(\Lambda)}$, describing Fock state n in a hadron with $\underline{P} = (P^+, \vec{P}_\perp)$, has the general form

$$\sum_{\lambda_i} \int \prod_i \frac{dx_i d^2\vec{k}_{\perp i}}{\sqrt{x_i} 16\pi^3} \psi_n^{(\Lambda)}(x_i, \vec{k}_{\perp i}, \lambda_i)\, T_n^{(\Lambda)}(x_i P^+, x_i \vec{P}_\perp + \vec{k}_{\perp i}, \lambda_i) \tag{53}$$

where $T_n^{(\Lambda)}$ is the irreducible scattering amplitude in LCPTh with the hadron replaced by Fock state n. If only the valence wavefunction is to be used, $T_n^{(\Lambda)}$ is irreducible with respect to the valence Fock state only: *e.g.* $T_n^{(\Lambda)}$ for a pion has no $q\bar{q}$ intermediate states. Otherwise contributions from all Fock states must be summed, and $T_n^{(\Lambda)}$ is completely irreducible.

$\underline{\pi \rightarrow \mu\nu}$

The leptonic width of the $\pi^\pm$ is one of the simplest processes because it involves only the $q\bar{q}$ Fock state. The sole contribution to π^- decay is from

$$\begin{aligned} \langle 0|\, \overline{\psi}_u \gamma^+(1-\gamma_5)\psi_d \,|\pi^-\rangle &= -\sqrt{2}P^+ f_\pi \\ &= \int \frac{dx\, d^2\vec{k}_\perp}{16\pi^3} \psi_{d\bar{u}}^{(\Lambda)}(x, \vec{k}_\perp) \frac{\sqrt{n_c}}{\sqrt{2}} \left\{ \frac{\overline{v}_\downarrow}{\sqrt{1-x}} \gamma^+(1-\gamma_5) \frac{u_\uparrow}{\sqrt{x}} \;+\; (\uparrow \leftrightarrow \downarrow) \right\} \end{aligned} \tag{54}$$

where $n_c = 3$ is the number of colors, $f_\pi \approx 93$ MeV, and where only the $L_z = S_z = 0$ component of the general $q\bar{q}$ wavefunction contributes. Thus we have

$$\int \frac{dx\, d^2\vec{k}_\perp}{16\pi^3} \psi_{d\bar{u}}^{(\Lambda)}(x, \vec{k}_\perp) = \frac{f_\pi}{2\sqrt{3}}. \tag{55}$$

This result must be independent of the cutoff Λ provided Λ is large compared with typical hadronic scales. This equation is an important constraint upon the normalization of the $d\bar{u}$ wavefunction, indicating among other things that there is a finite probability for finding a π^- in a pure $d\bar{u}$ Fock state.

Hadronic form factor

The electromagnetic form factor of a pion is defined by the relation

$$\langle \pi : \underline{P}' |\, J^{\mu}_{em} \,| \pi : \underline{P} \rangle = 2(P + P')^{\mu}\, F\left(-(P' - P)^2\right). \tag{56}$$

where J^{μ}_{em} is the electromagnetic-current operator for the quarks. The form factor is easily expressed in terms of the pion's Fock-state wavefunctions by examining the $\mu = +$ component of this equation in a frame where $\underline{P} = (1, 0)$ and $\underline{P}' = (1, \vec{q}_{\perp})$. Then the spinor algebra is trivial since $\overline{u}(\underline{k})\gamma^{+}u(\underline{l}) = 2\sqrt{k^{+}l^{+}}$, and the form factor is just a sum of overlap integrals that is quite analogous to the nonrelativistic result (Fig. 9a):[10]

$$F(\vec{q}_{\perp}^{\,2}) = \sum_{n,\lambda_i} \sum_{a} e_a \int \overline{\prod_i} \frac{dx_i\, d^2\vec{k}_{\perp i}}{16\pi^3}\, \psi_n^{(\Lambda)*}(x_i, \vec{l}_{\perp i}, \lambda_i)\, \psi_n^{(\Lambda)}(x_i, \vec{k}_{\perp i}, \lambda_i). \tag{57}$$

Here e_a is the charge of the struck quark, $\Lambda^2 \gg \vec{q}_{\perp}^{\,2}$, and

$$\vec{l}_{\perp i} \equiv \begin{cases} \vec{k}_{\perp i} - x_i \vec{q}_{\perp} + \vec{q}_{\perp} & \text{for the struck quark} \\ \vec{k}_{\perp i} - x_i \vec{q}_{\perp} & \text{for all other partons.} \end{cases} \tag{58}$$

Notice that the transverse momenta appearing as arguments of the first wavefunction correspond not to the actual momenta carried by the partons but to the actual momenta minus $x_i \vec{q}_{\perp}$, to account for the motion of the final hadron. Notice also that $\vec{l}_{\perp}$ and $\vec{k}_{\perp}$ become equal as $\vec{q}_{\perp} \to 0$, and that $F_{\pi} \to 1$ in this limit as a consequence of the unitarity condition Eq. (50). The behavior at large $\vec{q}_{\perp}^{\,2}$ is discussed at length in subsequent sections.

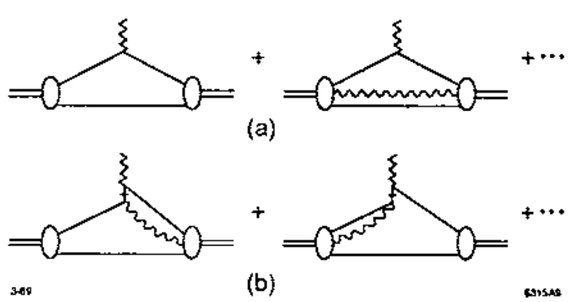

Figure 9. Diagrams contributing to the electromagnetic form factor of a hadron: a) only terms for $\mu = +$; b) additional terms for $\mu \neq +$.

It is interesting to note that a very different expression is obtained for the form factor if one examines some other component of the current, for example the $\mu = -$ component. Not only does the momentum dependence of the quark-photon become more complicated, but the vertex no longer conserves particle number since there are now terms involving transitions $q + \gamma^* \rightarrow q + g$ and $q + g + \gamma^* \rightarrow q$, as illustrated in Fig. 9b. These various expressions for the form factor must all be equal, and yet there is no simple way of demonstrating this fact. The problem is that rotations must be used to relate one expression to another, and the rotation operators are complicated in our formalism. The equality of these expressions implies a nontrivial relationship between different Fock states, a relationship that ought to be incorporated as much as possible into empirical models for the pion wavefunctions.

Note finally that our expression for the pion form factor is actually far more general. The helicity-conserving electromagnetic form factor of any hadron has precisely the same form.

Deep inelastic scattering

The proton's structure functions are determined to leading order in $\alpha_s(Q^2)$ by the τ-ordered diagrams in Fig. 10. Furthermore the only region to contribute in this order is $\vec{k}_\perp^2 \ll Q^2$ where $Q^2 \equiv \vec{q}_\perp^2$. This is because the hadronic wavefunctions are peaked at low $\vec{k}_\perp$. This has two important consequences: first, we can neglect $\vec{k}_\perp$ relative to $\vec{q}_\perp$ to leading order; and second, we can set the ultraviolet cutoff Λ equal to Q since only those Fock states with $\vec{k}_\perp^2 \ll Q^2$ are important. The structure functions are then

$$2M\, F_1(x,Q) = \frac{F_2(x,Q)}{x} \approx \sum_a e_a^2\, G_{a/p}(x,Q) \tag{59}$$

where, from Fig. 10,

$$G_{a/p}(x,Q) = \sum_{n,\lambda_i} \int \overline{\prod_i} \frac{dx_i d^2\vec{k}_{\perp i}}{16\pi^3} |\psi_n^{(Q)}(x_i, \vec{k}_{\perp i}, \lambda_i)|^2 \sum_{b=a} \delta(x_b - x) \tag{60}$$

is the number density of partons of type a with longitudinal momentum fraction x in the proton. (The $\sum_b$ is over all partons of type a in Fock state n.)

This equation leads immediately to a very useful interpretation of the structure

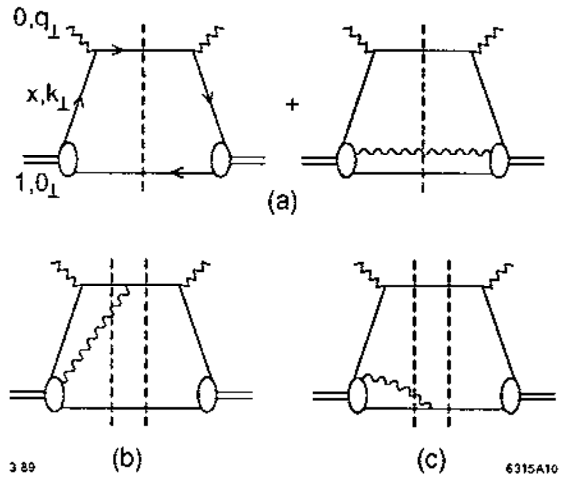

Figure 10. LCPTh diagrams contributing to the proton's structure functions for deep inelastic scattering.

function moments:

$$\int_0^1 dx\, x^{n+1} G_{a/p}(x,Q) = \frac{\langle p|\,\overline{\psi}_a \gamma^+ (i\overleftrightarrow{D}^+)^{n+1} \psi_a\,|p\rangle^{(Q)}}{(2P_p^+)^{n+2}} \tag{61}$$

where the matrix element is between proton states and is evaluated with ultraviolet cutoff $\Lambda = Q$, and where the gauge-covariant derivative is $D^+ = \partial^+$ in light-cone gauge. The Q-dependence of the moments is determined simply by the cutoff dependence of matrix elements of (twist-two) local operators!

4. A PERTURBATIVE ANALYSIS

In this section we develop the techniques needed to understand exclusive processes with large momentum transfer. This relativistic analysis is very similar to the nonrelativistic analysis given in Section 2, and, as in the nonrelativistic case, the result is both simple and intuitive. Generally one finds that the amplitudes for such processes can be written as a convolution of quark distribution amplitudes $\phi(x_i, Q)$, one for each hadron involved in the amplitude, with a hard-scattering amplitude T_H.[4,2] The pion's electromagnetic form factor, for example, can be written as[3,4,2]

$$F_\pi(Q^2) = \int_0^1 dx \int_0^1 dy\, \phi_\pi^*(y,Q)\, T_H(x,y,Q)\, \phi_\pi(x,Q)\, \left(1 + \mathcal{O}\left(\frac{1}{Q}\right)\right). \tag{62}$$

Here T_H is the scattering amplitude for the form factor but with the pions replaced by collinear $q\overline{q}$ pairs—i.e. the pions are replaced by their valence partons. The process-independent distribution amplitude[4] $\phi_\pi(x,Q)$ is just the probability amplitude for finding the $q\overline{q}$ pair in the pion with $x_q = x$ and $x_{\overline{q}} = 1 - x$:[#3]

$$\phi_\pi(x,Q) = \int \frac{d^2\vec{k}_\perp}{16\pi^3}\, \psi^{(Q)}_{q\overline{q}/\pi}(x,\vec{k}_\perp) \tag{63}$$

$$= P_\pi^+ \int \frac{dz^-}{4\pi}\, e^{ixP_\pi^+ z^-/2}\, \langle 0|\, \overline{\psi}(0)\, \frac{\gamma^+\gamma_5}{2\sqrt{2n_c}}\, \psi(z)\, |\pi\rangle^{(Q)}\Big|_{z^+ = \vec{z}_\perp = 0} \tag{64}$$

The $\vec{k}_\perp$ integration in Eq. (63) is cut off by the ultraviolet cutoff $\Lambda = Q$ implicit in the wavefunction; only Fock states with energies $|\mathcal{E}| < Q^2$ are important.

The structure of Eq. (62) is very reminiscent of that for the nonrelativistic form factor (Eq. (14)). The major difference is that here there is a convolution over the longitudinal momenta of the partons. In a nonrelativistic meson the longitudinal momentum is sharply peaked about $x = 1/2$, and thus the x-y dependence of T_H plays no role. One can set $x = y = 1/2$ in T_H, and factor it out of the integral in Eq. (62). Then one needs only $\int dx\, \phi$, which is just the wavefunction evaluated at the origin, to compute the form factor. As far as the nonrelativistic meson is concerned the hard subprocess occurs over very short distances. The situation is different for a relativistic meson, which is sensitive to the fact that the hard subprocess is not really a short-distance reaction. Although the volume within which the subprocess occurs is small in the transverse direction ($|\delta\vec{z}_\perp| \sim 1/Q$), it can extend over large longitudinal distances: $\delta z^- \sim 1/P_\pi^+ = 1/m_\pi$ in the pion's rest frame. A relativistic meson has structure over such distances, and therefore the asymptotic form factor is given by a convolution over

#3 The distribution amplitude is gauge invariant. In gauges other than light-cone gauge, a path-ordered "string operator" $P\exp(\int_0^1 ds\, ig\, A(sz)\cdot z)$ must be included between the $\overline{\psi}$ and ψ. The line integral vanishes in light-cone gauge because $A\cdot z = A^+ z^-/2 = 0$ and so the factor can be omitted in that gauge. This (non-perturbative) definition of ϕ uniquely fixes the definition of T_H which must itself then be gauge invariant.

longitudinal momentum. Note that the subprocess is still restricted to a region very near the light-cone—*i.e.* $\delta z^2 = \delta z^+ \delta z^- - \delta \vec{z}_\perp^{\,2} \sim -1/Q^2$. Such "light-cone dominated" processes can still be analyzed perturbatively.

The distribution amplitude is only weakly dependent on Q, as is evident from the evolution equation[4,2] (which we derive below):

$$Q\frac{\partial}{\partial Q}\phi_\pi(x,Q) = \int_0^1 dy\, V(x,y,\alpha_s(Q^2))\,\phi_\pi(y,Q) \tag{65}$$

$$V(x,y,\alpha_s(Q^2)) = \alpha_s(Q^2)\,V_1(x,y) + \alpha_s^2(Q^2)\,V_2(x,y) + \cdots \tag{66}$$

The bulk of the Q dependence comes from T_H. To leading order in $\alpha_s(Q^2)$, T_H is obtained directly from the form factor for $\gamma^* + q\overline{q} \to q\overline{q}$, where the mesons have been replaced by collinear $q\overline{q}$ pairs:

$$T_H(x,y,Q) = \frac{F_{q\overline{q}}(x,y,Q)}{[x(1-x)y(1-y)]^{1/2}} \qquad \text{(leading order)}. \tag{67}$$

Beyond leading order only the "collinear-irreducible" part of $F_{q\overline{q}}$ is retained: all mass singularities are systematically subtracted out since contributions from low momenta are already included in the distribution amplitudes. Therefore we can neglect all quark and meson masses in T_H, leaving Q as the only scale. The amplitude must then have the general form

$$T_H(x,y,Q) = \frac{1}{Q^n}\,f(x,y,\alpha_s(Q^2)) \tag{68}$$

where $n = 2$ from simple dimensional arguments. This means that the pion form factor falls as $1/Q^2$, up to logarithms of Q. In general the dimension of an amplitude is $[\text{energy}]^{-n}$ where n is the total number of quarks, gluons, and leptons in the initial and final states of the process: *e.g.* $n = 6 - 4$ for the pion form factor since the process $e\pi \to e\pi$ involves four partons and two leptons. This "dimensional-counting rule" implies that the nucleon form factor falls off roughly like $1/Q^4$ with increasing Q, since there is one additional parton in each of the initial and final states of T_H relative to the pion case and thus $n = 8 - 4$. Generally the more partons that must be scattered from the initial to the final direction, the more powers of $1/Q$ there are in the form factor.

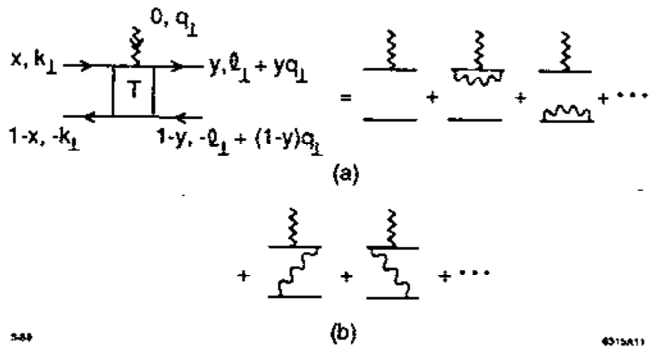

Figure 11. The $q\overline{q}$-irreducible diagrams contributing to the $q\overline{q}$ form factor.

A second consequence of neglecting masses in T_H is that total quark helicity is conserved[6] since the vector couplings with gluons cannot flip the helicity of massless quarks.[#4] By its definition ϕ carries no helicity, and so the helicity of the hadron equals the sum of the helicities of its valence quarks in T_H. Thus, for example, hadronic helicity is conserved in high-Q^2 form factors—*i.e.* helicity-flip form factors such as the nucleon form factor F_2 are suppressed by additional powers of m/Q.

In the following sections we derive these results for the pion's electromagnetic form factor; the techniques generalize readily to other large-$p_\perp$ processes. We discuss how the distribution amplitudes might be computed nonperturbatively. We examine problems that arise in certain processes due to singularities in T_H. Finally, we address the critical question of how large Q must be for these asymptotic results to hold. We do this by examining competing mechanisms and by investigating the self-consistency of perturbation theory.

4.1. Factorization—Leading Order Analysis

The pion's form factor can be written in terms of its $q\overline{q}$ wavefunction alone:

$$F_\pi(Q^2) = \int \frac{dx\, d^2\vec{k}_\perp}{16\pi^3} \int \frac{dy\, d^2\vec{l}_\perp}{16\pi^3}\, \psi^{(\Lambda)*}(y, \vec{l}_\perp)\, \frac{T(x, \vec{k}_\perp; y, \vec{l}_\perp; \vec{q}_\perp)}{[x(1-x)y(1-y)]^{1/2}}\, \psi^{(\Lambda)}(x, \vec{k}_\perp). \tag{69}$$

Here T is the sum of all $q\overline{q}$-irreducible LCPTh amplitudes contributing to the $q\overline{q}$ form factor for $\gamma^* + q\overline{q} \to q\overline{q}$ (Fig. 11). The ultraviolet cutoff is $\Lambda \gg Q$.

#4 The helicity-projection operators for massless quarks are just $1 \pm \gamma_5$. Noting that, for example, that the vertex $\overline{u}\gamma^\mu(1-\gamma_5)u$ equals $u^\dagger(1-\gamma_5)^\dagger\gamma^0\gamma^\mu u$, we see that the vector coupling of the gluons with the quarks preserves quark helicity. This would not be the case if the gluon was a scalar where, for example, the coupling might be $\overline{u}(1-\gamma_5)u$ which equals $u^\dagger(1+\gamma_5)^\dagger\gamma^0 u$ and flips the quark's helicity. This same sort of argument can also be used to explain why massless neutrinos are always left-handed.

Consider first the disconnected part of T (Fig. 11a). For the moment we ignore renormalization diagrams, and consider only terms where the photon attaches to the quark line. The disconnected part then gives a contribution

$$e_q \int_0^1 dx \int \frac{d^2\vec{k}_\perp}{16\pi^3}\, \psi^{(\Lambda)*}(x, \vec{k}_\perp + (1-x)\vec{q}_\perp)\, \psi^{(\Lambda)}(x, \vec{k}_\perp) \tag{70}$$

to F_π, where e_q is the quark's electric charge. The analysis of this contribution follows closely that of the nonrelativistic form factor. The integral is dominated by two regions of phase space when Q^2 is large since the wavefunctions are sharply peaked at low transverse momentum:

1) $|\vec{k}_\perp| \ll (1-x)Q$, where $\psi^{(\Lambda)}(x, \vec{k}_\perp)$ is large;

2) $|\vec{k}_\perp + (1-x)\vec{q}_\perp| \ll (1-x)Q$, where $\psi^{(\Lambda)*}(x, \vec{k}_\perp + (1-x)\vec{q}_\perp)$ is large.

In region 1), $\vec{k}_\perp$ can be neglected in $\psi^{(\Lambda)*}(x, \vec{k}_\perp + (1-x)\vec{q}_\perp)$ until $|\vec{k}_\perp| \approx (1-x)Q$, at which point $\psi^{(\Lambda)}$ begins to cut off the $\vec{k}_\perp$ integration. Thus in region 1) we can approximate Eq. (70) by

$$e_q \int_0^1 dx\, \psi^{(\Lambda)*}(x, (1-x)\vec{q}_\perp) \int^{(1-x)Q} \frac{d^2\vec{k}_\perp}{16\pi^3}\, \psi^{(\Lambda)}(x, \vec{k}_\perp). \tag{71}$$

The bulk of the integral comes from $|\vec{k}_\perp| \ll (1-x)Q$. Similarly we obtain the following contribution from region 2):

$$e_q \int_0^1 dx \left\{ \int^{(1-x)Q} \frac{d^2\vec{k}_\perp}{16\pi^3}\, \psi^{(\Lambda)*}(x, \vec{k}_\perp) \right\} \psi^{(\Lambda)}(x, -(1-x)\vec{q}_\perp). \tag{72}$$

One can easily show that these approximations are valid to "leading-log" order—*i.e.* up to corrections of $\mathcal{O}(1/\log(Q^2))$—given that ψ falls off roughly as $1/\vec{k}_\perp^2$ in QCD.

Again as in the nonrelativistic case, we can use the bound-state equation for the valence wavefunction (*c.f.* , Eq. (32)) to further simplify these expressions by isolating the $\vec{q}_\perp$ dependence of the stressed wavefunctions. The equation for

$\psi^{(\Lambda)}(x,(1-x)\vec{q}_\perp)$ is

$$\psi^{(\Lambda)}(x,(1-x)\vec{q}_\perp) = \frac{1}{-\vec{q}_\perp^{\,2}(1-x)/x} \int_0^1 dy \int \frac{d^2\vec{l}_\perp}{16\pi^3} V_{\rm eff}(x,(1-x)\vec{q}_\perp; y, \vec{l}_\perp)\, \psi^{(\Lambda)}(y,\vec{l}_\perp) \tag{73}$$

where we have neglected masses in the energy denominator. As above the dominant contribution here is from $|\vec{l}_\perp| \ll (1-y)Q$, and so we can approximate this equation to leading-log order by

$$\psi^{(\Lambda)}(x,(1-x)\vec{q}_\perp) \approx \int_0^1 dy \, \frac{V_{\rm eff}(x,(1-x)\vec{q}_\perp; y, 0)}{-\vec{q}_\perp^{\,2}(1-x)/x} \int^{(1-y)Q} \frac{d^2\vec{l}_\perp}{16\pi^3}\, \psi^{(\Lambda)}(y,\vec{l}_\perp). \tag{74}$$

It is readily demonstrated that $V_{\rm eff}(x,(1-x)\vec{q}_\perp; y, 0)$ is free of mass singularities in light-cone gauge.#5 Consequently all loop momenta are of order Q or larger, and perturbation theory can be used to compute $V_{\rm eff}$. To leading order $V_{\rm eff}$ involves the exchange of a single gluon between the quark and antiquark.

Combining Eq. (74) with Eqs. (71) and (72) we arrive at a simple expression for the contribution to F_π coming from the disconnected part of T (Eq. (70)):

$$\int_0^1 dx \int_0^1 dy\, \phi_0^*(y,(1-y)Q)\, e_q\, T_H^{(a)}(x,y,Q)\, \phi_0(x,(1-x)Q). \tag{75}$$

Here the unrenormalized quark distribution amplitude ϕ_0 is defined by

$$\phi_0(x,Q) = \int^{Q^2} \frac{d\vec{k}_\perp^{\,2}}{16\pi^2}\, \psi^{(\Lambda)}(x,\vec{k}_\perp), \tag{76}$$

#5 Mass singularities do occur in $V_{\rm eff}(x,(1-x)\vec{q}_\perp; y, 0)$ when using covariant gauges. They arise because the external quarks that carry no transverse momentum in this amplitude are effectively on energy-shell. In most covariant gauges such a quark couples strongly to a nearly collinear gluon, resulting in an integral over the gluon's transverse momentum that is logarithmically sensitive to masses and other low-momentum scales: *e.g.* $\int d\vec{l}_\perp^{\,2}/(\vec{l}_\perp^{\,2} + \mathcal{O}(m^2))$. In light-cone gauge the coupling between a gluon and an on-shell quark vanishes as the gluon becomes collinear with the quark. This means there is an extra factor $\vec{l}_\perp/Q$ in the integral over the gluon's momentum $\vec{l}_\perp$, and thus the logarithmic dependence upon masses is removed. Indeed all contributions from $|\vec{l}_\perp| \ll Q$ are strongly suppressed. The only diagrams that lead to collinear singularities in light-cone gauge are ones in which a gluon is exchanged between two nearly on-shell quarks (or gluons) that are collinear with each other. Such diagrams do not contribute to $V_{\rm eff}$ since they are not two particle irreducible.

and the hard-scattering amplitude $T_H^{(a)}$ is given by

$$T_H^{(a)} = V_{\text{eff}}(x,(1-x)\vec{q}_\perp; y, 0)\frac{1}{-\vec{q}_\perp^{\,2}(1-x)/x} + (x \leftrightarrow y). \tag{77}$$

Note that $T_H^{(a)}$ comes from part of the LCPTh amplitude for $\gamma^* + q\bar{q} \to q\bar{q}$ (Fig. 12a).

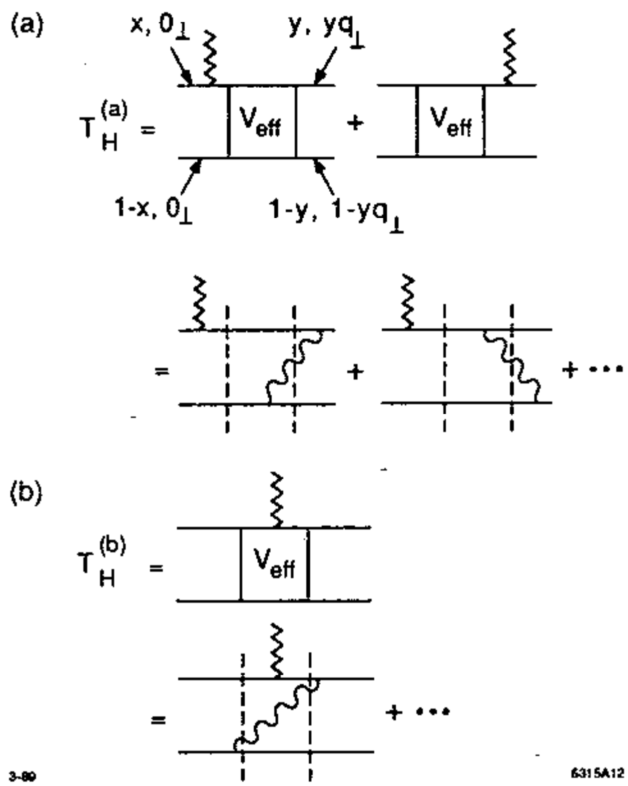

Figure 12. The unrenormalized hard-scattering amplitude for the pion form factor.

In addition to the disconnected parts, the connected part T_c of T contributes to Eq. (69) as $Q \to \infty$ (Fig. 11b). By the same reasoning used above, we can neglect $\vec{l}_\perp$ and $\vec{k}_\perp$ relative to $\vec{q}_\perp$ in T_c to obtain a formula that is identical to Eq. (75) but with $e_q T_H^{(a)}$ replaced by (Fig. 12b)

$$e_q T_H^{(b)} = \frac{T_c(x,0;y,0;\vec{q}_\perp)}{[x(1-x)y(1-y)]^{1/2}}. \tag{78}$$

Again T_c is free of mass singularities (in $A^+ = 0$ gauge) and can be computed perturbatively.

Still ignoring renormalization, the otherwise complete result is therefore

$$F_\pi^0(Q^2) \approx \int_0^1 dx \int_0^1 dy \Big\{ \phi_0^*(y,(1-y)Q)\, e_q\, T_H^0(x,y,Q)\, \phi_0(x,(1-x)Q) + \phi_0^*(y,yQ)\, e_{\bar{q}}\, T_H^0(1-x,1-y,Q)\, \phi_0(x,xQ) \Big\} \tag{79}$$

where we have now included contributions for the photon attaching to each of the quark and the antiquark. The unrenormalized hard-scattering amplitude in lowest order is given by

$$T_H^0(x,y,Q) = T_H^{(a)} + T_H^{(b)} = \frac{16\pi\, C_F\, \alpha_s(\Lambda^2)}{(1-x)(1-y)Q^2} \tag{80}$$

which is just the Born amplitude for a collinear $q\bar{q}$ pair to scatter with the virtual photon (divided by $[x(1-x)y(1-y)]^{1/2}$).

Finally we must consider the effects of vertex and propagator corrections in T_H (Fig. 13). Each of these corrections involves propagators off energy shell

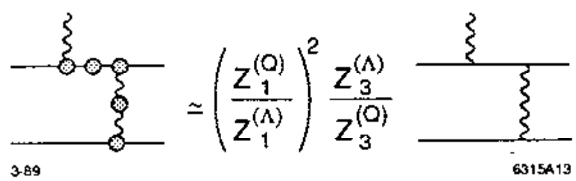

$$\simeq \left(\frac{Z_1^{(Q)}}{Z_1^{(\Lambda)}}\right)^2 \frac{Z_3^{(\Lambda)}}{Z_3^{(Q)}}$$

Figure 13. Vertex and propagator corrections to the hard-scattering amplitude.

by $\mathcal{O}(Q^2)$ and therefore all loop momenta are of order Q or larger (in $A^+ = 0$ gauge). It is then a straightforward consequence of renormalization theory that the propagators and vertices are modified only by the factors

$$\begin{aligned} &Z_i^{(\Lambda)}/Z_i^{(Q)} \text{ for propagators} \\ &Z_i^{(Q)}/Z_i^{(\Lambda)} \text{ for vertices} \end{aligned} \tag{81}$$

up to corrections of $\mathcal{O}(\alpha_s(Q^2))$, where $Z_i^{(\Lambda)}$ is the usual renormalization constant with ultraviolet cutoff Λ.#6 Thus in leading order T_H^0 is multiplied by (Fig. 13)

$$\left(\frac{Z_{1F}^{(Q)}}{Z_{1F}^{(\Lambda)}}\right)^2 \frac{Z_3^{(\Lambda)}}{Z_3^{(Q)}} = \left(\frac{Z_2^{(Q)}}{Z_2^{(\Lambda)}}\right)^2 \frac{\alpha_s(Q^2)}{\alpha_s(\Lambda^2)} \tag{82}$$

where $Z_{1F}^{(\Lambda)}$ renormalizes quark-gluon vertices, and $Z_2^{(\Lambda)}$ and $Z_3^{(\Lambda)}$ renormalize the quark and gluon propagators. Here we use the fact that α_s is renormalized by $Z_3(Z_2/Z_{1F})^2$—i.e. that $\alpha_s(\Lambda^2)Z_3^{(\Lambda)}(Z_2^{(\Lambda)}/Z_{1F}^{(\Lambda)})^2$ is independent of Λ. Also the photon-quark vertex correction in this amplitude cancels the quark-propagator correction by the QED Ward identity. So Eq. (79) is corrected to give

$$F_\pi(Q^2) \approx \int_0^1 dx \int_0^1 dy \, \{\phi^*(y,(1-y)Q)\, e_q\, T_H(x,y,Q)\, \phi(x,(1-x)Q) + (q \leftrightarrow \bar{q})\} \tag{83}$$

where now the leading-order hard-scattering amplitude is

$$T_H(x,y,Q) = \frac{16\pi\, C_F\, \alpha_s(Q^2)}{(1-x)(1-y)Q^2} \tag{84}$$

and the distribution amplitude is given by

$$\phi(x,Q) = \frac{Z_2^{(Q)}}{Z_2^{(\Lambda)}} \int^{Q^2} \frac{d\vec{k}_\perp^{\,2}}{16\pi^2}\, \psi^{(\Lambda)}(x,\vec{k}_\perp). \tag{85}$$

Since the bulk of the integral in Eq. (85) comes from $\vec{k}_\perp^{\,2} \ll Q^2$, we can use Eq. (49) to redefine

$$\varphi(x,Q) = \int \frac{d\vec{k}_\perp^{\,2}}{16\pi^2}\, \psi^{(Q)}(x,\vec{k}_\perp) \tag{86}$$

where now the $\vec{k}_\perp$ cutoff at $|\vec{k}_\perp| \sim Q$ is implicit in the definition of the wavefunction. Our equations now have the general form proposed in the introduction to this section.

#6 For example, the full unrenormalized quark propagator has the form $d_F(\Lambda/Q,\alpha_s(\Lambda^2))/(q\cdot\gamma)$ as $Q^2 = -q^2 \to \infty$. Since the quark is far off energy shell d_F is independent of masses in this limit. Furthermore the Λ dependence can be removed by dividing with the renormalization constant $Z_2^{(\Lambda)}$. Thus the quantity $d_F(\Lambda/Q,\alpha_s(\Lambda^2))/Z_2^{(\Lambda)}$ must equal $d_F(1,\alpha_s(Q^2))/Z_2^{(Q)}$, up to corrections of $\mathcal{O}(\alpha_s(Q))$ due to the fact that Λ/Q is not large in the second case. Since $d_F(1,\alpha_s(Q^2)) = 1 + \mathcal{O}(\alpha_s(Q^2))$, the final result is $d_F(\Lambda/Q,\alpha_s(\Lambda^2)) = Z_2^{(\Lambda)}/Z_2^{(Q)}$, again up to corrections of $\mathcal{O}(\alpha_s(Q^2))$.

The major effect of the renormalization corrections is to replace $\alpha_s(\Lambda^2)$ by $\alpha_s(Q^2)$ in the hard-scattering amplitude, and $\psi^{(\Lambda)}$ by $\psi^{(Q)}$ in the distribution amplitude. This is exactly what is expected on the basis of our earlier discussion of renormalization. The only physical scale in T_H is Q and so $\alpha_s(Q^2)$ is the natural expansion parameter. Furthermore T_H only probes structure in the wavefunctions down to distances of $\mathcal{O}(1/Q)$. Thus the wavefunction $\psi^{(Q)}$, defined in a theory with cutoff Q, incorporates hadronic structure over all distance scales relevant to the physical process. Structure at distances smaller than $1/Q$ is irrelevant except insofar as it determines $\alpha_s(Q^2)$, $m(Q)\ldots$.

The leading order result for T_H is consistent with the dimensional-counting prediction for the pion form factor: *i.e.* $T_H \sim 1/Q^2$ up to logarithms of Q. This rule also shows why it is that only the valence Fock state is relevant for large Q. For example, the hard-scattering amplitude for scattering a collinear $q\overline{q}q\overline{q}$ state has four additional partons and so must fall as $1/Q^6$; this amplitude has many more far off-shell ($\sim Q^2$) internal propagators than does the $q\overline{q}$ amplitude. The same is true of states with additional gluons provided that one is working in light-cone gauge.[#7]

4.2. The Quark Distribution Amplitude

Everything one needs to know about the pion in order to compute the asymptotic form factor is lumped into the quark distribution amplitude $\phi(x,Q)$.[4,2] Obviously ϕ is intrinsically nonperturbative. However its variation with Q can be studied in perturbation theory. To see this we differentiate Eq. (85) with respect to Q to obtain

$$Q\frac{\partial}{\partial Q}\phi(x,Q) = \frac{Z_2^{(Q)}}{Z_2^{(\Lambda)}}\,\frac{Q^2}{8\pi^2}\,\psi^{(\Lambda)}(x,\vec{q}_\perp) - \gamma_F(\alpha_s(Q^2))\,\phi(x,Q) \tag{87}$$

#7 A hard-scattering amplitude with additional gluons can contribute to leading order in $1/Q$ when covariant gauges are used. For example, adding a single gluon to the $q\overline{q}$ hard scattering amplitude introduces one additional denominator of $\mathcal{O}(Q^2)$. In addition there is typically a numerator factor of $\mathcal{O}(\varepsilon\cdot q)$, where ε is the gluon's polarization vector. So such an amplitude is suppressed by $\varepsilon\cdot q/Q^2 \sim 1/Q$ in light-cone gauge where $\varepsilon^+ = 0$. However other gauges can have $\varepsilon\cdot q \approx \varepsilon^+ q^- \sim Q^2$, in which case the amplitude with an additional gluon is not suppressed at all.

where γ_F is the anomalous dimension associated with Z_2—

$$
\begin{aligned}
Q\frac{d}{dQ}Z_2^{(Q)} &= -\gamma_F(\alpha_s(Q^2))\,Z_2^{(Q)} \\
&= -\left\{\frac{C_F\,\alpha_s(Q^2)}{\pi}\int_0^1 dy\,\frac{1+(1-y)^2}{y} + \mathcal{O}(\alpha_s^2)\right\} Z_2^{(Q)}.
\end{aligned}
\tag{88}
$$

(The singularity at $y=0$ in this equation cancels in the final result because the meson is a color singlet.) The first term in Eq. (87) represents the change in the probability amplitude ϕ due to the addition of more $q\bar{q}$ states as the cutoff Q is increased, while the second term represents the loss of probability from those already present, as $Z_2^{(Q)}$ decreases. By using the bound-state equation as in Eq. (74), we can express $\psi^{(\Lambda)}(x,\vec{q}_\perp)$ in terms of $\phi(x,Q)$. To leading order we need only consider one-gluon exchange between the quark and antiquark, and this gives (Fig. 14)

$$
\frac{Z_2^{(Q)}}{Z_2^{(\Lambda)}}\,\psi^{(\Lambda)}(x,\vec{q}_\perp) = \frac{4\pi\,\alpha_s(Q^2)}{\vec{q}_\perp^{\,2}}\int_0^1 dy\,\frac{\widetilde{V}(x,y)}{y(1-y)}\,\phi(y,Q) \tag{89}
$$

where again $\alpha_s(\Lambda^2)$ is converted to $\alpha_s(Q^2)$ by propagator and vertex corrections. Substituting into Eq. (87) we obtain finally the leading-order evolution equation[4]

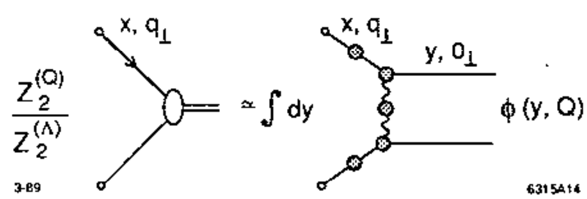

Figure 14. The $q\bar{q}$ wavefunction for $\vec{q}_\perp^{\,2} = Q^2$ large.

for ϕ:

$$
Q\frac{\partial}{\partial Q}\phi(x,Q) = \frac{\alpha_s(Q^2)}{4\pi}\left\{\int_0^1 dy\,\frac{V(x,y)}{y(1-y)}\,\phi(y,Q) - 2\phi(x,Q)\right\} \tag{90}
$$

where the evolution potential is

$$V(x,y) = 4C_F \left\{ x(1-y)\,\theta(y-x)\left(\delta_{-h,\bar{h}} + \frac{\Delta}{y-x}\right) + \begin{pmatrix} x \leftrightarrow 1-x \\ y \leftrightarrow 1-y \end{pmatrix} \right\} = V(y,x). \tag{91}$$

Operator Δ in the potential is defined by

$$\Delta \frac{\phi(y,Q)}{y(1-y)} \equiv \frac{\phi(y,Q)}{y(1-y)} - \frac{\phi(x,Q)}{x(1-x)}. \tag{92}$$

Also h and $\bar{h}$ are the helicities of the quark and antiquark ($\delta_{-h,\bar{h}} = 1$ for pions).

The evolution equation completely specifies the Q dependence of $\phi(x,Q)$: given $\phi(x,Q_0)$, $\phi(x,Q)$ is determined for any other Q by integrating this equation, numerically or otherwise. Still it is instructive to exhibit explicitly the most general Q dependence. Using the symmetry $V(x,y) = V(y,x)$ to diagonalize V, the general solution of Eq. (90) is easily shown to be[#8]

$$\phi(x,Q) = x(1-x)\sum_{n=0}^{\infty} a_n\, C_n^{3/2}(2x-1)\left(\log\frac{Q^2}{\Lambda_{QCD}^2}\right)^{-\gamma_n/2\beta_0}. \tag{93}$$

where[#9]

$$\gamma_n = 2C_F\left\{1 + 4\sum_{k=2}^{n+1}\frac{1}{k} - \frac{2\delta_{-h,\bar{h}}}{(n+1)(n+2)}\right\} \geq 0. \tag{94}$$

By combining the orthogonality condition for the Gegenbauer polynomials and the operator definition of ϕ (Eq. (64)), we obtain an interpretation for the ex-

#8 The evolution potential $V(x,y)$ can be treated as an integral operator. Being symmetric it has real eigenvalues $\tilde{\gamma}_n$ and eigensolutions $\phi_n(y)$ that satisfy $\int dy\, V(x,y)\, w(y)\, \phi_n(y) = \tilde{\gamma}_n\, \phi_n(x)$ where integration weight $w(y) \equiv 1/(y(1-y))$. The eigensolutions must be orthogonal with respect to weight $w(x)$, from which it immediately follows that $\phi_n(x) \propto x(1-x)\, C_n^{3/2}(2x-1)$ where $C_n^{3/2}$ is a Gegenbauer polynomial. It is a straightforward exercise to now extract analytic expressions for the eigenvalues. Given the eigenvalues a general solution of the evolution equation can be written down as an expansion on the complete set of eigensolutions, as we do here.

#9 Note that Λ_{QCD} is the scale appearing in the running coupling constant; it has *nothing* to do with the ultraviolet cutoff Λ. Recall also that $C_F = 4/3$ and $\beta_0 = 11 - 2n_f/3$ where n_f is the number of quark flavors.

pansion constants in Eq. (93):

$$a_n \left(\log \frac{Q^2}{\Lambda_{QCD}^2}\right)^{-\gamma_n/2\beta_0} = \frac{4(2n+1)}{(2+n)(1+n)} \int_0^1 dx\, C_n^{3/2}(2x-1)\,\phi(x,Q)$$
$$= \frac{4(2n+3)}{(2+n)(1+n)} \langle 0|\,\overline{\psi}\,\frac{\gamma^+\gamma_5}{2\sqrt{2n_c}}\,C_n^{3/2}(\overleftrightarrow{D}^+)\,\psi\,|\pi\rangle^{(Q)} \tag{95}$$

—the a_n's are just matrix elements of local operators.

This analysis shows that the distribution amplitude can be expressed as a sum of matrix elements of local (twist-two) operators.[11,12] This sum is just the operator-product expansion of the operator $\overline{\psi}(0)\gamma^+\gamma_5\psi(z)$ in Eq. (64). Such an expansion is warranted since the separation between the fields is very nearly on the light cone: $z^2 = z^+z^- - \vec{z}_\perp^2 = \mathcal{O}(1/Q^2)$. The Gegenbauer polynomials also appear very naturally in this context, as a consequence of the residual conformal symmetry of QCD at short distances. All of the dimensionful couplings in the QCD lagrangian can be dropped at very short distances, and so the classical theory (*i.e.* tree order in perturbation theory) becomes invariant under conformal mappings of the space-time coordinates. This conformal symmetry is destroyed in the quantum field theory by renormalization, which necessarily introduces a dimensionful parameter such as the cutoff Λ. However the evolution potential for ϕ is given by tree diagrams in leading order, and so the leading-order potential ought still to be consistent with the requirements of conformal symmetry. One such requirement is that local operators that are multiplicatively renormalizable must transform irreducibly under conformal transformations. In the case of meson operators conformal symmetry is enough by itself to uniquely specify the structure of the these local operators. As these are the operators that appear in the operator-product expansion, conformal symmetry completely specifies the structure of the expansion for ϕ. These ideas do not easily generalize beyond leading order.[13]

The operator-product analysis of the distribution amplitude suggests an important constraint on ϕ. The $n = 0$ Gegenbauer moment of the distribution amplitude is proportional to the amplitude for pion decay (*c.f.* Eq. (55)):

$$\int_0^1 dx\, \phi(x,Q) = \frac{f_\pi}{2\sqrt{n_c}}. \tag{96}$$

Given the shape of $\phi(x,Q)$ this equation normalizes it for any Q. Note that the value of this moment is Q independent. This is because the $n = 0$ operator is just the axial-vector current operator. As far as its ultraviolet behavior is concerned, this operator is conserved and so its anomalous dimension vanishes: $\gamma_{n=0} = 0$. Notice also that $\gamma_n > 0$ for all other n. Thus only the $n = 0$ term in the expansion of $\phi(x, Q)$ survives when Q becomes infinite:

$$\phi(x, Q) \to \frac{3f_\pi}{\sqrt{n_c}} x(1-x) \qquad \text{as } Q \to \infty. \tag{97}$$

So $\phi(x, Q)$ is completely determined for pions when Q is very, very large.

Notice finally from Eq. (89) that $\psi^{(\Lambda)}(x, \vec{q}_\perp)$ does in fact fall as $1/\vec{q}_\perp^{\,2}$, up to logarithms, as $\vec{q}_\perp$ grows. The high-momentum or short-distance behavior of the Fock-state wavefunctions is perturbative in nature, and as a general rule is crudely that of simple Born amplitudes in light-cone perturbation theory. In particular wavefunctions are *not* exponentially damped at large $\vec{q}_\perp$, as is frequently assumed in phenomenological studies.

4.3. Determination of Distribution Amplitudes

Large-$p_\perp$ exclusive processes, like most other high-energy processes, involve physics both at short distances and at long distances. A special feature of the large-$p_\perp$ processes is that we are able to separate short from long distance physics in a relatively simple fashion. This allows us to analyze each regime separately, using the tools best suited to that regime. The hard-scattering amplitudes and the evolution potentials for distribution amplitudes embody the short-distance physics; they are most effectively analyzed using perturbation theory. However perturbation theory is largely useless for determining anything about the distribution amplitudes beyond their Q-dependence. The distribution amplitudes contain the long-distance physics of a large-$p_\perp$ process, and as such require some sort of nonperturbative treatment.

Given that the distribution amplitude is intrinsically nonperturbative one might wonder whether it isn't just as well to treat the entire process nonperturbatively. This is generally a very bad idea. Any nonperturbative analysis of a large-$p_\perp$ process would have to deal accurately with QCD dynamics over a huge range of momentum scales—*e.g.* a vast grid would be required in lattice QCD if one wanted to accommodate both the relatively small momenta that characterize hadronic structure and the very large momenta transferred in the process. Such an analysis would be very inefficient. Instead we can use our renormalization-group analysis to "divide and conquer" the problem in pieces. First we compute the distribution amplitude $\phi(x, Q_0)$ for some small Q_0, of order a few GeV, using a nonperturbative technique. The range of relevant momentum scales is quite modest for this part of the analysis. Then we use the perturbative evolution equations to evolve $\phi(x, Q)$ out to the large values of Q characteristic of the process. The evolution equations build up the short-distance structure of the hadronic wavefunction and are trivial to apply. Finally we combine the distribution amplitudes with the hard-scattering amplitude, which incorporates (perturbatively) the short-distance structure particular to the process.

We can illustrate the nonperturbative analysis of distribution amplitudes with a brief discussion of two such analyses, one using lattice QCD[14,15] and the other QCD sum rules.[16] Both methods are based upon the behavior of matrix elements of the form $\langle 0|\, T\, \Gamma_i(0)\, \Gamma_j(t)\, |0\rangle^{(Q_0)}$ where each $\Gamma_i(t)$ is the spatial average of a local operator like those in Eq. (95):

$$\Gamma_i(t) \equiv \frac{1}{V} \int_V d^3\vec{x}\, \Gamma_i(\vec{x}, t). \tag{98}$$

By inserting a complete set $\{|n\rangle\}$ of hadronic eigenstates between the two operators it is easy to see that

$$\langle 0|\, \Gamma_i(t)\, \Gamma_j(0)\, |0\rangle^{(Q_0)} = \sum_n \langle 0|\, \Gamma_i(0)\, |n\rangle^{(Q_0)}\ \langle n|\, \Gamma_j(0)\, |0\rangle^{(Q_0)}\ e^{-iE_n t} \tag{99}$$

when $t > 0$. The matrix elements multiplying the exponential in the sum are precisely those that determine the moments of the distribution amplitude for state $|n\rangle$.

In the lattice analysis ordinary time is analytically continued to euclidean time so that $it \to t$, and the cutoff Q_0 is determined by the lattice spacing. The matrix element in Eq. (99) is computed for large t. The sum is then dominated by the lowest mass state $|n_0\rangle$ that couples both to Γ_i and Γ_j—*e.g.* the pion for operators taken from Eq. (95)—and so for sufficiently large t the expectation value has the form

$$\langle 0|\, \Gamma_i(t)\, \Gamma_j(0)\, |0\rangle^{(Q_0)} \to \langle 0|\, \Gamma_i(0)\, |n_0\rangle^{(Q_0)}\ \langle n_0|\, \Gamma_j(0)\, |0\rangle^{(Q_0)}\ e^{-M_0 t} \tag{100}$$

where M_0 is the mass of state $|n_0\rangle$. The moments of the distribution amplitude for the lowest-lying state can be read off directly from the large-t behavior of the $\Gamma_i\, \Gamma_j$-amplitude.

QCD sum rules[16] can be derived for the Fourier transform of the matrix element,

$$I_{ij}(q^2) = \int dt\, e^{iqt}\, \langle 0|\, \Gamma_i(t)\, \Gamma_j(0)\, |0\rangle^{(Q_0)}, \tag{101}$$

analytically continued deep into the euclidean region $q^2 < 0$. Amplitude $I_{ij}(q^2)$ can be computed in two ways as $q^2 \to -\infty$. First, since the two operators are forced together in this limit, the operator product expansion can be used to relate the amplitude to vacuum expectation values of such local operators as $\alpha_s F_{\mu\nu}^2$ and $\sqrt{\alpha_s}\,\overline{u}u$. These matrix elements are universal and their values are usually inferred from other processes. On the other hand, the spectral decomposition Eq. (99) can be used to relate $I_{ij}(q^2)$ to the moments of the distribution amplitudes for hadronic states $|n\rangle$. In practice the sum over hadronic states is replaced by a sum over a few low lying hadrons together with a continuum contribution approximated by the formula for free quarks, the threshold being a tunable parameter of the model. The moments are extracted by fitting the spectral formula for $I_{ij}(q^2)$ to its operator product expansion.[#10]

Each of these methods currently suffers from large systematic uncertainties and so one must be cautious in accepting results derived using them. Nevertheless such results form a reasonable starting point for phenomenological studies. Furthermore these methods have played an important role in alerting us to the potential complexity of hadronic distribution amplitudes. For example, one might have expected a relatively smooth distribution amplitude for the pion, not too different perhaps from its asymptotic form $x(1-x)$. However the sum rules, for example, seem to imply a double-humped distribution $x(1-x)(2x-1)^2$. The sum rule predictions for baryons are even more remarkable—*e.g.* 65% of the proton momentum is carried by the u-quark with helicity parallel to the proton, while the remaining quarks split the remainder in this model. It is unclear how seriously one should take such predictions, but it is clear that unusual x-dependence is a distinct possibility for hadronic distribution amplitudes. It is also clear that the reliability of the these nonperturbative techniques, particularly the lattice analysis, will improve substantially in the not-too-distant future.

Note finally that it was essential for our nonperturbative calculations that the distribution amplitude have a nonperturbative definition—*i.e.* in terms of operator matrix elements in a cut off field theory. Had the distribution amplitude been

---

#10 In actual practice this procedure is modified to employ a Borel transform so as to de-emphasize the high-mass region.

defined in terms of perturbative constructs, it would have been almost impossible to carry that definition over into a nonperturbative framework such as that provided by lattice QCD. In general it is important to provide a nonperturbative characterization for the contributions omitted from the perturbative analysis of a process.

4.4. Higher Order Analysis

The leading-order formula for the asymptotic pion form factor results from a series of approximations. One can systematically undo these approximations to obtain[17,18] $\mathcal{O}(\alpha_s(Q^2))$ corrections to $F_\pi(Q^2)$. For example in our leading-order analysis of the disconnected contribution

$$e_q \int_0^1 dx \int \frac{d^2\vec{k}_\perp}{16\pi^3}\, \psi^{(\Lambda)*}(x, \vec{k}_\perp + (1-x)\vec{q}_\perp)\, \psi^{(\Lambda)}(x, \vec{k}_\perp) \tag{102}$$

we assumed that large transverse momentum flows through one or the other wavefunction. We ignored the contribution from the region where large momentum flows through both wavefunctions: $\vec{k}_\perp \sim \vec{k}_\perp + (1-x)\vec{q}_\perp \sim (1-x)\vec{q}_\perp$. The contribution from the latter region is easily estimated. We can use the bound state equation to replace both wavefunctions by a convolution of the perturbative potential with the distribution amplitude (Eq. (74)) to obtain a contribution

$$\int_0^1 dy \int_0^1 dz\, \phi_0^*(z, (1-z)Q)\, T_2(y, z, Q)\, \phi_0(y, (1-y)Q). \tag{103}$$

where

$$T_2(y,z,Q) = \int_0^1 dx \int \frac{d^2\vec{k}_\perp}{16\pi^3}\, \frac{V_{\text{eff}}(z, 0; x, \vec{k}_\perp + (1-x)\vec{q}_\perp)}{-(\vec{k}_\perp + (1-x)\vec{q}_\perp)^2/x(1-x)}\, e_q\, \frac{V_{\text{eff}}(x, \vec{k}_\perp; y, 0)}{-\vec{k}_\perp^2/x(1-x)}.$$

The $\vec{k}_\perp$ integration in this expression must be restricted to the region where both $\vec{k}_\perp$ and $\vec{k}_\perp + (1-x)\vec{q}_\perp$ are large, because the contributions from the regions where one or the other vector is small are already included in the leading-order result. One way to restrict the range of $\vec{k}_\perp$ is to introduce collinear subtractions that remove precisely the contribution included in the leading-order analysis. The region where $\vec{k}_\perp$ is small is removed by subtracting

$$T_2^{s1}(y,z,Q) = \int_0^1 dx \int^{(1-x)Q} \frac{d^2\vec{k}_\perp}{16\pi^3} \frac{V_{\text{eff}}(z,0;x,(1-x)\vec{q}_\perp)}{-((1-x)\vec{q}_\perp)^2/x(1-x)}\, e_q\, \frac{V_{\text{eff}}(x,\vec{k}_\perp;y,0)}{-\vec{k}_\perp^2/x(1-x)}. \tag{104}$$

where we neglect $\vec{k}_\perp$ relative to $(1-x)\vec{q}_\perp$ and integrate over $|\vec{k}_\perp| < (1-x)Q$, just as in the leading-order analysis (*c.f.* , Eq. (71)). Similarly the region where $\vec{k}_\perp + (1-z)\vec{q}_\perp$ is small is removed by

$$T_2^{s2}(y,z,Q) = \int_0^1 dx \int^{(1-x)Q} \frac{d^2\vec{k}_\perp}{16\pi^3} \frac{V_{\text{eff}}(z,0;x,\vec{k}_\perp)}{-\vec{k}_\perp^2/x(1-x)}\, e_q\, \frac{V_{\text{eff}}(x,-(1-x)\vec{q}_\perp;y,0)}{-((1-x)\vec{q}_\perp)^2/x(1-x)}. \tag{105}$$

where we have changed variables so that $\vec{k}_\perp + (1-x)\vec{q}_\perp \to \vec{k}_\perp$. The subtracted amplitude (Fig. 15a) contains only large momenta when Q is large, and thus it can be computed perturbatively and gives an $\mathcal{O}(\alpha_s^2(Q^2))$ contribution to the hard-scattering amplitude T_H. All masses can be neglected, and no logarithms of Q can arise from the $\vec{k}_\perp$-integration since Q is the only scale left after the subtractions.

A similar analysis can be applied to the bound state equation to obtain higher order corrections to the formula relating the high-$\vec{q}_\perp$ wavefunction and the distribution amplitude (Eq. (74)). These corrections lead to additional $\mathcal{O}(\alpha_s^2)$ contributions to T_H (Fig. 15b), and to $\mathcal{O}(\alpha_s^2)$ contributions to the evolution potential V. In addition to these higher-order corrections, there are corrections coming from the one-loop (and higher) $q\bar{q}$-irreducible diagrams, both for T_H (Fig. 15c) and for V. As discussed in earlier sections, these irreducible amplitudes have no sensitivity to low momenta when they are computed in light-cone gauge, and thus they are perturbative when Q is large.

This procedure can iterated to produce still higher-order corrections to the hard-scattering amplitude and to the evolution potential. In this way one establishes the self-consistency of the factored perturbative result to all orders in perturbation theory. The only complication arises when endpoint and/or pinch singularities appear in the hard-scattering amplitude, and these we discuss in the next section.

A systematic analysis of higher order corrections, based upon Mueller's cut-vertex formalism, has been given in Ref. 19. Using this method, the validity of the perturbative expression for the meson form factor has been established to all

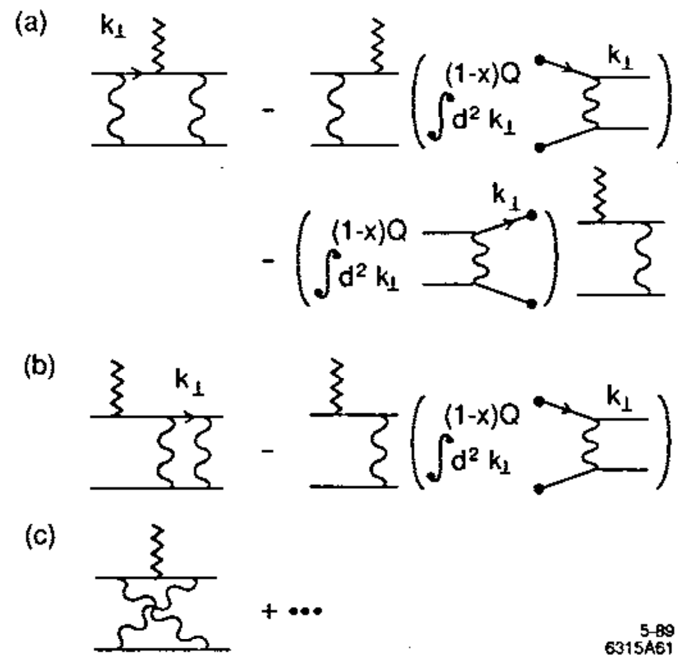

Figure 15. Diagrams contributing to the second-order hard-scattering amplitude for the pion form factor.

orders in perturbation theory. The one-loop corrections have also been calculated for the meson form factor.[17,18]

4.5. Complications

The perturbative analysis of large-$p_\perp$ processes relies upon the fact that the hard subprocess is confined to a small volume near the light-cone. This is a consequence not of the kinematics of the process but rather of the dynamical behavior of the hard-scattering amplitude T_H, all of whose internal propagators are typically far off shell ($|\mathcal{E}| \sim Q^2$). Unfortunately the x integrations in the perturbative formula can include points where internal lines in T_H go on shell. In form factors these points show up as singularities in T_H at the endpoints of the integration—*i.e.* $x = 0$ or $x = 1$—and so they are referred to as endpoint singularities.[19] Singularities can also occur at intermediate values of x in hard-scattering amplitudes for hadronic scattering amplitudes;[20] these are referred to as pinch singularities.[#11] Perturbation theory breaks down in the vicinity of such

#11 In the covariant calculation of a Feynman amplitude every internal propagator has singular points. Usually these singularities are avoided by deforming the integration contours into the complex momentum plane. A singularity that occurs at the endpoint of a consingularities, and so our perturbative results are jeopardized if large contributions come from such regions.

Remarkably it is just in the endpoint[19,4] and pinch regions[21] that Sudakov form factors appear. In these regions individual quarks (or gluons) tend to scatter independently of the other partons comprising the hadrons. An isolated, nearly on-shell quark wants to radiate gluons when it scatters, the amount of radiation increasing as the change in the quark's state of motion becomes more drastic. In an exclusive process such *bremsstrahlung* is prohibited, and as a result the amplitude is suppressed. This phenomenon is apparent in perturbation theory. For example, in computing the electromagnetic form factor of a single quark one obtains double logarithms of Q^2 coming from the radiative corrections to the quark-photon vertex. These exponentiate when summed to all orders to give a quark form factor that ultimately falls faster than any power of $1/Q$. This is the Sudakov form factor. Such form factors tend to suppress contributions coming from the endpoint and pinch regions.

Note that double logarithms of Q and Sudakov form factors only appear in the vicinity of singularities in T_H. In other regions all of the constituents of each hadron are involved in the same hard subprocess. The collinear bunches of partons representing each hadron in T_H carry no color charge, and thus the soft gluons that normally build up Sudakov form-factors decouple.

In this section we examine the contributions coming from the endpoint and pinch regions. We show where these contributions come from and why Sudakov suppression is expected.

Endpoint Singularities

Our analysis of the $q\overline{q}$ contribution to $F_\pi(Q^2)$ for large Q^2 depends upon the assumption that either $\vec{k}_\perp$ or $\vec{k}_\perp + (1-x)\vec{q}_\perp$ is $\mathcal{O}(\vec{q}_\perp)$ in the overlap integral

$$e_q \int_0^1 dx \int \frac{d^2\vec{k}_\perp}{16\pi^3}\, \psi^{(\Lambda)*}(x, \vec{k}_\perp + (1-x)\vec{q}_\perp)\, \psi^{(\Lambda)}(x, \vec{k}_\perp) \tag{106}$$

—*i.e.* that large momentum flows through one or the other of the wavefunctions. This is certainly the case except in the infinitesimal region where

$$1 - x \sim \lambda/Q \tag{107}$$

if λ is the typical transverse momentum in the wavefunction. Within this "end-

tour obviously cannot be avoided in this fashion; this is how endpoint singularities arise in exclusive amplitudes. In addition it is possible for a contour to be trapped or pinched between two singularities. This is how pinch singularities arise.

point region" both wavefunctions carry small transverse momentum ($\sim \lambda$). The meson form factor receives a contribution from this region of order

$$F_{EP}(Q^2) \sim \int_{1-\frac{\lambda}{Q}}^{1} dx\, |\psi^{(\Lambda)}(x,\lambda)|^2 \sim \left(\frac{\lambda}{Q}\right)^{1+2\delta} \tag{108}$$

when $\psi^{(\Lambda)}(x,\lambda)$ vanishes like $(1-x)^\delta$ as $x \to 1$. This mechanism, in which spectator quarks are stopped rather than turned, was actually the first parton model suggested for hadronic form factors. To assess its importance here we require information about the $q\overline{q}$ wavefunction as $x \to 1$.[#12] The $q\overline{q}$ state in the pion is far off shell in the endpoint region—

$$|\mathcal{E}| \sim \frac{\lambda^2}{x(1-x)} \sim \lambda Q \tag{109}$$

—suggesting that perturbation theory might be a reasonable guide to the behavior of the wavefunction (Fig. 16). Perturbation theory implies $\delta = 1$ and thus the

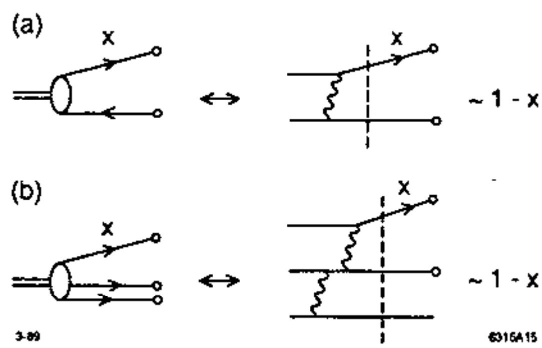

Figure 16. Born amplitudes whose behavior might be similar to that of the hadronic wavefunctions as $x \to 1$.

endpoint contributions fall as $(\lambda/Q)^3$, down by a full power of λ/Q relative to the hard-scattering contributions.

#12 We consider only the valence Fock state here since the phase space in the case of n spectator partons goes like $(\lambda/Q)^n$—small numbers of spectators are favored.

The analysis is similar for baryon form factors where

$$F_{EP}(Q^2) \sim \int_{1-\frac{\lambda}{Q}}^{1} dx_1 \int_{0}^{\lambda/Q} dx_2 \, |\psi^{(\Lambda)}(x_i,\lambda)|^2 \sim \left(\frac{\lambda}{Q}\right)^{2+2\delta} . \tag{110}$$

Perturbation theory again gives $\delta = 1$, but here the endpoint contribution seems to be suppressed by only two powers of $\alpha_s(\lambda Q)$ relative to the hard scattering prediction:

$$F_{EP} \sim \frac{\alpha_s^4(\lambda Q)}{Q^4} \sim \alpha_s^2(\lambda Q)\, F_{HS}. \tag{111}$$

Endpoint singularities are far more severe in the nucleon form factor than they are in the meson form factor. In general they are equally severe in more complicated process, such as hadron-hadron scattering.

In fact the suppression of the endpoint region is probably a good deal stronger than these equations indicate. As far as the photon is concerned the struck quark is very nearly on shell in the endpoint region since $|\mathcal{E}| \sim \lambda Q \ll Q^2$. Furthermore only the struck quark participates in the hard subprocess in this region; it behaves as though isolated from the other quarks over time scales of $\mathcal{O}(1/\sqrt{\lambda Q})$. Consequently the endpoint contribution to the amplitude is suppressed by a Sudakov form factor, and most likely is negligible when Q is sufficiently large.

Pinch Singularities

The pinch singularity[20,21,22] is most serious in hadron-hadron scattering. As an illustration consider the diagram in Fig. 17a, which contributes to π-π scattering. Three-momentum conservation requires

$$\begin{aligned} x_a + x_b &= x_c + x_d \\ \vec{k}_{\perp a} + \vec{k}_{\perp b} - \vec{k}_{\perp c} - \vec{k}_{\perp d} &= (x_c - x_a)\vec{r}_\perp \,+\, (x_d - x_a)\vec{q}_\perp \end{aligned} \tag{112}$$

where $\vec{k}_{\perp a} \ldots \vec{k}_{\perp d}$ are the transverse momenta appearing in the wavefunctions for each of the pions, $x_a \ldots x_d$ are the longitudinal momenta, and where the relativistic invariants for the process are

$$\begin{aligned} s &= \vec{r}_\perp^{\,2} + \vec{q}_\perp^{\,2} \\ t &= -\vec{q}_\perp^{\,2} \\ u &= -\vec{r}_\perp^{\,2} \end{aligned} \tag{113}$$

with $\vec{r}_\perp \cdot \vec{q}_\perp = 0$. At high energies and wide angles, $\vec{r}_\perp^{\,2}$ and $\vec{q}_\perp^{\,2}$ are both large, and so at least one of $\vec{k}_{\perp a} \ldots \vec{k}_{\perp d}$ must be large for most values of $x_a \ldots x_d$. Then, as in our analysis of the meson form factor, the wavefunction with large $\vec{k}_\perp$ is replaced by a gluon exchange to give a hard-scattering amplitude, as depicted in Fig. 17b (where $\vec{k}_{\perp a}$ is large). Dimensional counting then implies

$$T_H \sim \frac{\alpha_s^3}{s^2} f(\theta_{CM}; x_a \ldots x_d) \tag{114}$$

for this contribution. Also the energy denominator in D in Fig. 17a,

$$D = (x_c - x_a)\vec{r}_\perp^{\,2} + (x_d - x_a)\vec{q}_\perp^{\,2} + 2(\vec{k}_{\perp d} - \vec{k}_{\perp a})\cdot\vec{q}_\perp + 2(\vec{k}_{\perp c} - \vec{k}_{\perp a})\cdot\vec{r}_\perp + \ldots + i\epsilon, \tag{115}$$

is of $\mathcal{O}(s)$ indicating that the two quark-quark scatterings occur within a very short time of each other.

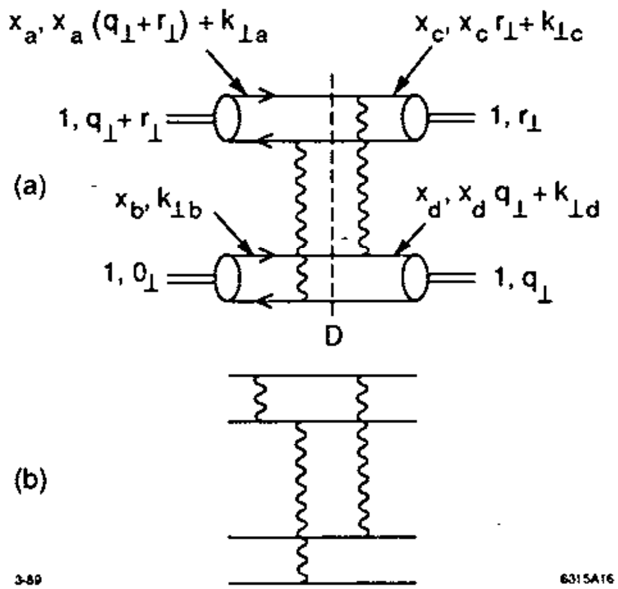

Figure 17. a) Diagram contributing to π-π scattering. b) Hard scattering amplitude coming from a).

Notice however that in the pinch region,

$$|x_c - x_a| \sim \frac{\lambda}{|\vec{r}_\perp|} \qquad |x_d - x_a| \sim \frac{\lambda}{|\vec{q}_\perp|}, \tag{116}$$

all wavefunction momenta $\vec{k}_{\perp a} \ldots \vec{k}_{\perp d}$ can be small ($\sim \lambda$). Furthermore the denominator D is $\mathcal{O}(\lambda\sqrt{s})$ or less, and can even vanish. Thus the two quark-quark scatterings can occur more or less independently, at widely separated points. The scattering process is no longer localized, and factorization does not occur. The s dependence of the contribution from this region can be readily estimated: a) the quark-quark scattering amplitudes each give $(1/s)^0$, by dimensional counting; b) phase space as restricted by in Eq. (116) gives a factor $(\lambda/\sqrt{s})^2$; c) the energy denominator gives a factor $1/D \sim 1/\lambda\sqrt{s}$. Thus the pinch region contributes

$$T_{PS} \sim \frac{1}{s^{3/2}}\, f(\theta_{CM}; x_a) \tag{117}$$

which apparently dominates the hard scattering contribution by a factor $\sqrt{s}$.

Two things work to suppress this pinch contribution. First the number of hard scattering amplitudes is much larger than the number of pinch singularity diagrams. More importantly, perhaps, radiative corrections to the individual quark-quark amplitudes build up Sudakov form factors that increase the effective power of $1/s$ to something like

$$\frac{3}{2} + \frac{4\,C_F}{\beta}\,\log\log\left(\frac{|t|}{\lambda^2}\right) \tag{118}$$

which grows infinitely large as $|t| \sim s \to \infty$. These corrections do not cancel here because the quarks and antiquarks scatter separately here, and not together as color singlets. So the pinch region is probably completely suppressed by Sudakov effects when s is sufficiently large. It turns out that a contribution still remains from a region intermediate between the pinch region and the hard-scattering region.[21] This results in a small correction to the power-law predicted by dimensional counting. For example, pp elastic scattering at wide angles should fall off roughly like $s^{-9.7}$, rather than s^{-10} as predicted by dimensional counting. Considerable progress has been made recently towards a complete analysis of such effects.[23]

Pinch singularities always show up as singularities in the hard scattering amplitude $T_H(x_a, x_b \ldots, Q)$ at points $x_a, x_b \ldots$ away from the endpoints 0 and 1. The integrals over $x_a, x_b \ldots$ are then singular. Not every midpoint singularity in T_H actually corresponds to a pinch. For example, singularities that are linear—*e.g.* $1/(x - c + i\epsilon)$—do not involve pinches. These cause no problems when integrating over x: the real part of the amplitude is obtained using a principal value prescription, while an imaginary part is generated by making the replacement $1/(x - c + i\epsilon) \to -2\pi i\delta(x - c)$. When the singularities are more severe they must be cut off by explicitly including Sudakov form factors in the pinch region. The dimensional-counting rule is modified only in these very singular situations.

4.6. How Large is Asymptotic Q?

The perturbative formalism we have described is only valid at large momentum transfers. A critical question[24] then is, How large is large? Here as in any application of perturbative QCD there are really two issues: 1) the convergence of perturbation theory; and 2) the relative importance of competing nonperturbative mechanisms. We examine each in term.

The perturbative expansion describing a short-distance process in QCD—e.g. $a_0+a_1\,\alpha_s(Q^2_{\rm eff})/\pi+\ldots$—converges quickly if the characteristic momentum $Q_{\rm eff}$ for the process is large compared with the QCD scale parameter $\Lambda_{QCD}\sim 200$ Mev. To determine $Q_{\rm eff}$ for large-$p_\perp$ exclusive processes we can examine the momentum flow in the hard-scattering amplitude. The pion's form factor, for example, is given by

$$F_\pi(Q^2)\approx\int_0^1 dx\int_0^1 dy\,\{\phi^*(y,(1-y)Q)\,e_q\,T_H(x,y,Q)\,\phi(x,(1-x)Q)+(q\leftrightarrow\overline{q})\}\tag{119}$$

where the hard-scattering amplitude is

$$T_H(x,y,Q)=\frac{16\pi\,C_F\,\alpha_s}{(1-x)(1-y)Q^2}.\tag{120}$$

The running coupling in T_H is associated with gluon-exchange between the quark and the antiquark as they scatter from the initial to the final direction. Thus it is natural to set the scale of this coupling equal to the square of the gluon's four momentum: $\alpha_s\to\alpha_s((1-x)(1-y)Q^2)$ in T_H.[#13] The defining relation for $Q_{\rm eff}$ then is obviously

$$\int_0^1 dx\int_0^1 dy\,\phi^*\,\frac{\alpha_s((1-x)(1-y)Q^2)}{(1-x)(1-y)}\,\phi=\int_0^1 dx\int_0^1 dy\,\phi^*\,\frac{\alpha_s(Q^2_{\rm eff})}{(1-x)(1-y)}\,\phi.\tag{121}$$

A small complication is that the usual perturbative formula for $\alpha_s(Q^2)$ has an unphysical singularity at $Q=\Lambda_{QCD}$, and so the integral on the left-hand-side

#13 In earlier sections we set the scale equal to Q^2. The changes that result from the replacement $Q^2\to(1-x)(1-y)Q^2$ are higher order in α_s and so are irrelevant at very large Q^2. However we are now concerned with how small Q^2 can be made before perturbation theory fails, and for this purpose it is important to use the more physical scale in α_s.

of this equation is ill-defined. This is easily remedied by redefining the running coupling so that

$$\alpha_s(Q^2) = \frac{4\pi}{\beta_0 \log(c + Q^2/\Lambda^2_{QCD})} \tag{122}$$

where c is a constant ($\sim$ 1–3). This is a rather *ad hoc* remedy, but the ratio Q_{eff}/Q that results is fairly insensitive to both c and Q unless Q is very small.

The ratio Q_{eff}/Q is clearly quite sensitive to the x-dependence of the distribution amplitudes, with broader amplitudes giving more emphasis to the region $x, y \sim 1$ and thus lower Q_{eff}'s. Assuming the asymptotic dependence $x(1-x)$, one finds that $Q_{\text{eff}}/Q \approx 0.2$. In this case a form factor with momentum transfer of say 2 Gev actually probes QCD at scales of order only 400 MeV. The effective momentum transfer is smaller still with the broader distribution amplitudes suggested by QCD sum rules ($Q_{\text{eff}}/Q \approx 0.1$). The running coupling constant is of order unity for such small Q_{eff}'s and so perturbation theory is not likely to converge very well, if at all. Some perturbative properties, such as the dimensional-counting and helicity-conservation rules, are valid to all orders in perturbation theory; these might well be applicable even for such Q_{eff}'s. However it should not be surprising if predictions for things like the magnitude of the form factor are off by factors of 2 or more. (Note, for example, that replacing $\alpha_s(Q^2)$ by $\alpha_s(Q^2_{\text{eff}})$ more than doubles the perturbative prediction for the form factor at $Q = 2$ GeV.)

It has proven difficult to measure meson form factors for Q's much above a couple of GeV. However the proton form factor has been measured out beyond 5 Gev. Unfortunately the hard-scattering amplitudes for baryon form factors tend to be more singular in the low-momentum region than meson amplitudes resulting in smaller ratios of Q_{eff}/Q: e.g. one finds that $Q_{\text{eff}}/Q \approx 0.1$ for the asymptotic distribution amplitude $x_1x_2x_3$, and the ratio is smaller by another factor of a half to a third for the broader distribution amplitudes predicted by sum rules. So existing data for the proton form factor, although more accurate, still probes much the same region in effective momentum as does the data for the pion form factor.

The ratio Q_{eff}/Q is also relevant to the second important issue—the relative importance of nonperturbative contributions. We expect the quark-antiquark interaction in T_H to evolve smoothly from nonperturbative to perturbative behavior as Q_{eff} increases, with the crossover occurring around a few hundred MeV. Consequently the pion form factor, for example, could be predominantly perturbative by $Q = 2$ GeV since Q_{eff} is then of order a few hundred MeV. This is despite the fact that perturbative interactions bring in factors of α_s: the coupling $\alpha_s(Q^2_{\text{eff}})$

is not particularly small when $Q_{\rm eff}$ is small, and thus it does not suppress such interactions much.[#14] With protons, perturbative behavior might set in at 3 GeV or higher, depending upon the distribution amplitude.

For larger Q's one must also worry about nonperturbative contributions coming from the endpoint region, particularly in the case of baryon form factors and scattering amplitudes. Perturbative arguments indicate that such contributions are suppressed by Sudakov form factors, but the extent of this suppression at accessible Q's is uncertain. The importance of this region also depends sensitively upon the behavior of the hadronic wavefunctions in the endpoint region: it is easy to make model wavefunctions in which there is little contribution from the endpoint region for Q's greater than a few GeV;[25,26,27] it is also easy to make models in which the region is important even at several GeV (ignoring Sudakov effects).[24] The situation is further complicated in the case of hadronic scattering amplitudes by our incomplete understanding of the Sudakov suppression of pinch singularities.

In the light of these uncertainties the best one can do is to assume the validity of the perturbative analysis, at least as a qualitative or semi-quantitative guide to large-$p_\perp$ exclusive processes. This model is quite plausibly correct, and in any case there is currently no other comprehensive theory of these processes. The validity of the perturbative model can then be judged by the extent to which it is capable of accounting for the broad range of available data.

#14 Of course perturbation theory will not converge well if α_s is large. When we speak of "perturbative behavior" here we are again thinking of behavior that is true to all orders—factorization, dimensional counting, helicity conservation.... It is important to realize that the validity of the factorized form for a large momentum transfer amplitude is not necessarily contingent on the applicability of perturbation theory. Indeed there is likely to be a region of momentum transfer where factorization, dimensional counting... are valid but where perturbation theory does not converge at all.

5. APPLICATIONS OF QCD TO THE PHENOMENOLOGY OF EXCLUSIVE REACTIONS

In the following sections we will discuss the phenomenology of exclusive reactions as tests of QCD and the structure of hadrons. The primary processes of interest are those in which all final particles are measured at large invariant masses compared to each other: *i.e.* large momentum transfer exclusive reactions. This includes form factors of hadrons and nuclei at large momentum transfer Q and large angle scattering reactions. Specific examples are reactions such as $e^-p \to e^-p$, $e^+e^- \to p\overline{p}$ which determine the proton form factor, two-body scattering reactions at large angles and energies such as $\pi^+p \to \pi^+p$ and $pp \to pp$, two-photon annihilation processes such as $\gamma\gamma \to K^+K^-$ or $\overline{p}p \to \gamma\gamma$, exclusive nuclear processes such as deuteron photo-disintegration $\gamma d \to np$, and exclusive decays such as $\pi^+ \to \mu^+\nu$ or $J/\psi \to \pi^+\pi^-\pi^0$. In this section we will summarize the main features of the QCD predictions developed in the previous sections.

QCD has two essential properties which make calculations of processes at short distance or high-momentum transfer tractable and systematic. The critical feature is asymptotic freedom: the effective coupling constant $\alpha_s(Q^2)$ which controls the interactions of quarks and gluons at momentum transfer Q^2 vanishes logarithmically at large Q^2 since it allows perturbative expansions in $\alpha_s(Q^2)$. Complementary to asymptotic freedom is the existence of *factorization theorems* for both exclusive and inclusive processes at large momentum transfer. In the case of "hard" exclusive processes (in which the kinematics of all the final state hadrons are fixed at large invariant mass), the hadronic amplitude can be represented as the product of a process-dependent hard-scattering amplitude $T_H(x_i, Q)$ for the scattering of the constituent quarks convoluted with a process-independent *distribution amplitude* $\phi(x, Q)$ for each incoming or outgoing hadron.[2] When Q^2 is large, T_H is computable in perturbation theory as is the Q-dependence of $\phi(x, Q)$. We have discussed the development of factorization for exclusive processes in detail in Section 4.

Quantum chromodynamics[1] has now been extensively tested in high momentum transfer inclusive reactions where the factorization theorems, perturbation theory, and jet evolution algorithms provide semi-quantitative predictions. Tests of the confining nonperturbative aspects of the theory are, however, either qualitative or at best indirect. In fact QCD is a theory of relatively low mass scales ($\Lambda_{\overline{MS}} \sim 200 \pm 100$ MeV, $< k_\perp^2 >^{1/2} \sim 300$ MeV), and eventually its most critical test as a viable theory of strong and nuclear interactions will involve relatively low energies and momentum transfer at the interface of the perturbative and nonperturbative domain.

The understanding of hadronization and the computation of hadron matrix elements clearly requires knowledge of the hadron wavefunctions. In Table I we give a summary of the main scaling laws and properties of large momentum transfer exclusive and inclusive cross sections which are derivable starting from the light-cone Fock space basis and the perturbative expansion for QCD.

As we have discussed in Section 3, a convenient relativistic description of hadron wavefunctions is given by the set of n-body momentum space amplitudes, $\psi_n(x_i, k_{\perp_i}, \lambda_i)$, $i = 1, 2, \ldots n$, defined on the free quark and gluon Fock basis at equal "light-cone time" $\tau = t + z/c$ in the physical "light-cone" gauge $A^+ \equiv A^0 + A^3 = 0$. (Here $x_i = k_i^+/p^+$, $\sum_i x_i = 1$, is the light-cone momentum fraction of quark or gluon i in the n — particle Fock state; $k_{\perp_i}$, with $\sum_i k_{\perp_i} = 0$, is its transverse momentum relative to the total momentum p^μ; and λ_i is its helicity.) The quark and gluon structure functions $G_{q/H}(x, Q)$ and $G_{g/H}(x, Q)$ which control hard inclusive reactions and the hadron distribution amplitudes $\phi_H(x, Q)$ which control hard exclusive reactions are simply related to these wavefunctions:

$$G_{q/H}(x, Q) \propto \sum_n \int^Q \Pi d^2 k_{\perp_i} \int \Pi dx_i \, |\psi_n(x_i, k_{\perp_i})|^2 \delta(x_q - x) \quad ,$$

and

$$\phi_H(x_i, Q) \propto \int^Q \Pi d^2 k_{\perp_i} \, \psi_{\text{valence}}(x_i, k_{\perp_i}) \quad .$$

In the case of inclusive reactions, such as deep inelastic lepton scattering, two basic aspects of QCD are relevant: (1) the scale invariance of the underlying lepton-quark subprocess cross section, and (2) the form and evolution of the structure functions. A structure function is a sum of squares of the light-cone wavefunctions. The logarithmic evolution of $G_q(x, Q^2)$ is controlled by the wavefunctions which fall off as $|\psi(x, \vec{k}_\perp)|^2 \sim \alpha_s(k_\perp^2)/k_\perp^2$ at large $k_\perp^2$. This form is a consequence of the pointlike $q \to gq$, $g \to gg$, and $g \to q\overline{q}$ splittings. By taking the logarithmic derivative of G with respect to Q one derives the evolution equations of the structure function. All of the hadron's Fock states generally participate; the necessity for taking into account the (non-valence) higher-particle Fock states in the proton is apparent from two facts: (1) the proton's large gluon momentum fraction and (2) the recent results from the EMC collaboration[28] suggesting that, on the average, little of the proton's helicity is carried by the light quarks.[29]

Table I

Table I Comparison of Exclusive and Inclusive Cross Sections

Exclusive Amplitudes	Inclusive Cross Sections
$\mathcal{M} \sim \Pi\, \phi(x_i, Q) \otimes T_H(x_i, Q)$	$d\sigma \sim \Pi\, G(x_a, Q) \otimes d\hat{\sigma}(x_a, Q)$
$\phi(x,Q) = \int^{Q} [d^2k_\perp]\, \psi^{Q}_{\rm val}(x, k_\perp)$	$G(x,Q) = \sum_n \int^{Q} [d^2k_\perp]\,[dx]'\, \lvert\psi^{Q}_n(x,k_\perp)\rvert^2$
Measure ϕ in $\gamma \to M\overline{M}$	Measure G in $\ell p \to \ell X$
$\sum_{i\in H} \lambda_i = \lambda_H$	$\sum_{i\in H} \lambda_i \neq \lambda_H$
	Evolution
$\frac{\partial\phi(x,Q)}{\partial \log Q^2} = \alpha_s \int [dy]\; V(x,y)\,\phi(y)$	$\frac{\partial G(x,Q)}{\partial \log Q^2} = \alpha_s \int dy\; P(x/y)\, G(y)\,.$
$\lim_{Q\to\infty} \phi(x,Q) = \prod_i x_i \cdot C_{\rm flavor}$	$\lim_{Q\to\infty} G(x,Q) = \delta(x)\, C$
	Power Law Behavior
$\frac{d\sigma}{dx}(A+B \to C+D) \cong \frac{1}{s^{n-2}} f(\theta_{c.m.})$	$\frac{d\sigma}{d^2p/E}(AB \to CX) \cong \sum \frac{(1-x_T)^{2n_s-1}}{(Q^2)^{n_{act}-2}} f(\theta_{c.m.})$
$n = n_A + n_B + n_C + n_D$	$n_{act} = n_a + n_b + n_c + n_d$
T_H : expansion in $\alpha_s(Q^2)$	$d\hat{\sigma}$: expansion in $\alpha_s(Q^2)$
	Complications
End point singularities	Multiple scales
Pinch singularities	Phase-space limits on evolution
High Fock states	Heavy quark thresholds
	Higher twist multiparticle processes
	Initial and final state interactions

In the case of exclusive electroproduction reactions such as the baryon form factor, again two basic aspects of QCD are relevant: (1) the scaling of the underlying hard scattering amplitude (such as $l + qqq \to l + qqq$), and (2) the form and evolution of the hadron distribution amplitudes. The distribution amplitude is defined as an integral over the lowest (valence) light-cone Fock state. The logarithmic variation of $\phi(x, Q^2)$ is derived from the integration at large $k_\perp$, *i.e.* wavefunctions which behave as $\psi(x, \vec{k}_\perp) \sim \alpha_s(k_\perp^2)/k_\perp^2$ at large $k_\perp^2$ This behavior follows from the simple one-gluon exchange contribution to the tail of the valence wavefunction. By taking the logarithmic derivative, one then obtains the evolution equation for the hadron distribution amplitude.

As we showed in Section 3, the form factor of a hadron at any momentum transfer can be computed exactly in terms of a convolution of initial and final light-cone Fock state wavefunctions.[10] In general, all of the Fock states contribute. In contrast, exclusive reactions with high momentum transfer Q, perturbative QCD predicts that only the lowest particle number (valence) Fock state is required to compute the contribution to the amplitude to leading order in $1/Q$.

For example, in the light-cone Fock expansion the proton is represented as a column vector of states ψ_{qqq}, ψ_{qqqg}, $\psi_{qqq\bar{q}q}\ldots$ In the light-cone gauge, $A^+ = A^0 + A^3 = 0$, only the minimal "valence" three-quark Fock state needs to be considered at large momentum transfer since any additional quark or gluon forced to absorb large momentum transfer yields a power-law suppressed contribution to the hadronic amplitude. Thus at large Q^2, the baryon form factor can be systematically computed by iterating the equation of motion for its valence Fock state wherever large relative momentum occurs. To leading order the kernel is effectively one-gluon exchange. The sum of the hard gluon exchange contributions can be arranged as the gauge invariant amplitude T_H, the final form factor having the form

$$F_B(Q^2) = \int_0^1 [dy] \int_0^1 [dx]\ \phi_B^\dagger(y_j, Q) T_H(x_i, y_j, Q) \phi_B(x_i, Q)\ .$$

The essential gauge-invariant input for hard exclusive processes is the distribution amplitude $\phi_H(x, Q)$. For example $\phi_\pi(x, Q)$ is the amplitude for finding a quark and antiquark in the pion carrying momentum fractions x and $1 - x$ at impact (transverse space) separations less than $b_\perp < 1/Q$. The distribution amplitude thus plays the role of the "wavefunction at the origin" in analogous non-relativistic calculations of form factors. In the relativistic theory, its dependence on log Q is controlled by evolution equations derivable from perturbation theory or the operator product expansion. A detailed discussion of the light-cone Fock state wavefunctions and their relation to observables is given in Section 3 and in Ref. 30.

The distribution amplitude contains all of the bound-state dynamics and specifies the momentum distribution of the quarks in the hadron. The hard-scattering amplitude for a given exclusive process can be calculated perturbatively as a function of $\alpha_s(Q^2)$. Similar analyses can be applied to form factors, exclusive photon-photon reactions, and with increasing degrees of complication, to photoproduction, fixed-angle scattering, etc. In the case of the simplest processes, $\gamma\gamma \to M\overline{M}$ and the meson form factors, the leading order analysis can be readily extended to all-orders in perturbation theory.

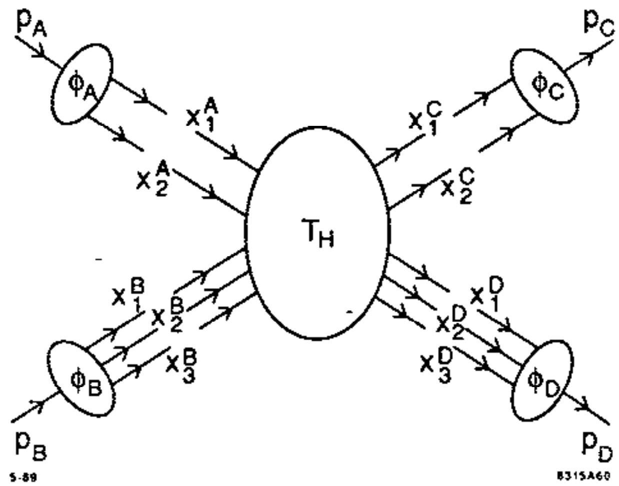

Figure 18. QCD factorization for two-body amplitudes at large momentum transfer.

In the case of exclusive processes such as photo-production, Compton scattering, meson-baryon scattering, etc., the leading hard scattering QCD contribution at large momentum transfer $Q^2 = tu/s$ has the form (helicity labels and suppressed) (see Fig. 18)

$$\mathcal{M}_{A+B-C+D}(Q^2, \theta_{\text{c.m.}}) = \int [dx] \phi_C(x_c, \tilde{Q}) \; \phi_D(x_d, \tilde{Q}) \; T_H(x_i; Q^2, \theta_{\text{c.m.}}) \\ \times \phi_A(x_a, \tilde{Q}) \; \phi_B(x_b, \tilde{Q})$$

In general the distribution amplitude is evaluated at the characteristic scale $\tilde{Q}$ set by the effective virtuality of the quark propagators.

By definition, the hard scattering amplitude T_H for a given exclusive process is constructed by replacing each external hadron with its massless, collinear valence partons, each carrying a finite fraction x_i of the hadron's momentum. Thus T_H is the scattering amplitude for the constituents. The essential behavior of the amplitude is determined by T_H, computed where each hadron is replaced by its (collinear) quark constituents. We note that T_H is "collinear irreducible," *i.e.* the transverse momentum integrations of all reducible loop integration are restricted to $k_\perp^2 > \mathcal{O}(Q^2)$ since the small $k_\perp$ region is already contained in ϕ. If the internal propagators in T_H are all far-off-shell $\mathcal{O}(Q^2)$, then a perturbative expansion in $\alpha_s(Q^2)$ can be carried out.

Higher twist corrections to the quark and gluon propagator due to mass terms and intrinsic transverse momenta of a few hundred MeV give nominal corrections of higher order in $1/Q^2$. These finite mass corrections combine with the leading twist results to give a smooth approach to small Q^2. It is thus reasonable that PQCD scaling laws become valid at relatively low momentum transfer of order of a few GeV.

5.1. General Features of Exclusive Processes in QCD

The factorization theorem for large-momentum-transfer exclusive reactions separates the dynamics of hard-scattering quark and gluon amplitudes T_H from process-independent distribution amplitudes $\phi_H(x,Q)$ which isolates all of the bound state dynamics. However, as seen from Table I, even without complete information on the hadronic wave functions, it is still possible to make predictions at large momentum transfer directly from QCD.

Although detailed calculations of the hard-scattering amplitude have not been carried out in all of the hadron-hadron scattering cases, one can abstract some general features of QCD common to all exclusive processes at large momentum transfer:

1. Since the distribution amplitude ϕ_H is the $L_z = 0$ orbital-angular-momentum projection of the hadron wave function, the sum of the interacting constituents' spin along the hadron's momentum equals the hadron spin:[6]

$$\sum_{i\in H} s_i^z = s_H^z .$$

   In contrast, there are any number of non-interacting spectator constituents in inclusive reactions, and the spin of the active quarks or gluons is only statistically related to the hadron spin (except at the edge of phase space $x \to 1$).

2. Since all loop integrations in T_H are of order $\tilde{Q}$, the quark and hadron masses can be neglected at large Q^2 up to corrections of order $\sim m/\tilde{Q}$. The vector-gluon coupling conserves quark helicity when all masses are neglected–*i.e.* $\overline{u}_{\downarrow}\gamma^{\mu}u_{\uparrow} = 0$. Thus total quark helicity is conserved in T_H. In addition, because of (2), each hadron's helicity is the sum of the helicities of its valence quarks in T_H. We thus have the selection rule

$$\sum_{\text{initial}} \lambda_H - \sum_{\text{final}} \lambda_H = 0,$$

i.e. total hadronic helicity is conserved up to corrections of order m/Q or higher. Only (flavor-singlet) mesons in the 0^{-+} nonet can have a two-gluon valence component and thus even for these states the quark helicity equals the hadronic helicity. Consequently hadronic-helicity conservation applies for all amplitudes involving light meson and baryons.[31] Exclusive reactions which involve hadrons with quarks or gluons in higher orbital angular states are suppressed by powers.

3. The nominal power-law behavior of an exclusive amplitude at fixed $\theta_{c.m.}$ is $(1/Q)^{n-4}$, where n is the number of external elementary particles (quarks, gluons, leptons, photons, ...) in T_H. This dimensional-counting rule[5] is modified by the Q^2 dependence of the factors of $\alpha_s(Q^2)$ in T_H, by the Q^2 evolution of the distribution amplitudes, and possibly by a small power correction associated with the Sudakov suppression of pinch singularities in hadron-hadron scattering.

The dimensional-counting rules for the power-law falloff appear to be experimentally well established for a wide variety of processes.[32,33] The helicity-conservation rule is also one of the most characteristic features of QCD, being a direct consequence of the gluon's spin. A scalar-or tensor-gluon-quark coupling flips the quark's helicity. Thus, for such theories, helicity may or may not be conserved in any given diagram contribution to T_H depending upon the number of interactions involved. Only for a vector theory, such as QCD, can one have a helicity selection rule valid to all orders in perturbation theory.

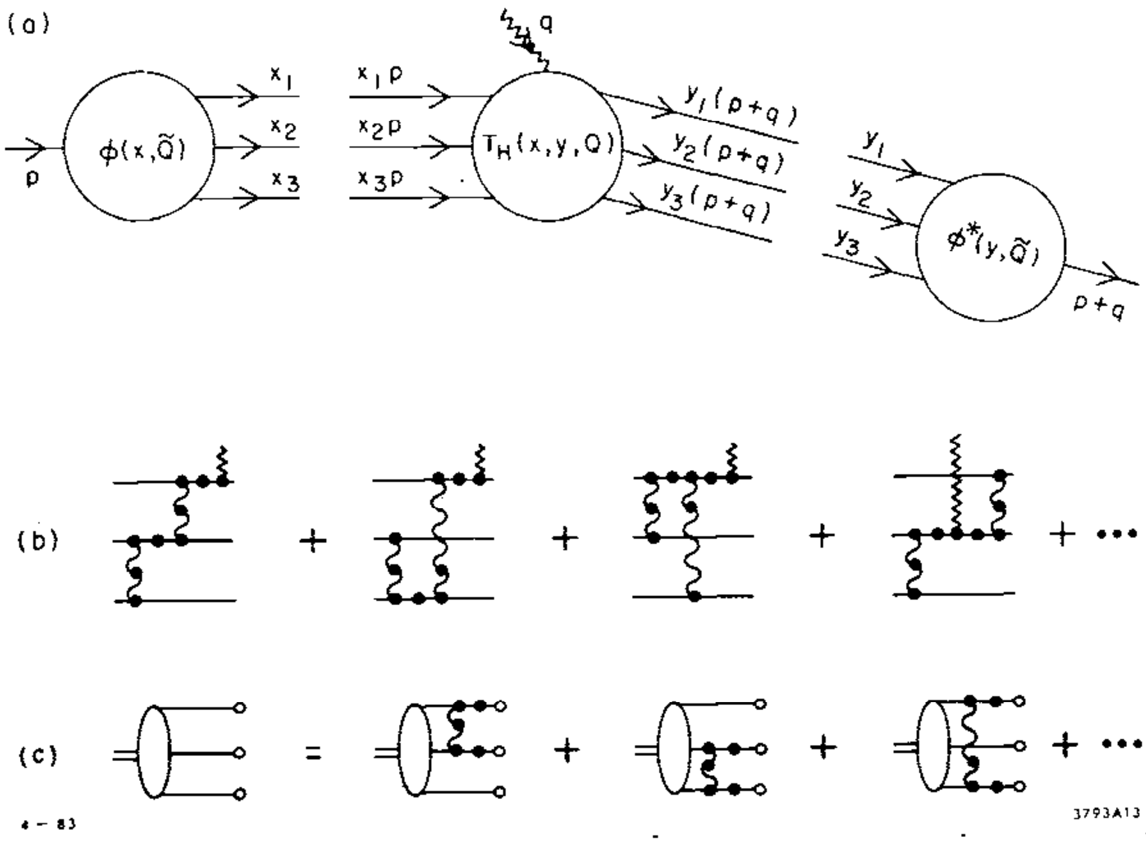

Figure 19. (a) Factorization of the nucleon form factor at large Q^2 in QCD. (b) The leading order diagrams for the hard scattering amplitude T_H. The dots indicate insertions which enter the renormalization of the coupling constant. (c) The leading order diagrams which determine the Q^2 dependence of the distribution amplitude $\phi(x,Q)$.

5.2. Electromagnetic Form Factors

Any helicity conserving baryon form factor at large Q^2 has the form: [see Fig. 19(a)]

$$F_B(Q^2) = \int_0^1 [dy] \int_0^1 [dx] \; \phi_B^\dagger(y_j,Q) T_H(x_i,y_j,Q) \phi_B(x_i,Q) \quad ,$$

where to leading order in $\alpha_s(Q^2)$, T_H is computed from $3q + \gamma^* \to 3q$ tree graph amplitudes: [Fig. 19(b).]

$$T_H = \left[\frac{\alpha_s(Q^2)}{Q^2}\right]^2 f(x_i,y_j)$$

and

$$\phi_B(x_i, Q) = \int [d^2k_\perp]\, \psi_V(x_i, \vec{k}_{\perp i})\theta(k_{\perp i}^2 < Q^2)$$

is the valence three-quark wavefunction [Fig. 19(c)] evaluated at quark impact separation $b_\perp \sim \mathcal{O}(Q^{-1})$. More detailed formulae for the baryon form factor are presented in Appendix I. Since ϕ_B only depends logarithmically on Q^2 in QCD, the main dynamical dependence of $F_B(Q^2)$ is the power behavior $(Q^2)^{-2}$ derived from scaling of the elementary propagators in T_H. More explicitly, the proton's magnetic form factor has the form:[4]

$$G_M(Q^2) = \left[\frac{\alpha_s(Q^2)}{Q^2}\right]^2 \sum_{n,m} a_{nm} \left(\log\ \frac{Q^2}{\Lambda^2}\right)^{-\gamma_n - \gamma_m}$$

$$\times \left[1 + \mathcal{O}(\alpha_s(Q)) + \mathcal{O}\left(\frac{1}{Q}\right)\right].$$

The first factor, in agreement with the quark counting rule, is due to the hard scattering of the three valence quarks from the initial to final nucleon direction. Higher Fock states lead to form factor contributions of successively higher order in $1/Q^2$. The logarithmic corrections derive from an evolution equation for the nucleon distribution amplitude. The γ_n are the computed anomalous dimensions, reflecting the short distance scaling of three-quark composite operators.[12] The results hold for any baryon to baryon vector or axial vector transition amplitude that conserves the baryon helicity. Helicity non-conserving form factors should fall as an additional power of $1/Q^2$.[6] Measurements[34] of the transition form factor to the $J = 3/2$ $N(1520)$ nucleon resonance are consistent with $J_z = \pm 1/2$ dominance, as predicted by the helicity conservation rule.[6] A review of the data on spin effects in electron nucleon scattering in the resonance region is given in Ref. 34. It is important to explicitly verify that $F_2(Q^2)/F_1(Q^2)$ decreases at large Q^2. The angular distribution decay of the $J/\psi \to p\overline{p}$ is consistent with the QCD prediction $\lambda_p + \lambda_{\overline{p}} = 0$.

Thus, modulo logarithmic factors, one obtains a dimensional counting rule for any hadronic or nuclear form factor at large Q^2 ($\lambda = \lambda' = 0$ or $1/2$)

$$F(Q^2) \sim \left(\frac{1}{Q^2}\right)^{n-1},$$

$$F_1^N \sim \frac{1}{Q^4}, \quad F_\pi \sim \frac{1}{Q^2}, \quad F_d \sim \frac{1}{Q^{10}},$$

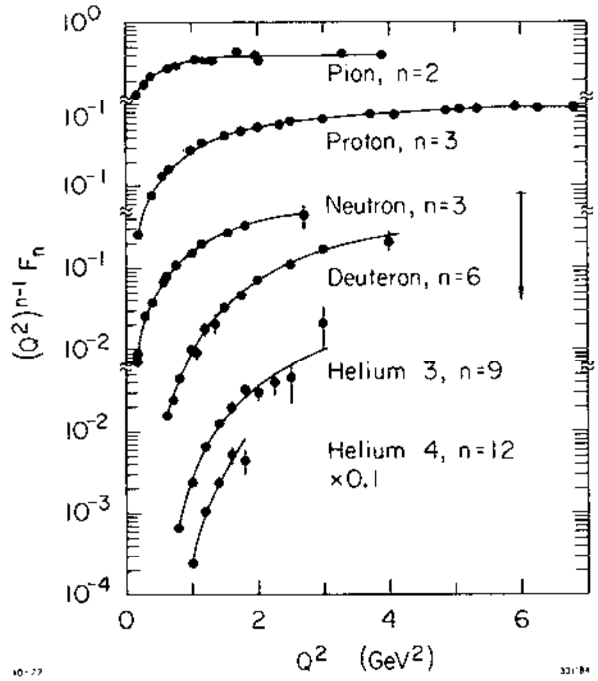

Figure 20. Comparison of experiment[35] with the QCD dimensional counting rule $(Q^2)^{n-1}F(Q^2) \sim const$ for form factors. The proton data extends beyond 30 GeV^2.

where n is the minimum number of fields in the hadron. Since quark helicity is conserved in T_H and $\phi(x_i, Q)$ is the $L_z = 0$ projection of the wavefunction, total hadronic helicity is conserved at large momentum transfer for any QCD exclusive reaction. The dominant nucleon form factor thus corresponds to $F_1(Q^2)$ or $G_M(Q^2)$; the Pauli form factor $F_2(Q^2)$ is suppressed by an extra power of Q^2. Similarly, in the case of the deuteron, the dominant form factor has helicity $\lambda = \lambda' = 0$, corresponding to $\sqrt{A(Q^2)}$.

The comparison of experimental form factors with the predicted nominal power-law behavior is shown in Fig. 20. We will discuss predictions for the normalization of the leading power terms in Section 5.6. As we have discussed in Section 4, the general form of the logarithmic corrections to the leading power contributions form factors can be derived from the operator product expansion at short distance[11,12] or by solving an evolution equation[4] for the distribution amplitude computed from gluon exchange [Fig. 19(c)], the only QCD contribution which falls sufficiently small at large transverse momentum to effect the large Q^2 dependence.

The comparison of the proton form factor data with the QCD prediction arbitrarily normalized is shown in Fig. 21. The fall-off of $(Q^2)^2 G_M(Q^2)$ with Q^2

is consistent with the logarithmic fall-off of the square of QCD running coupling constant. As we shall discuss below, the QCD sum rule[16] model form for the nucleon distribution amplitude together with the QCD factorization formulae, predicts the correct sign and magnitude as well as scaling behavior of the proton and neutron form factors.[36]

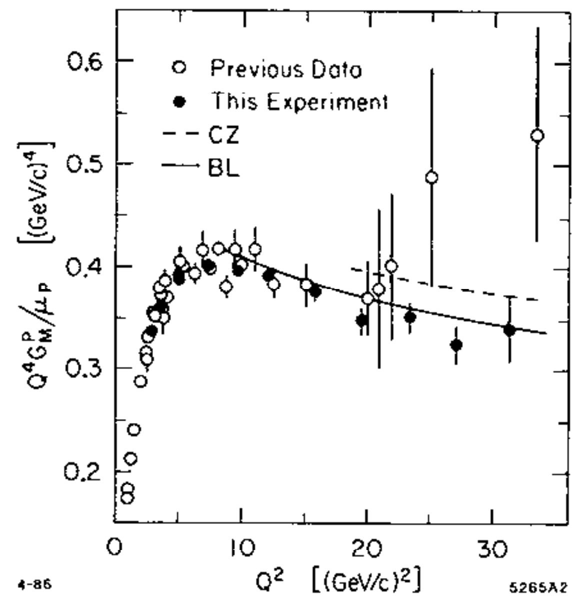

Figure 21. Comparison of the scaling behavior of the proton magnetic form factor with the theoretical predictions of Refs. 4 and 16. The CZ predictions[16] are normalized in sign and magnitude. The data are from Ref. 36.

5.3. Comparison of QCD Scaling with Experiment

Phenomenologically the dimensional counting power laws appear consistent with measurements of form factors, photon-induced amplitudes, and elastic hadron-hadron scattering at large angles and momentum transfer.[33] The successes of the quark counting rules can be taken as strong evidence for QCD since the derivation of the counting rules require scale invariant tree graphs, soft corrections from higher loop corrections to the hard scattering amplitude, and strong suppression of pinch singularities. QCD is the only field theory of spin $\frac{1}{2}$ fields that has all of these properties.

As shown in Fig. 22, the data for $\gamma p \to \pi^+ n$ cross section at $\theta_{CM} = \pi/2$ are consistent with the normalization and scaling $d\sigma/dt\ (\gamma p \to \pi^+ n) \simeq [1\,\mathrm{nb}/(s/10\ \mathrm{GeV})^7]\ f(t/s)$.

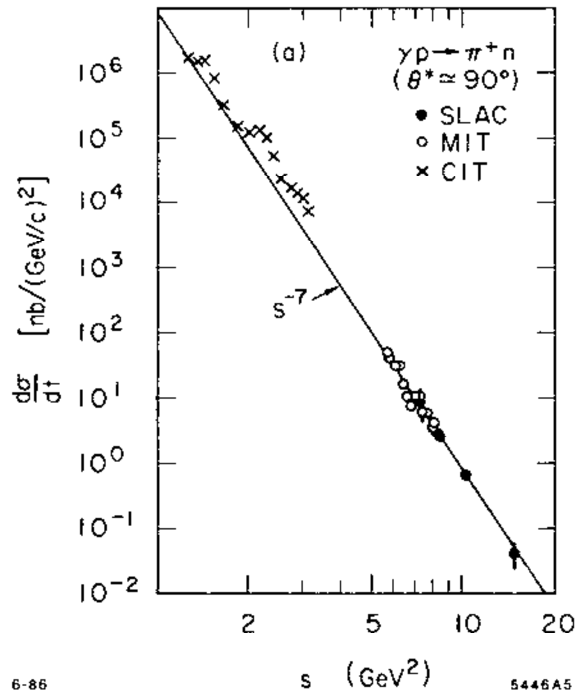

Figure 22. Comparison of photoproduction data with the dimensional counting power-law prediction. The data are summarized in Ref. 37.

The check of fixed angle scaling in proton-proton elastic scattering is shown in Figs. 23. Extensive measurements of the $pp \to pp$ cross section have been made at ANL, BNL and other laboratories. The scaling law $s^{10} d\sigma/dt(pp \to pp) \simeq const.$ predicted by QCD seems to work quite well over a large range of energy and angle. The best fit gives the power $N = 9.7 \pm 0.5$ compared to the dimensional counting prediction N=10. There are, however, measurable deviations from fixed power dependence which are not readily apparent on the log-log plot. As emphasized by Hendry[38] the $s^{10} d\sigma/dt$ cross section exhibits oscillatory behavior with p_T (see Section 9). Even more serious is the fact that polarization measurements[40] show significant spin-spin correlations (A_{NN}), and the single spin asymmetry (A_N) is not consistent with predictions based on hadron helicity conservation (see Section 6) which is expected to be valid for the leading power behavior.[6] Recent discussions of these effects have been given by Farrar[41] and Lipkin.[42] We discuss a new explanation of all of these effects in Section 9.

As emphasized by Landshoff, the ISR data for high energy elastic pp scattering at small $|t|/s$ can be parameterized in the form $d\sigma/dt \sim const/t^8$ for $2\ GeV^2 < |t| < 10\ GeV^2$. This suggests a role for triple gluon exchange pinch contributions at large energies where multiple vector exchange diagrams could

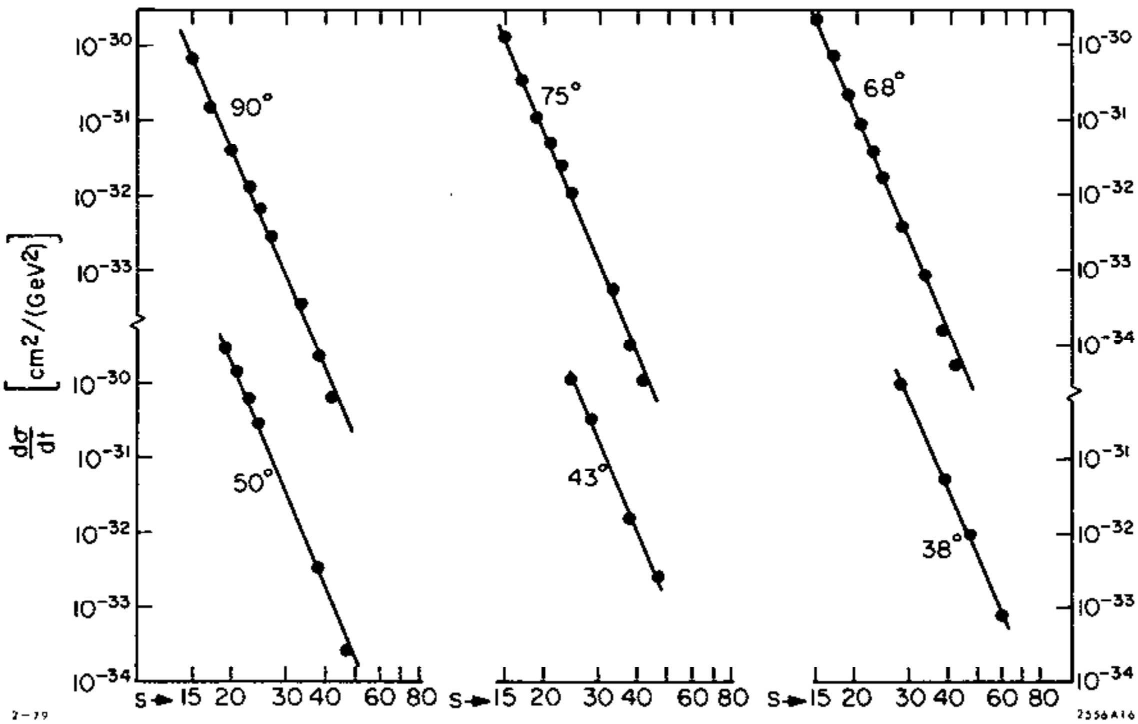

Figure 23. Test of fixed θ_{CM} scaling for elastic pp scattering. The data compilation is from Landshoff and Polkinghorne.

dominate. However, from Mueller's analysis[21] one expects stronger fall-off in t due to the Sudakov form factor suppression. This paradox implies that the role of the pinch singularity in large momentum transfer exclusive reactions is not well understood and deserve further attention.[43] As discussed in Section 4.5, pinch singularities are also expected to modify the dimensional counting scaling laws for wide-angle scattering, but the change in the exponent of s is small and hard to detect experimentally. However, Ralston and Pire[43] have suggested that the oscillatory behavior in the wide-angle pp scattering amplitude results from interference between the pinch contributions and the ordinary hard-scattering contributions to the pp amplitude. Thus pp scattering may provide a experimental handle on pinch contribution. However it is possible that the oscillations are specific to particular channels, in which case an alternative explanation is necessary. We discuss this further in Section 9. Pinch singularities do not arise in form factors, or such photon-induced processes as $\gamma\gamma \to M\overline{M}$,[16] $\gamma^* + \gamma \to M$,[4] $\gamma^* \to M_1 ... M_N$ at fixed angle,[44] $\gamma\gamma \to B\overline{B}$, $\gamma B \to \gamma B$, etc.[45,46]

5.4. Exclusive Anti-Proton Proton Annihilation Processes

Anti-proton annihilation has a number of important advantages as a probe of QCD in the low energy domain. Exclusive reaction in which *complete* annihilation of the valance quarks occur ($\overline{p}p \to \ell\overline{\ell}$, $\gamma\gamma$, $\phi\phi$, etc.) necessarily involve impact distances $b_\perp$ smaller than $1/M_p = 5\ \text{fm}^{-1}$ since baryon number is exchanged in the t-channel. There are a number of exclusive and inclusive $\overline{p}$ reactions which can provide useful constraints on hadron wavefunctions or test novel features of QCD involving both perturbative and nonperturbative dynamics. In several cases ($\overline{p}p \to \overline{\ell}\ell$, $\overline{p}p \to J/\psi$, $\overline{p}p \to \gamma\gamma$), complete leading twist (leading power law) predictions are available. These reactions not only probe the subprocesses $\overline{qqq}\ qqq \to \gamma\gamma$, etc., but they also are sensitive to the normalization and shape of the proton distribution amplitude $\phi_p(x_i, x_2, x_3; Q)$, the basic measure of the proton's three-quark valance wavefunction.

The fixed angle scaling laws for the $\overline{p}p$ channels are:

$$\frac{d\sigma}{d\Omega}\,(\overline{p}p \to e^+e^-) \simeq \frac{\alpha^2}{(p_T^2)^5}\, f^{e^+e^-}(\cos\theta, \ell n p_T)$$

$$\frac{d\sigma}{d\Omega}\,(\overline{p}p \to \gamma\gamma) \simeq \frac{\alpha^2}{(p_T^2)^5}\, f^{\gamma\gamma}(\cos\theta, \ell n p_T)$$

$$\frac{d\sigma}{d\Omega}\,(\overline{p}p \to \gamma M) \simeq \frac{\alpha^2}{(p_T^2)^6}\, f^{\gamma M}(\cos\theta, \ell n p_T)$$

$$\frac{d\sigma}{d\Omega}\,(p\overline{p} \to M\overline{M}) \simeq \frac{1}{(p_T^2)^7}\, f^{M\overline{M}}(\cos\theta, \ell n p_T)$$

$$\frac{d\sigma}{d\Omega}\,(p\overline{p} \to B\overline{B}) \simeq \frac{1}{(p_T^2)^9}\, f^{B\overline{B}}(\cos\theta, \ell n p_T) \quad .$$

The angular dependence reflects the structure of the hard-scattering perturbative T_H amplitude, which in turn follows from the flavor pattern of the contributing duality diagrams.

It is important to note that the leading power-law behavior originates in the minimum three-particle Fock state of the $\overline{p}$ and p, at least in physical gauge, such as $A^+ = 0$. Higher Fock states give contributions higher order in $1/s$. For $\overline{p}p \to \ell\overline{\ell}$ this means that initial-state interaction such as one gluon exchange are dynamically suppressed (see Fig. 24). Soft-gluon exchange is suppressed since the incident p or $\overline{p}$ color neutral wavefunction in the three-parton state with impact operation $b_\perp \sim 0(1/\sqrt{s})$. Hard-gluon exchange is suppressed by powers of $\alpha_s(s)$. The absence of a soft initial-state interaction in these reactions is a remarkable consequence of gauge theory, and is quite contrary to normal treatments of initial interactions based on Glauber theory.

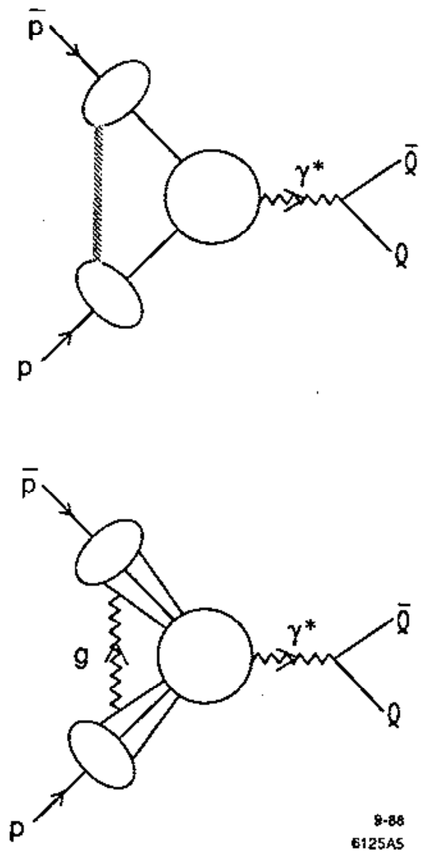

Figure 24. Analysis of initial-state interactions in PQCD.

We will discuss in Section 8.1 another class of exclusive reactions in QCD involving light nuclei, such as $\bar{p}d \to \gamma n$ and $\bar{p}d \to \pi^- p$ which can probe quark and gluon degrees of freedom of the nucleus at surprisingly low energy. We will also discuss the "color transparency" of nuclei in quasi-elastic processes like $\bar{p}A \to \ell\bar{\ell}(A-1)$.

5.5. Additional Tests of Gluon Spin in Exclusive Processes

The spin of the gluon can be tested in a wide variety of exclusive processes:

(a) $\gamma\gamma \rightarrow \rho\rho, K^*K^*, \ldots$. These cross sections can be measured using e^+e^- colliding beams. At large energies ($s \gtrsim 2-4 GeV^2$) and wide angles, the final-state helicities must be equal and opposite. These processes can also be used as a sensitive probe of the structure of the quark distribution amplitudes.[16]

(b) Electroweak form factors of baryons. Relations, valid to all order in α_s, can be found among the various electromagnetic and weak-interaction for factors of the nucleons and other baryons.[47] These relations depend crucially upon quark-helicity conservation and as such test the vector nature of the gluon. Current data for the axial-vector and electromagnetic form factors of the nucleons is in excellent agreement with these QCD predictions, although a definitive test requires higher energies.

(c) $\pi p \rightarrow \pi p, pp \rightarrow pp, \ldots$. QCD predicts that total hadronic helicity is conserved from the initial state to the final state in all high-energy, wide-angle, elastic, and quasi-elastic hadronic amplitudes. One immediate consequence of this is the suppression of the backward peak relative to the forward peak in scalar-meson- baryon scattering. This follows because angular momentum cannot be conserved along the beam axis if only the baryons carry helicity, helicity is conserved, and the baryons scatter through 180°. Data[32] for πp and Kp scattering is consistent with this observation. However the hard-scattering amplitudes for these processes must be computed before a detailed interpretation of the data is possible.

In the case of $pp \rightarrow pp$ scattering, there are in general five independent parity-conserving and time-reversal-invariant amplitudes $\mathcal{M}(++ \rightarrow ++), \mathcal{M}(+- \rightarrow +-)$, $\mathcal{M}(-+ \rightarrow +-), \mathcal{M}(++ \rightarrow +-)$, and $\mathcal{M}(-- \rightarrow ++)$. Total-hadron-helicity conservation implies that $\mathcal{M}(++ \rightarrow +-)$ and $\mathcal{M}(-- \rightarrow ++)$ are power-law suppressed. The vanishing of the double-flip amplitude implies $A_{NN} = A_{SS}$, and

$$2A_{NN} - A_{LL} = 1 \quad (\theta_{c.m.} = 90^\circ).$$

Here A_{NN} is the spin asymmetry for incident nucleons polarized normal ($\hat{x}$) to the scattering plane. A_{LL} refers to initial spins polarized along the laboratory beam direction ($\hat{z}$) and A_{SS} refers to initial spin polarized (sideways) along y. Data at $p_{\mathrm{lab}} = 11.75\ GeV/c$ from Argonne[48] appears to be consistent with this prediction.

(d) Zeros of meson form factors. Asymptotically, the electromagnetic form factors of charged π's, K's, and $\rho(\lambda = 0)$'s have a positive sign in QCD. In a theory of scalar gluons, these form factors become negative for Q^2 large, and thus must vanish at some finite Q^2 since $F(Q^2 = 0) = 1$ by definition. Consequently the absence of zeros in $F_\pi(Q^2)$ is further evidence for a vector gluon. We discuss this in detail in the next section.

5.6. Hadronic Wavefunction Phenomenology

Let us now return to the question of the normalization of exclusive amplitudes in QCD. It should be emphasized that because of the uncertain magnitude of corrections of higher order in $\alpha_s(Q^2)$, comparisons with the normalization of experiment with model predictions could be misleading. Nevertheless, it this section we shall assume that the leading order normalization is at least approximately accurate. If the higher order corrections are indeed small, then the normalization of the proton form factor at large Q^2 is a non-trivial test of the distribution amplitude shape; for example, if the proton wave function has a non-relativistic shape peaked at $x_i \sim 1/3$ then one obtains the wrong sign for the nucleon form factor. Furthermore symmetrical distribution amplitudes predict a very small magnitude for $Q^4 G_M^p(Q^2)$ at large Q^2.

The phenomenology of hadron wavefunctions in QCD is now just beginning. Constraints on the baryon and meson distribution amplitudes have been recently obtained using QCD sum rules and lattice gauge theory. The results are expressed in terms of gauge-invariant moments $< x_j^m >= \int \Pi dx_i \, x_j^m \, \phi(x_i, \mu)$ of the hadron's distribution amplitude. A particularly important challenge is the construction of the baryon distribution amplitude.In the case of the proton form factor, the constants a_{nm} in the QCD prediction for G_M must be computed from moments of the nucleon's distribution amplitude $\phi(x_i, Q)$. There are now extensive theoretical efforts to compute this nonperturbative input directly from QCD. The QCD sum rule analysis of Chernyak *et al.*[16,49] provides constraints on the first 12 moments of $\phi(x, Q)$. Using as a basis the polynomials which are eigenstates of the nucleon evolution equation, one gets a model representation of the nucleon distribution amplitude, as well as its evolution with the momentum transfer scale. The moments of the proton distribution amplitude computed by Chernyak *et al.*, have now been confirmed in an independent analysis by Sachrajda and King.[50]

A three-dimensional "snapshot" of the proton's uud wavefunction at equal light-cone time as deduced from QCD sum rules at $\mu \sim 1$ GeV by Chernyak *et al.*[49] and King and Sachrajda[50] is shown in Fig. 25. The QCD sum rule analysis predicts a surprising feature: strong flavor asymmetry in the nucleon's momentum distribution. The computed moments of the distribution amplitude imply that 65% of the proton's momentum in its 3-quark valence state is carried by the u-quark which has the same helicity as the parent hadron.

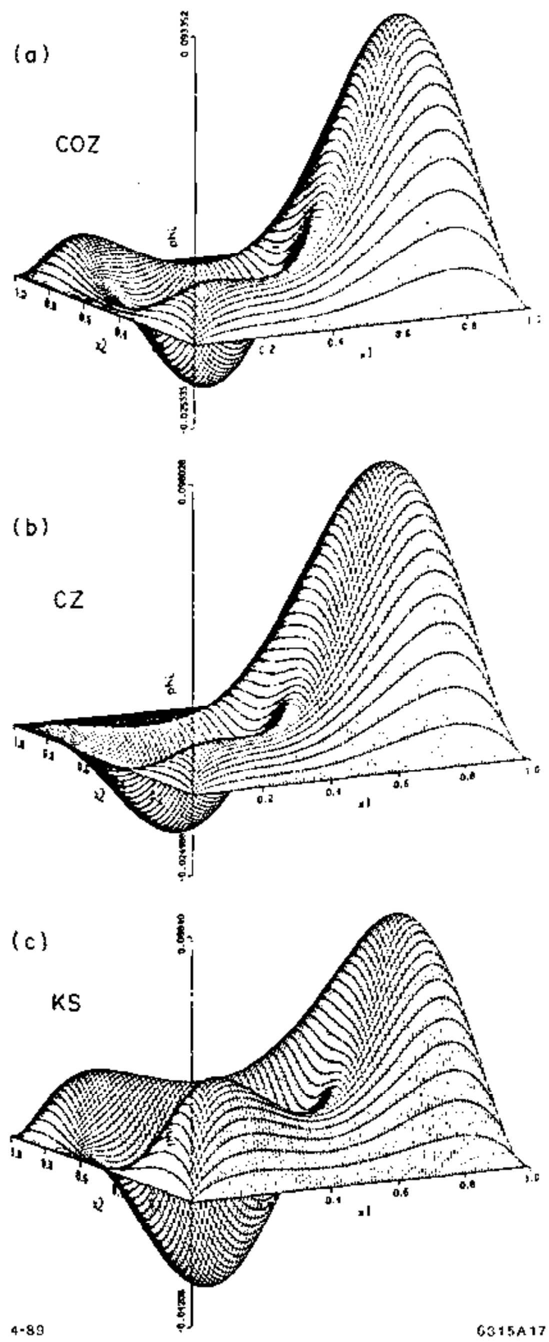

Figure 25. The proton distribution amplitude $\phi_p(x_i, \mu)$ determined at the scale $\mu \sim 1$ GeV from QCD sum rules.

Dziembowski and Mankiewicz[27] have recently shown that the asymmetric form of the CZ distribution amplitude can result from a rotationally-invariant CM wave function transformed to the light cone using free quark dynamics. They find that one can simultaneously fit low energy phenomena (charge radii, magnetic moments, etc.), the measured high momentum transfer hadron form factors, and the CZ distribution amplitudes with a self-consistent ansatz for the quark wave functions. Thus for the first time one has a somewhat complete model for the relativistic three-quark structure of the hadrons. In the model the transverse size of the valence wave function is not found to be significantly smaller than the mean radius of the proton–averaged over all Fock states as argued in Ref. 51. Dziembowski *et al.* also find that the perturbative QCD contribution to the form factors in their model dominates over the soft contribution (obtained by convoluting the non-perturbative wave functions) at a scale $Q/N \approx 1$ GeV, where N is the number of valence constituents. (This criterion was also derived in Ref. 52.)

Gari and Stefanis[53] have developed a model for the nucleon form factors which incorporates the CZ distribution amplitude predictions at high Q^2 together with VMD constraints at low Q^2. Their analysis predicts sizeable values for the neutron electric form factor at intermediate values of Q^2.

A detailed phenomenological analysis of the nucleon form factors for different shapes of the distribution amplitudes has been given by Ji, Sill, and Lombard-Nelsen.[54] Their results show that the CZ wave function is consistent with the sign and magnitude of the proton form factor at large Q^2 as recently measured by the American University/SLAC collaboration[36] (see Fig. 26).

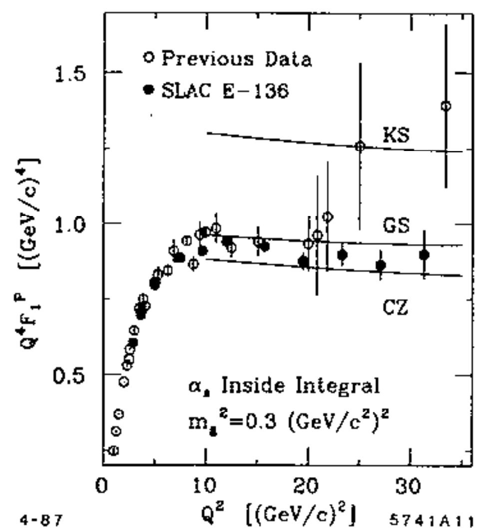

Figure 26. Predictions for the normalization and sign of the proton form factor at high Q^2 using perturbative QCD factorization and QCD sum rule predictions for the proton distribution amplitude (from Ref. 54.) The predictions use forms given by Chernyak and Zhitnitsky, King and Sachrajda,[50] and Gari and Stefanis.[53]

It should be stressed that the magnitude of the proton form factor is sensitive to the $x \sim 1$ dependence of the proton distribution amplitude, where non-perturbative effects could be important.[55] The asymmetry of the distribution amplitude emphasizes contributions from the large x region. Since non-leading corrections are expected when the quark propagator scale $Q^2(1-x)$ is small, in principle relatively large momentum transfer is required to clearly test the perturbative QCD predictions. Chernyak *et al.*[49] have studied this effect in some detail and claim that their QCD sum rule predictions are not significantly changed when higher moments of the distribution amplitude are included.

The moments of distribution amplitudes can also be computed using lattice gauge theory.[14] In the case of the pion distribution amplitudes, there is good agreement of the lattice gauge theory computations of Martinelli and Sachrajda[15] with the QCD sum rule results. This check has strengthened confidence in the reliability of the QCD sum rule method, although the shape of the meson distribution amplitudes are unexpectedly structured: the pion distribution amplitude is broad and has a dip at $x = 1/2$. The QCD sum rule meson distributions, combined with the perturbative QCD factorization predictions, account well for the scaling, normalization of the pion form factor and $\gamma\gamma \to M^+M^-$ cross sections.

In the case of the baryon, the asymmetric three-quark distributions are consistent with the normalization of the baryon form factor at large Q^2 and also the branching ratio for $J/\psi \to p\overline{p}$. The data for large angle Compton scattering $\gamma p \to \gamma p$ are also well described.[56] However, a very recent lattice calculation of the lowest two moments by Martinelli and Sachrajda[15] does not show skewing of the average fraction of momentum of the valence quarks in the proton. This lattice result is in contradiction to the predictions of the QCD sum rules and does cast some doubt on the validity of the model of the proton distribution proposed by Chernyak *et al.*[49] The lattice calculation is performed in the quenched approximation with Wilson fermions and requires an extrapolation to the chiral limit.

The contribution of soft momentum exchange to the hadron form factors is a potentially serious complication when one uses the QCD sum rule model distribution amplitudes. In the analysis of Ref. 24 it was argued that only about 1% of the proton form factor comes from regions of integration in which all the propagators are hard. A new analysis by Dziembowski *et al.*[57] shows that the QCD sum rule[16] distribution amplitudes of Chernyak *et al.*[16] together with the perturbative QCD prediction gives contributions to the form factors which agree with the measured normalization of the pion form factor at $Q^2 >$

4 GeV^2 and proton form factor $Q^2 > 20\ GeV^2$ to within a factor of two. In the calculation the virtuality of the exchanged gluon is restricted to $|k^2| > 0.25\ GeV^2$. The authors assume $\alpha_s = 0.3$ and that the underlying wavefunctions fall off exponentially at the $x \simeq 1$ endpoints. Another model of the proton distribution amplitude with diquark clustering[58] chosen to satisfy the QCD sum rule moments come even closer. Considering the uncertainty in the magnitude of the higher order corrections, one really cannot expect better agreement between the QCD predictions and experiment.

The relative importance of non-perturbative contributions to form factors is also an issue. Unfortunately, there is little that can be said until we have a deeper understanding of the end-point behavior of hadronic wavefunctions, and of the role played by Sudakov form factors in the end-point region. Models have been constructed in which non-perturbative effects persist to high Q.[24] Other models have been constructed in which such effects vanish rapidly as Q increases.[25,26,27]

If the QCD sum rule results are correct then, the light hadrons are highly structured oscillating momentum-space valence wavefunctions. In the case of mesons, the results from both the lattice calculations and QCD sum rules show that the light quarks are highly relativistic. This gives further indication that while nonrelativistic potential models are useful for enumerating the spectrum of hadrons (because they express the relevant degrees of freedom), they may not be reliable in predicting wave function structure.

5.7. Calculating T_H

The calculation of hard-scattering diagrams for exclusive processes in QCD becomes increasingly arduous as the number of incident and final parton lines increases. The tree-graph calculations of T_H have been completed for the meson and baryon form factors, as well as for many exclusive two-photon processes such as $\gamma\gamma \to p\overline{p}$ for both real and virtual photons and various Compton scattering reactions. Further discussion of the two-photon predictions is given in Section 7.

The most efficient computational methods involve two-component spinor techniques where the amplitude itself can be converted to a trace. This method was first used by Bjorken and Chen[59] for their calculation of the QED "trident" amplitudes for $\mu Z \to \mu\mu\mu$. It was further developed by the CALKUL group and applied to exclusive processes by Farrar[60] and Gunion[61] and their co-workers.

The large number of PQCD tree graph (300,000 for pp scattering) may help to explain the relatively large normalization of the pp amplitude at large momentum transfer. For example the nominal one-gluon exchange amplitude $4\pi C_F(s/t)\alpha_s(t)[F_1^p(t)]^2$ gives a contribution only about 10^{-3} of that required by the large angle pp scattering data. It is clearly necessary to develop highly efficient and automatic methods for evaluating multi-particle hard scattering amplitudes T_H for reactions such as pp scattering. The light-cone quantization method could prove highly effective. In this method one expands the S-matrix in the τ-ordered perturbation theory. For numerical computations one can use a discrete basis, such that in each intermediate state one sums over a complete set of discretized Fock states, defined using periodic or anti-periodic boundary conditions. The matrix elements of the light-cone Hamiltonian $H_{QCD}^{interaction}$ are simple to compute. In the expansion all Feynman diagrams and all time-orderings are automatically summed.

In principle the perturbative QCD predictions can be calculated systematically in powers of $\alpha_s(Q^2)$. In practice the calculations are formidable, and thus far only the next-to-leading correction to the pion form factor and the $\gamma\gamma \rightarrow \pi\pi$ amplitude have been systematically studied. The two-photon amplitude analysis is given by Nizic[62] and is discussed further in Section 7. The complete analysis of the meson form factor to this order requires evaluating the one-loop corrections to the hard-scattering amplitude for $\gamma q\overline{q} \rightarrow q\overline{q}$, plus a corresponding correction to the kernel for the meson distribution amplitude. The one-loop corrections to T_H for the meson form factor have been evaluated by several groups. Because of different conventions the results differ in detail; however Braaten and Tse[18] have resolved the discrepancies between the three previous calculations. An important feature is the presence of correction terms of order $\frac{\alpha_s}{4\pi}(\frac{11}{3}C_A - \frac{2}{3})\log[(1-x)(1-y)Q^2]$ which sets the scale of the running coupling constant in the leading order contribution at $Q^2_{eff} = (1-x)(1-y)Q^2$. This is consistent with the expectation that the running coupling constant scale is set by the virtuality of the exchanged gluon propagator, just as in Abelian QED. This is also consistent with the automatic scale-fixing scheme of Ref. 63. Thus a significant part of the PQCD higher order corrections can be absorbed by taking the natural choice for the argument of the running coupling constant. The next-to-leading correction to the kernel for the meson distribution amplitude has also been evaluated by several groups. A surprising feature of this analysis is the fact that conformal symmetry cannot be used as a guide to predict the form the results even when the β-function is set to zero.[13] This is discussed in further detail in Section 4.2

5.8. THE PRE-QCD DEVELOPMENT OF EXCLUSIVE REACTIONS

The study of exclusive processes in terms of underlying quark subprocesses in fact began before the discovery of QCD. The advent of the parton model and Bjorken scaling for deep inelastic structure functions in the late 1960's brought a new focus to the structure of form factors and exclusive processes at large momentum transfer. The underlying theme of the parton model was the concept that quarks carried the electromagnetic current within hadrons. The use of time-ordered perturbation theory in an "infinite momentum frame", or equivalently, quantization on the light cone, provided a natural language for hadrons as composites of relativistic partons, *i.e.* point-like constituents.[64] As discussed in Section 3, Drell and Yan[10] introduced Eq. (57) for current matrix elements in terms of a Fock state expansion at infinite momentum. (Later this result was shown to be an exact result using light-cone quantization.)

Drell and Yan suggested that the form factor is dominated by the end-point region $x \approx 1$. Then it is clear from the Drell-Yan formula that the form factor fall-off at large Q^2 is closely related to the $x \to 1$ behavior of the hadron structure function. The relation found by Drell and Yan was

$$F(Q^2) \sim \frac{1}{(Q^2)^n} \quad \text{if} \quad F_2(x, Q^2) \sim (1-x)^{2n-1}.$$

Gribov and Lipatov[65] extended this relationship to fragmentation functions $D(z, Q^2)$ at $z \to 1$, taking into account cancellations due to quark spin. Feynman[66] noted that the Drell-Yan relationship was also true in gauge theory models in which the endpoint behavior of structure functions is suppressed due to the emission of soft or "wee" partons by charged lines. However, as discussed in Section 4, the endpoint region is suppressed in QCD relative to the leading perturbative contributions.

The parton model was extended to exclusive processes such as hadron-hadron scattering and photoproduction by Blankenbecler, Brodsky, and Gunion[67] and by Landshoff and Polkinghorne.[68] It was recognized that independent of specific dynamics, hadrons could interact and scatter simply by exchanging their common constituents. These authors showed that the amplitude due to quark interchange (or rearrangement) could be written in closed form as an overlap of the light-cone wavefunctions of the incident and final hadrons. In order to make definite predictions, model wavefunctions were chosen to reproduce the fall-off of the form factors obtained from the Drell-Yan formula. Two-body exclusive amplitudes in the "constituent interchange model" then take the form of "fixed-angle" scaling laws

$$\frac{d\sigma}{dt}(AB \to CD) \sim \frac{f(\theta_{cm})}{s^N}$$

where the power N reflects the power-law fall-off of the elastic form factors of the scattered hadrons. The form of the angular dependence $f(\theta_{cm})$ reflects the number of interchanged quarks.

Even though the constituent interchange is model was motivated in part by the Drell-Yan endpoint analysis of form factors, many of the predictions and systematics of quark interchange remain applicable in the QCD analysis.[67] A comprehensive series of measurements of elastic meson nucleon scattering reactions has recently been carried out by Baller *et al.*[69] at BNL. Empirically, the quark interchange amplitudes gives a reasonable account of the scaling, angular dependence, and relative magnitudes of the various channels. For example, the strong differences between K^+p and K^-p scattering is accounted for by u quark interchange in the K^+p amplitude. It is inconsistent with gluon exchange as the dominant amplitude since this produces equal scattering for the two channels. The dominance of quark interchange over gluon exchange is a surprising result which eventually needs to be understood in the context of QCD.

The prediction of fixed angle scaling laws laid the groundwork for the derivation of the "dimensional counting rules." As discussed in Ref. 5, it is natural to assume that at large momentum transfer, an exclusive amplitude factorize as a convolution of hadron wavefunctions which couple the hadrons to their quark constituents with a hard scattering amplitude T_H which scatters the quarks from the initial to final direction. Since the hadron wavefunction is maximal when the quarks are nearly collinear with each parent hadron, the large momentum transfer occurs in T_H. The pre-QCD argument went as follows: the dimension of T_H is $[L^{n-4}]$ where $n = n_A + n_B + n_C + n_D$ is the total number of fields entering T_H. In a renormalizable theory where the coupling constant is dimensionless and masses can be neglected at large momentum transfer, all connected tree-graphs for T_H then scale as $[1/\sqrt{s}]^{n-4}$ at fixed t/s. This immediately gives the dimensional counting law[5]

$$\frac{d\sigma}{dt}(AB \to CD) \sim \frac{f(\theta_{cm})}{s^{n_A+n_B+n_C+n_D-2}}.$$

In the case of incident or final photons or leptons $n = 1$. Specializing to elastic lepton-hadron scattering, this also implies $F(Q^2) \sim 1/(Q^2)^{n_H-1}$ for the spin averaged form factor, where n_H is the number of constituents in hadron H. These results were obtained independently by Matveev *et al.*[5] on the basis of an "automodality" principle, that the underlying constituent interactions are scale free.

As we have seen, the dimensional counting scaling laws will generally be modified by the accumulation of logarithms from higher loop corrections to the hard scattering amplitude T_H; the phenomenological success of the counting rules in their simplest form thus implies that the loop corrections be somewhat mild. As we have seen, it is the asymptotic freedom property of QCD which in fact makes higher order corrections an exponentiation of a $\log\log Q^2$ series, thus preserving the form of the dimensional counting rules modulo only logarithmic corrections.

6. EXCLUSIVE e^+e^- ANNIHILATION PROCESSES

The study of time-like hadronic form factors using e^+e^- colliding beams can provide very sensitive tests of the QCD helicity selection rule. This follows because the virtual photon in $e^+e^- \to \gamma^* \to h_A \bar{h}_B$ always has spin ± 1 along the beam axis at high energies.[#15] Angular-momentum conservation implies that the virtual photon can "decay" with one of only two possible angular distributions in the center-of-momentum frame: $(1+\cos^2\theta)$ for $|\lambda_A - \lambda_B| = 1$, and $\sin^2\theta$ for $|\lambda_A - \lambda_B| = 0$, where $\lambda_{A,B}$ are the helicities of hadron $h_{A,B}$. Hadronic-helicity conservation, Eq. (7), as required by QCD greatly restricts the possibilities. It implies that $\lambda_A + \lambda_B = 2\lambda_A = -2\lambda_B$. Consequently, angular-momentum conservation requires $|\lambda_A| = |\lambda_B| = \frac{1}{2}$ for baryons and $|\lambda_A| = |\lambda_B| = 0$ for mesons; and the angular distributions are now completely determined:

$$\frac{d\sigma}{d\cos\theta}(e^+e^- \to B\overline{B}) \propto 1 + \cos^2\theta(\text{baryons}),$$
$$\frac{d\sigma}{d\cos\theta}(e^+e^- \to M\overline{M}) \propto \sin^2\theta(\text{mesons}).$$

It should be emphasized that these predictions are far from trivial for vector mesons and for all baryons. For example, one expects distributions like $\sin^2\theta$ for baryon pairs in theories with a scalar or tensor gluon. Simply verifying these angular distributions would give strong evidence in favor of a vector gluon.

#15 This follows from helicity conservation as well, which is a well-known property of QED at high energies. The electron and positron must have opposite helicities; *i.e.* $\gamma_e + \gamma_{\bar{e}} = 0$, since it is the total helicity carried by fermions (alone) which is conserved, and there are no fermions in the intermediate state. In the laboratory frame ($\to p_e = - \to p_{\bar{e}}$), their *spins* must be parallel, resulting in a virtual photon with spin ± 1 along the beam.

The power-law dependence on s of these cross sections is also predicted in QCD, using the dimensional-counting rule. Such "all-orders" predictions for QCD allowed processes are summarized in Table II.[6,70] Processes suppressed in QCD are also listed there; these all violate hadronic-helicity conservation, and are suppressed by powers of m^2/s in QCD. This would not necessarily be the case in scalar or tensor theories.

Table II

Exclusive channels in e^+e^- annihilation. The $h_A\overline{h}_B\gamma^*$ couplings in allowed processes are $-ie(p_A - p_B)^\mu F(s)$ for mesons, $-ie\overline{v}(p_B)\gamma^\mu G(s)u(p_A)$ for baryons, and $-ie^2\epsilon_{\mu\nu\rho}p^\nu_M\epsilon^\rho p^\sigma_\gamma F_{M\gamma}(s)$ for meson-photon final states. Similar predictions apply to decays of heavy-quark vector states, such as $\psi, \psi', \ldots$, produced in e^+e^- collisions.

	$e^+e^- \to h_A(\lambda_A)\overline{h}_B(\lambda_B)$	Angular distribution	$\frac{\sigma(e^+e^-\to h_A\overline{h}_B)}{\sigma(e^+e^-\to\mu^+\mu^-)}$
	$e^+e^- \to \pi^+\pi^-, K^+K^-$	$\sin^2\theta$	$\frac{1}{4}\|F(s)\|^2 \sim c/s^2$
	$e^+e^- \to \rho^+\rho^-(0), K^{*+}K^{*-}$	$\sin^2\theta$	$\frac{1}{4}\|F(s)\|^2 \sim c/s^2$
Allowed	$e^+e^- \to \pi^0\gamma(\pm1), \eta\gamma, \eta'\gamma$	$1+\cos^2\theta$	$(\pi\alpha/2)s\|F_{M\gamma}(s)\|^2 \sim c/s$
in QCD	$e^+e^- \to p(\pm\frac{1}{2})\overline{p}(\mp\frac{1}{2}), n\overline{n}, \ldots$	$1+\cos^2\theta$	$\|G(s)\|^2 \sim c/s^4$
	$e^+e^- \to p(\pm\frac{1}{2})\overline{\Delta}(\mp\frac{1}{2}), \overline{n}\Delta \ldots$	$1+\cos^2\theta$	$\|G(s)\|^2 \sim c/s^4$
	$e^+e^- \to \Delta(\pm\frac{1}{2})\overline{\Delta}(\mp\frac{1}{2}), y^*\overline{y}^*, \ldots$	$1+\cos^2\theta$	$\|G(s)\|^2 \sim c/s4$
	$e^+e^- \to \rho^+(0)\rho^-(\pm1), \pi^+\rho^-, K^+K^{*-}, \ldots$	$1+\cos^2\theta$	$< c/s^3$
Suppressed	$e^+e^- \to \rho^+(\pm1)\rho^-(\pm1), \ldots$	$\sin^2\theta$	$< c/s^3$
in QCD	$e^+e^- \to p(\pm\frac{1}{2})\overline{p}(\pm\frac{1}{2}), p\overline{\Delta}, \Delta\overline{\Delta}, \ldots$	$\sin 2\theta$	$< c/s^5$
	$e^+e^- \to p(\pm\frac{1}{2})\overline{\Delta}(\pm\frac{3}{2}), \Delta\overline{\Delta}, \ldots$	$1+\cos^2\theta$	$< c/s^5$
	$e^+e^- \to \Delta(\pm\frac{3}{2})\overline{\Delta}(\pm\frac{3}{2}), \ldots$	$\sin^2\theta$	$< c/s^5$

Table II

All of these perturbative predictions assume that s is sufficiently far from resonance contributions.

Notice the $e^+e^- \to \pi\rho, \pi\omega, KK^*, \ldots$, are all suppressed in QCD. This occurs because the $\gamma - \pi - \rho$ can couple through only a single form factor – $\epsilon^{\mu\nu\tau\sigma}\epsilon^{(\gamma)}_\mu\epsilon^{(\rho)}_\nu p^{(\pi)}_\tau p^{(\rho)}_\sigma F_{\pi\rho}(s)$ — and this requires $|\ \lambda_\rho\ | = 1$ in e^+e^- collisions. Hadronic-helicity conservation requires $\lambda = 0$ for mesons, and thus these amplitudes are suppressed in QCD (although, again, not in scalar or tensor theories). Notice however that the processes $e^+e^- \to \gamma\pi, \gamma\eta, \gamma\eta'$ are allowed by the helicity selection rule; helicity conservation applies only to the hadrons. Unfortunately the form factors governing these last processes are not expected to be large, *e.g.* $F_{\pi\gamma}(s) \sim 2f_\pi/s$.

These form factors can also tell us about the quark distribution amplitudes $\phi_H(x_i, Q)$. For example sum rules require (to all orders in α_s) that $\pi^+\pi^-, K^+K^-$, and $\rho^+\rho^-$ (helicity-zero) pairs are produced in the ratio of $f_\pi^4 : f_K^4 : 4f_\rho^4 \sim 1 : 2 : 7$, respectively if the π, K, and ρ distribution amplitudes are of similar shape. These ratios must apply at very large energies, where all distribution amplitudes tend to $\phi \propto x(1-x)$. On the other hand, the kaon's distribution amplitude may be quite asymmetric about $x = \frac{1}{2}$ at low energies due to the large difference between s and u, d quark masses. This could enhance K^+K^- production. (Distribution amplitudes for π's and ρ's must be symmetric due to isospin.) The process $e^+e^- \to K_L K_S$ is only possible if the kaon distribution amplitude is asymmetric;[#16] the presence or absence of $K_L K_S$ pairs relative to K^+K^- pairs is thus a sensitive indicator of asymmetry in the wave function.

6.1. J/ψ Decay to Hadron Pairs

The exclusive decays of heavy-quark atoms $(J/\psi, \psi', \ldots)$ into light hadrons can also be analyzed in QCD.[71] The decay $\psi \to p\overline{p}$, for example, proceeds via diagrams such as those in Fig. 27. Since ψ's produced in e^+e^- collisions must also have spin ± 1 along the beam direction and since they can only couple to light quarks via gluons, all the properties listed in Table II apply to $\psi, \psi', \Upsilon, \Upsilon', \ldots$ decays as well. Already there is considerable experimental data for the ψ and ψ' decays.[72,73]

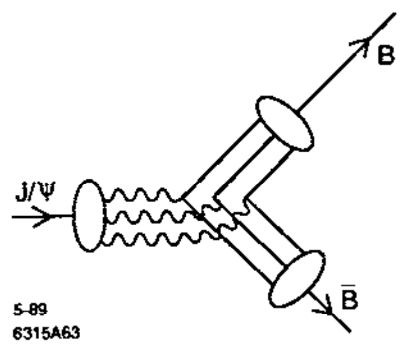

Figure 27. Quark-gluon subprocesses for $\psi \to B\overline{B}$.

#16 For example, this amplitude vanishes under the (stronger) assumption of exact flavor-$SU(3)$ symmetry. This is easily seen by defining G_U parity, in analogy to G parity: $G_U = C\exp(i\pi U_2)$, where the U_i are the isospin-like generators of $SU(3)_f$ which connect the K_0 and $\overline{K}_0$. The final state in $e^+e^- \to K_L K_S$ has positive G_U parity, while the intermediate photon has negative G_U parity. G_U parity is conserved if $SU(3)_f$ is exact, and $e^+e^- \to K_L K_S$ then vanishes.

Perhaps the most significant are the decays $\psi, \psi' \rightarrow p\overline{p}, n\overline{n}, \ldots$. The predicted angular distribution $1+ \cos^2\theta$ is consistent with published data.[73] This is important evidence favoring a vector gluon, since scalar- or tensor-gluon theories would predict a distribution of $\sin^2\theta + O(\alpha_s)$. Dimensional-counting rules can be checked by comparing the ψ and ψ' rates into $p\overline{p}$, normalized by the total rates into light-quark hadrons so as to remove dependence upon the heavy-quark wave functions. Theory predicts that the ratio of branching fractions for the $p\overline{p}$ decays of the ψ and ψ' is

$$\frac{B(\psi' \rightarrow p\overline{p})}{B(\psi \rightarrow p\overline{p})} \sim Q_{e^+e^-} \left(\frac{M_\psi}{M'_\psi}\right)^8 ,$$

where $Q_{e^+e^-}$ is the ratio of branching fractions into e^+e^-:

$$Q_{e^+e^-} \equiv \frac{B(\psi' \rightarrow e^+e^-)}{B(J/\psi \rightarrow e^+e^-)} = 0.135 \pm 0.023 \quad .$$

Existing data suggest a ratio $(M_{\psi'}/M_\psi)^n$ with $n = 6 \pm 3$, in good agreement with QCD. One can also use the data for $\psi \rightarrow p\overline{p}, \Lambda\overline{\Lambda}, \Xi\Xi, \ldots$, to estimate the relative magnitudes of the quark distribution amplitudes for baryons. Correcting for phase space, one obtains $\phi_p \sim 1.04(13)\ \phi_n \sim 0.82(5)\ \phi_\Xi \sim 1.08(8)\ \phi_\Sigma \sim 1.14(5)\ \phi_\Lambda$ by assuming similar functional dependence on the quark momentum fractions x_i for each case.

As is well known, the decay $\psi \rightarrow \pi^+\pi^-$ must be electromagnetic if G-parity is conserved by the strong interactions. To leading order in α_s, the decay is through a virtual photon (*i.e.* $\psi \rightarrow \gamma^* \rightarrow \pi^+\pi^-$) and the rate is determined by the pion's electromagnetic form factor:

$$\frac{\Gamma(\psi \rightarrow \pi^+\pi^-)}{\Gamma(\psi \rightarrow \mu^+\mu^-)} = \frac{1}{4}[F_\pi(s)]^2[1 + O(\alpha_s(s))],$$

where $s = (3.1GeV)^2$. Taking $F_\pi(s) \simeq (1 - s/m_\rho^2)^{-1}$ gives a rate $\Gamma(\psi \rightarrow \pi^+\pi^-) \sim 0.0011\ \Gamma(\psi \rightarrow \mu^+\mu^-)$, which compares well with the measured ratio 0.0015(7). This indicates that there is indeed little asymmetry in the pion's wave function.

The same analysis applied to $\psi \rightarrow K^+K^-$ suggests that the kaon's wave function is nearly symmetric about $x = \frac{1}{2}$. The ratio $\Gamma(\psi \rightarrow K^+K^-)/\Gamma(\psi \rightarrow \pi^+\pi^-)$ is 2 ± 1, which agrees with the ratio $(f_K/f_\pi)^4 \sim 2$ expected if π and K have similar quark distribution amplitudes. This conclusion is further supported by measurements of $\psi \rightarrow K_L K_S$ which vanishes completely if the K distribution amplitudes are symmetric; experimentally the limit is $\Gamma(\psi \rightarrow K_L K_S)/\Gamma(\psi \rightarrow K^+K^-) \lesssim \frac{1}{2}$.

6.2. THE π-ρ PUZZLE

We have emphasized that a central prediction of perturbative QCD for exclusive processes is hadron helicity conservation: to leading order in $1/Q$, the total helicity of hadrons in the initial state must equal the total helicity of hadrons in the final state. This selection rule is independent of any photon or lepton spin appearing in the process. The result follows from (a) neglecting quark mass terms, (b) the vector coupling of gauge particles, and (c) the dominance of valence Fock states with zero angular momentum projection.[6] The result is true in each order of perturbation theory in α_s.

Hadron helicity conservation appears relevant to a puzzling anomaly in the exclusive decays J/ψ and $\psi' \to \rho\pi, K^*\overline{K}$ and possibly other Vector-Pseudoscalar (VP) combinations. One expects the J/ψ and ψ' mesons to decay to hadrons via three gluons or, occasionally, via a single direct photon. In either case the decay proceeds via $|\Psi(0)|^2$, where $\Psi(0)$ is the wave function at the origin in the nonrelativistic quark model for $c\bar{c}$. Thus it is reasonable to expect on the basis of perturbative QCD that for any final hadronic state h that the branching fractions scale like the branching fractions into e^+e^-:

$$Q_h \equiv \frac{B(\psi' \to h)}{B(J/\psi \to h)} \cong Q_{e^+e^-}$$

Usually this is true, as is well documented in Ref. 74 for $p\bar{p}\pi^0$, $2\pi^+2\pi^-\pi^0$, $\pi^+\pi^-\omega$, and $3\pi^+3\pi^-\pi^0$, hadronic channels. The startling exceptions occur for $\rho\pi$ and $K^*\overline{K}$ where the present experimental limits[74] are $Q_{\rho\pi} < 0.0063$ and $Q_{K^*\overline{K}} < 0.0027$.

Perturbative QCD quark helicity conservation implies[6] $Q_{\rho\pi} \equiv [B(\psi' \to \rho\pi)/B(J/\psi \to \rho\pi)] \le Q_{e^+e^-}[M_{J/\psi}/M_{\psi'}]^6$ This result includes a form factor suppression proportional to $[M_{J/\psi}/M_{\psi'}]^4$ and an additional two powers of the mass ratio due to helicity flip. However, this suppression is not nearly large enough to account for the data.[#17]

From the standpoint of perturbative QCD, the observed suppression of $\psi' \to VP$ is to be expected; it is the J/ψ that is anomalous.[75] The ψ' obeys the perturbative QCD theorem that total hadron helicity is conserved in high-momentum

---

#17 There is the possibility is the these form factors are dominated by end-point contributions for which quark masses may be less relevant. Such terms are expected to be strongly suppressed by quickly falling Sudakov form factors. This could also explain the rapid falloff of the $\psi - \pi - \rho$ form factor with increasing M_ψ^2.

transfer exclusive processes. The general validity of the QCD helicity conservation theorem at charmonium energies is of course open to question. An alternative model[76] based on nonperturbative exponential vertex functions, has recently been proposed to account for the anomalous exclusive decays of the J/ψ. However, helicity conservation has received important confirmation in $J/\psi \to p\overline{p}$ where the angular distribution is known experimentally to follow $[1 + \cos^2\theta]$ rather than $\sin^2\theta$ for helicity flip, so the decays $J/\psi \to \pi\rho$, and $K\overline{K}$ seem truly exceptional.

The helicity conservation theorem follows from the assumption of short-range point-like interactions among the constituents in a hard subprocess. One way in which the theorem might fail for $J/\psi \to$ gluons $\to \pi\rho$ is if the intermediate gluons resonate to form a gluonium state $\mathcal{O}$. If such a state exists, has a mass near that of the J/ψ, and is relatively stable, then the subprocess for $J/\psi \to \pi\rho$ occurs over large distances and the helicity conservation theorem need no longer apply. This would also explain why the J/ψ decays into $\pi\rho$ and not the ψ'.

Tuan *et al.*[75] have thus proposed, following Hou and Soni,[77] that the enhancement of $J/\psi \to K^*\overline{K}$ and $J/\psi \to \rho\pi$ decay modes is caused by a quantum mechanical mixing of the J/ψ with a $J^{PC} = 1^{--}$ vector gluonium state $\mathcal{O}$ which causes the breakdown of the QCD helicity theorem. The decay width for $J/\psi \to \rho\pi(K^*\overline{K})$ via the sequence $J/\psi \to \mathcal{O} \to \rho\pi(K^*\overline{K})$ must be substantially larger than the decay width for the (non-pole) continuum process $J/\psi \to 3$ gluons $\to \rho\pi(K^*\overline{K})$. In the other channels (such as $p\overline{p}, p\overline{p}\pi^0, 2\pi^+2\pi^-\pi^0$, etc.), the branching ratios of the $\mathcal{O}$ must be so small that the continuum contribution governed by the QCD theorem dominates over that of the $\mathcal{O}$ pole. For the case of the ψ' the contribution of the $\mathcal{O}$ pole must always be inappreciable in comparison with the continuum process where the QCD theorem holds. The experimental limits on $Q_{\rho\pi}$ and $Q_{K^*\overline{K}}$ are now substantially more stringent than when Hou and Soni made their estimates of $M_{\mathcal{O}}$, $\Gamma_{\mathcal{O}\to\rho\pi}$ and $\Gamma_{\mathcal{O}\to K^*\overline{K}}$ in 1982.

A gluonium state of this type was first postulated by Freund and Nambu[78] based on OZI dynamics soon after the discovery of the J/ψ and ψ' mesons. In fact, Freund and Nambu predicted that the $\mathcal{O}$ would decay copiously precisely into $\rho\pi$ and $K^*\overline{K}$ with severe suppression of decays into other modes like e^+e^- as required for the solution of the puzzle.

Branching fractions for final states h which can proceed only through the intermediate gluonium state have the ratio:

$$Q_h = Q_{e^+e^-} \frac{(M_{J/\psi} - M_{\mathcal{O}})^2 + \frac{1}{4}\,\Gamma_0^2}{(M_{\psi'} - M_{\mathcal{O}})^2 + \frac{1}{4}\,\Gamma_0^2} \ .$$

It is assumed that the coupling of the J/ψ and ψ' to the gluonium state scales as the e^+e^- coupling. The value of Q_h is small if the $\mathcal{O}$ is close in mass to the J/ψ. Thus one requires $(M_{J/\psi} - M_{\mathcal{O}})^2 + \frac{1}{4}\,\Gamma_{\mathcal{O}}^2 \lesssim 2.6\, Q_h$ GeV^2. The experimental limit for $Q_{K^*\overline{K}}$ then implies $\left[(M_{J/\psi} - M_{\mathcal{O}})^2 + \frac{1}{4}\,\Gamma_{\mathcal{O}}^2\right]^{1/2} \lesssim 80$ MeV. This implies $\mid M_{J/\psi} - M_{\mathcal{O}} \mid < 80$ MeV and $\Gamma_{\mathcal{O}} < 160$ MeV. Typical allowed values are $M_{\mathcal{O}} =$ 3.0 GeV, $\Gamma_{\mathcal{O}} = 140$ MeV or $M_{\mathcal{O}} = 3.15$ GeV, $\Gamma_{\mathcal{O}} = 140$ MeV. Notice that the gluonium state could be either lighter or heavier than the J/ψ. The branching ratio of the $\mathcal{O}$ into a given channel must exceed that of the J/ψ.

It is not necessarily obvious that a $J^{PC} = 1^{--}$ gluonium state with these parameters would necessarily have been found in experiments to date. One must remember that though $\mathcal{O} \to \rho\pi$ and $\mathcal{O} \to K^*\overline{K}$ are important modes of decay, at a mass of order 3.1 GeV many other modes (albeit less important) are available. Hence, a total width $\Gamma_{\mathcal{O}} \cong 100$ to 150 MeV is quite conceivable. Because of the proximity of $M_{\mathcal{O}}$ to $M_{J/\psi}$, the most important signatures for an $\mathcal{O}$ search via exclusive modes $J/\psi \to K^*\overline{K}h$, $J/\psi \to \rho\pi h$; $h = \pi\pi, \eta, \eta'$, are no longer available by phase-space considerations. However, the search could still be carried out using $\psi' \to K^*\overline{K}h$, $\psi' \to \rho\pi h$; with $h = \pi\pi$, and η. Another way to search for $\mathcal{O}$ in particular, and the three-gluon bound states in general, is via the inclusive reaction $\psi' \to (\pi\pi) + X$, where the $\pi\pi$ pair is an isosinglet. The three-gluon bound states such as $\mathcal{O}$ should show up as peaks in the missing mass (*i.e.* mass of X) distribution.

The most direct way to search for the $\mathcal{O}$ is to scan $\overline{p}p$ or e^+e^- annihilation at $\sqrt{s}$ within ~ 100 MeV of the J/ψ, triggering on vector/pseudoscalar decays such as $\pi\rho$ or $\overline{K}K^*$.

The fact that the $\rho\pi$ and $K^*\overline{K}$ channels are strongly suppressed in ψ' decays but not in J/ψ decays clearly implies dynamics beyond the standard charmonium analysis. The hypothesis of a three-gluon state $\mathcal{O}$ with mass within $\cong 100$ MeV of the J/ψ mass provides a natural, perhaps even compelling, explanation of this anomaly. If this description is correct, then the ψ' and J/ψ hadronic decays not only confirm hadron helicity conservation (at the ψ' momentum scale), but they also provide a signal for bound gluonic matter in QCD.

6.3. Form Factor Zeros in QCD

The exclusive pair production of heavy hadrons $|Q_1\overline{Q}_2\rangle$, $|Q_1Q_2Q_3\rangle$ consisting of higher generation quarks ($Q_i = t, b, c$, and possibly s) can be reliably predicted within the framework of perturbative QCD, since the required wavefunction input is essentially determined from nonrelativistic considerations.[79] The results can be applied to e^+e^- annihilation, $\gamma\gamma$ annihilation, and W and Z decay into higher generation pairs. The normalization, angular dependence and helicity structure can be predicted away from threshold, allowing a detailed study of the basic elements of heavy quark hadronization.

A particularly striking feature of the QCD predictions is the existence of a zero in the form factor and e^+e^- annihilation cross section for zero-helicity hadron pair production close to the specific timelike value $q^2/4M_H^2 = m_h/2m_\ell$ where m_h and m_ℓ are the heavier and lighter quark masses, respectively. This zero reflects the destructive interference between the spin-dependent and spin-independent (Coulomb exchange) couplings of the gluon in QCD. In fact, all pseudoscalar meson form factors are predicted in QCD to reverse sign from spacelike to timelike asymptotic momentum transfer because of their essentially monopole form. For $m_h > 2m_\ell$ the form factor zero occurs in the physical region.

To leading order in $1/q^2$, the production amplitude for hadron pair production is given by the factorized form

$$M_{H\overline{H}} = \int [dx_i] \int [dy_j]\, \phi_H^\dagger(x_i, \widetilde{q}^2)\, \phi_{\overline{H}}^\dagger(y_j, \widetilde{q}^2)\, T_H(x_i, y_j; \widetilde{q}^2, \theta_{CM})$$

where $[dx_i] = \delta\left(\sum_{k=1}^n x_k - 1\right) \prod_{k=1}^n dx_k$ and $n = 2, 3$ is the number of quarks in the valence Fock state. The scale $\widetilde{q}^2$ is set from higher order calculations, but it reflects the minimum momentum transfer in the process. The main dynamical dependence of the form factor is controlled by the hard scattering amplitude T_H which is computed by replacing each hadron by collinear constituents $P_i^\mu = x_i P_H^\mu$. Since the collinear divergences are summed in ϕ_H, T_H can be systematically computed as a perturbation expansion in $\alpha_s(q^2)$.

The distribution amplitude required for heavy hadron production $\phi_H(x_i, q^2)$ is computed as an integral of the valence light-cone Fock wavefunction up to the scale Q^2. For the case of heavy quark bound states, one can assume that the constituents are sufficiently non-relativistic that gluon emission, higher Fock states, and retardation of the effective potential can be neglected. The analysis of Section 2 is thus relevant. The quark distributions are then controlled by a simple nonrelativistic wavefunction, which can be taken in the model form:

$$\psi_M(x_i, \vec{k}_{\perp i}) = \frac{C}{x_1^2 x_2^2 \left[M_H^2 - \dfrac{\vec{k}_{\perp 1}^2 + m_1^2}{x_1} - \dfrac{\vec{k}_{\perp 2}^2 + m_2^2}{x_2}\right]^2}$$

This form is chosen since it coincides with the usual Schrödinger- Coulomb wavefunction in the nonrelativistic limit for hydrogenic atoms and has the correct large momentum behavior induced from the spin- independent gluon couplings. The wavefunction is peaked at the mass ratio $x_i = m_i/M_H$:

$$\left(x_i - \frac{m_i}{M_H}\right)^2 \sim \frac{\langle k_z^2 \rangle}{M_H^2}$$

where $\langle k_z^2 \rangle$ is evaluated in the rest frame. Normalizing the wavefunction to unit probability gives

$$C^2 = 128\pi \left(\langle v^2 \rangle\right)^{5/2} m_r^5 (m_1 + m_2)$$

where $\langle v^2 \rangle$ is the mean square relative velocity and $m_r = m_1 m_2/(m_1 + m_2)$ is the reduced mass. The corresponding distribution amplitude is

$$\begin{aligned}\phi(x_i) &= \frac{C}{16\pi^2} \frac{1}{[x_1 x_2 M_H^2 - x_2 m_1^2 - x_1 m_2^2]} \\ &\cong \frac{1}{\sqrt{2\pi}} \frac{\gamma^{3/2}}{M_H^{1/2}} \delta\left(x_1 - \frac{m_1}{m_1 + m_2}\right) .\end{aligned}$$

It is easy to see from the structure of T_H for $e^+e^- \to M\overline{M}$ that the spectator quark pair is produced with momentum transfer squared $q^2 x_s y_s = 4m_s^2$. Thus heavy hadron pair production is dominated by diagrams in which the primary coupling of the virtual photon is to the heavier quark pair. The perturbative predictions are thus expected to be accurate even near threshold to leading order in $\alpha_s(4m_\ell^2)$ where m_ℓ is the mass of lighter quark in the meson.

The leading order e^+e^- production helicity amplitudes for higher generation meson ($\lambda = 0, \pm 1$) and baryon ($\lambda = \pm 1/2, \pm 3/2$) pairs are computed in Ref. 79 as a function of q^2 and the quark masses. The analysis is simplified by using the peaked form of the distribution amplitude, Eq. (6). In the case of meson pairs the (unpolarized) e^+e^- annihilation cross section has the general form[#18]

#18 $F_{\lambda\overline{\lambda}}(q^2)$ is the form factor for the production of two mesons which have both spin and helicity (Z-component of spin) as λ and $\overline{\lambda}$ respectively. There are two Lorentz and gauge invariant form factors of vector pair production. However, one of them turns out to be the same as the form factor of pseudoscalar plus vector production multiplied by M_H. Therefore the differential cross section for the production of two mesons with spin 0 or 1 can be represented in terms of three independent form factors.

$$4\pi \frac{d\sigma}{d\Omega} (e^+e^- \to M_\lambda \overline{M}_{\overline{\lambda}}) = \frac{3}{4} \beta \sigma_{e^+e^- \to \mu^+\mu^-} \left[\frac{1}{2} \beta^2 \sin^2 \theta \right.$$

$$\times \left[|F_{0,0}(q^2)|^2 + \frac{1}{(1-\beta^2)^2} \left\{ (3 - 2\beta^2 + 3\beta^4) |F_{1,1}(q^2)|^2 \right.\right.$$

$$\left.\left. - 4(1+\beta^2) \operatorname{Re}(F_{1,1}(q^2) F^*_{0,1}(q^2)) + 4|F_{0,1}(q^2)|^2 \right\} \right]$$

$$\left. + \frac{3\beta^2}{2(1-\beta^2)} (1 + \cos^2\theta) |F_{0,1}(q^2)|^2 \right]$$

where $q^2 = s = 4M_H^2 \overline{q}^2$ and the meson velocity is $\beta = 1 - \frac{4M_H^2}{q^2}$. The production form factors have the general form

$$F_{\lambda\overline{\lambda}} = \frac{\langle v^2 \rangle^2}{(\overline{q}^2)^2} (A_{\lambda\overline{\lambda}} + \overline{q}^2 B_{\lambda\overline{\lambda}})$$

where A and B reflect the Coulomb-like and transverse gluon couplings, respectively. The results to leading order in α_s are given in Ref. 79. In general A and B have a slow logarithmic dependence due to the q^2-evolution of the distribution amplitudes. The form factor zero for the case of pseudoscalar pair production reflects the numerator structure of the T_H amplitude.

$$\text{Numerator} \sim \epsilon_1 \left(\overline{q}^2 - \frac{m_1^2}{4M_H^2} \frac{1}{x_2 y_1} - \frac{m_2^2}{4M_H^2} \frac{x_1}{x_2^2 y_2} \right)$$

For the peaked wavefunction,

$$F^M_{0,0}(q^2) \propto \frac{1}{(\overline{q}^2)^2} \left\{ \epsilon_1 \left(\overline{q}^2 - \frac{m_1}{2m_2} \right) + \epsilon_2 \left(\overline{q}^2 - \frac{m_2}{2m_1} \right) \frac{m_2^2}{m_1^2} \right\}$$

If m_1 is much greater than m_2 then the ϵ_1 is dominant and changes sign at $q^2/4M_H^2 = m_1/2m_2$. The contribution of the ϵ_2 term and higher order contributions are small and nearly constant in the region where the ϵ_1 term changes sign; such contributions can displace slightly but not remove the form factor zero.

These results also hold in quantum electrodynamics; *e.g.* pair production of muonium ($\mu - e$) atoms in $e_+ e_-$ annihilation. Gauge theory predicts a zero at $\overline{q}^2 = m_\mu / 2m_e$.

These explicit results for form factors also show that the onset of the leading power-law scaling of a form factor is controlled by the ratio of the A and B terms; *i.e.* when the transverse contributions exceed the Coulomb mass-dominated contributions. The Coulomb contribution to the form factor can also be computed directly from the convolution of the initial and final wavefunctions. Thus, contrary to the claim of Ref. 24 there are no extra factors of $\alpha_s(q^2)$ which suppress the "hard" versus nonperturbative contributions.

The form factors for the heavy hadrons are normalized by the constraint that the Coulomb contribution to the form factor equals the total hadronic charge at $q^2 = 0$. Further, by the correspondence principle, the form factor should agree with the standard non-relativistic calculation at small momentum transfer. All of these constraints are satisfied by the form

$$F^M_{0,0}(q^2) = e_1 \frac{16\gamma^4}{(q^2+\gamma^2)^2} \left(\frac{M_H^2}{m_2^2}\right)^2 \left(1 - \frac{q^2}{4M_H^2} \frac{2m_2}{m_1}\right) + 1 \leftrightarrow 2 \ .$$

At large q^2 the form factor can also be written as

$$F^M_{(0,0)} = e_1 \frac{16\pi\alpha_s f_M^2}{9q^2} \left(\frac{M_H^2}{m_2^2}\right) + (1 \leftrightarrow 2) \ , \quad \frac{f_M}{2\sqrt{3}} = \int\limits_0^1 dx\, \varphi(x, Q)$$

where $f_M = (6\gamma^3/\pi M_H)^{1/2}$ is the meson decay constant. Detailed results for $F\overline{F}$ and $B_c\overline{B}_c$ production are give in Ref. 79.

At low relative velocity of the hadron pair one also expects resonance contributions to the form factors. For these heavy systems such resonances could be related to $qq\overline{q}\overline{q}$ bound states. From Watson's theorem, one expects any resonance structure to introduce a final-state phase factor, but not destroy the zero of the underlying QCD prediction.

Analogous calculations of the baryon form factor, retaining the constituent mass structure have also been done. The numerator structure for spin 1/2 baryons has the form

$$A + B\overline{q}^2 + c\overline{q}^4 \ .$$

Thus it is possible to have two form factor zeros; *e.g.* at spacelike and timelike values of q^2.

Although the measurements are difficult and require large luminosity, the observation of the striking zero structure predicted by QCD would provide a unique test of the theory and its applicability to exclusive processes. The onset of leading power behavior is controlled simply by the mass parameters of the theory.

7. EXCLUSIVE $\gamma\gamma$ REACTIONS

Two-photon reactions have a number of unique features which are especially important for testing QCD, especially in exclusive channels:[80]

1. Any even charge conjugation hadronic state can be created in the annihilation of two photons—an initial state of minimum complexity. Because $\gamma\gamma$ annihilation is complete, there are no spectator hadrons to confuse resonance analyses. Thus, one has a clean environment for identifying the exotic color-singlet even C composites of quarks and gluons $|q\bar{q}>$, $|gg>$, $|ggg>$, $|q\bar{q}g>$, $|qq\overline{qq}>$, ... which are expected to be present in the few GeV mass range. (Because of mixing, the actual mass eigenstates of QCD may be complicated admixtures of the various Fock components.)
2. The mass and polarization of each of the incident virtual photons can be continuously varied, allowing highly detailed tests of theory. Because a spin-one state cannot couple to two on-shell photons, a $J = 1$ resonance can be uniquely identified by the onset of its production with increasing photon mass.[81]
3. Two-photon physics plays an especially important role in probing dynamical mechanisms. In the low momentum transfer domain, $\gamma\gamma$ reactions such as the total annihilation cross section and exclusive vector meson pair production can give important insights into the nature of diffractive reactions in QCD. Photons in QCD couple directly to the quark currents at any resolution scale (see Fig. 28). Predictions for high momentum transfer $\gamma\gamma$ reactions, including the photon structure functions, $F_2^\gamma(x,Q^2)$ and $F_L^\gamma(x,Q^2)$, high p_T jet production, and exclusive channels are thus much more specific than corresponding hadron-induced reactions. The pointlike coupling of the annihilating photons leads to a host of special features which differ markedly with predictions based on vector meson dominance models.
4. Exclusive $\gamma\gamma$ processes provide a window for viewing the wavefunctions of hadrons in terms of their quark and gluon degrees of freedom. In the case of $\gamma\gamma$ annihilation into hadron pairs, the angular distribution of the production cross section directly reflects the shape of the distribution amplitude (valence wavefunction) of each hadron.

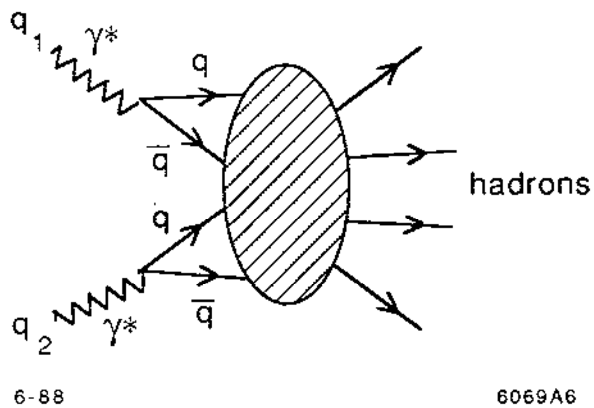

Figure 28. Photon-photon annihilation in QCD. The photons couple directly to one or two quark currents.

Thus far experiment has not been sufficiently precise to measure the logarithmic modification of dimensional counting rules predicted by QCD. Perturbative QCD predictions for $\gamma\gamma$ exclusive processes at high momentum transfer and high invariant pair mass provide some of the most severe tests of the theory.[82] A simple, but still very important example[4] is the Q^2-dependence of the reaction $\gamma^*\gamma \rightarrow M$ where M is a pseudoscalar meson such as the η. The invariant amplitude contains only one form factor:

$$M_{\mu\nu} = \epsilon_{\mu\nu\sigma\tau} p_\eta^\sigma q^\tau F_{\gamma\eta}(Q^2) \ .$$

It is easy to see from power counting at large Q^2 that the dominant amplitude (in light-cone gauge) gives $F_{\gamma\eta}(Q^2) \sim 1/Q^2$ and arises from diagrams (see Fig. 29) which have the minimum path carrying Q^2: *i.e.* diagrams in which there is only a single quark propagator between the two photons. The coefficient of $1/Q^2$ involves only the two-particle $q\bar{q}$ distribution amplitude $\phi(x, Q)$, which evolves logarithmically on Q. Higher particle number Fock states give higher power-law falloff contributions to the exclusive amplitude.

The TPC/$\gamma\gamma$ data[83] shown in Fig. 30 are in striking agreement with the predicted QCD power: a fit to the data gives $F_{\gamma\eta}(Q^2) \sim (1/Q^2)^n$ with $n = 1.05 \pm 0.15$. Data for the η' from Pluto and the TPC/$\gamma\gamma$ experiments give similar results, consistent with scale-free behavior of the QCD quark propagator and the point coupling to the quark current for both the real and virtual photons. In the case of deep inelastic lepton scattering, the observation of Bjorken scaling tests these properties when both photons are virtual.

The QCD power law prediction, $F_{\gamma\eta}(Q^2) \sim 1/Q^2$, is consistent with dimensional counting[5] and also emerges from current algebra arguments (when both

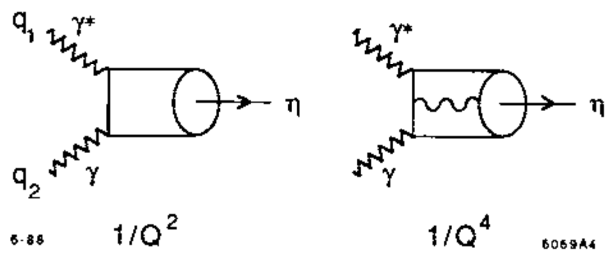

Figure 29. Calculation of the $\gamma - \eta$ transition form factor in QCD from the valence $q\bar{q}$ and $q\bar{q}g$ Fock states.

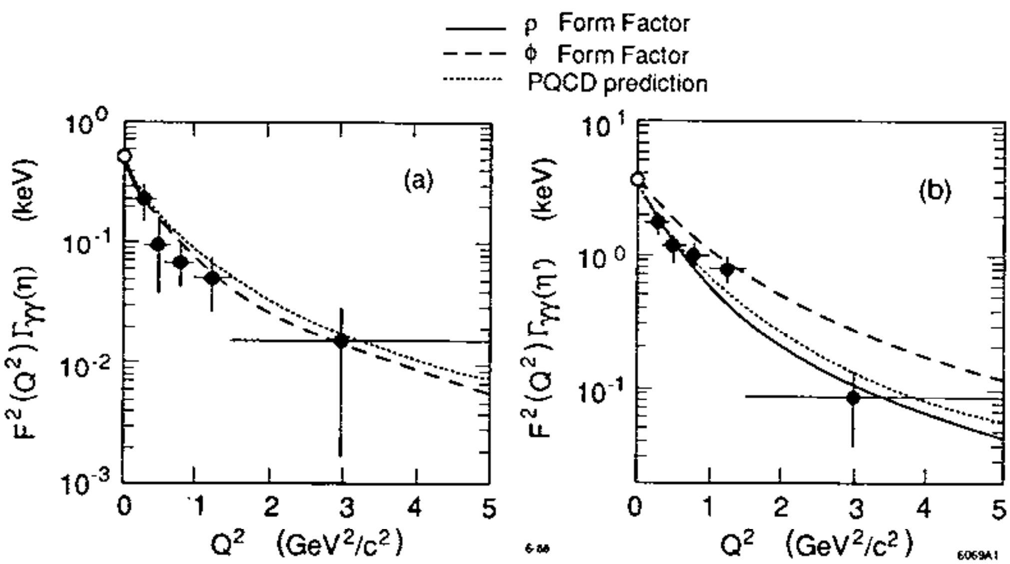

Figure 30. Comparison of TPC/$\gamma\gamma$ data[83] for the $\gamma - \eta$ and $\gamma - \eta'$ transition form factors with the QCD leading twist prediction of Ref. 82. The VMD predictions are also shown. See S. Yellin, this meeting.

photons are very virtual).[84] On the other hand, the $1/Q^2$ falloff is also expected in vector meson dominance models. The QCD and VDM predictions can be readily discriminated by studying $\gamma^*\gamma^* \to \eta$. In VMD one expects a product of form factors; in QCD the falloff of the amplitude is still $1/Q^2$ where Q^2 is a linear combination of Q_1^2 and Q_2^2. It is clearly very important to test this essential feature of QCD.

Exclusive two-body processes $\gamma\gamma \to H\overline{H}$ at large $s = W_{\gamma\gamma}^2 = (q_1 + q_2)^2$ and fixed $\theta_{cm}^{\gamma\gamma}$ provide a particularly important laboratory for testing QCD, since the large momentum-transfer behavior, helicity structure, and often even the absolute normalization can be rigorously predicted.[82,56] The angular dependence of some of the $\gamma\gamma \to H\overline{H}$ cross sections reflects the shape of the hadron distribution amplitudes $\phi_H(x_i, Q)$. The $\gamma_\lambda\gamma_{\lambda'} \to H\overline{H}$ amplitude can be written as a factorized form

$$\mathcal{M}_{\lambda\lambda'}(W_{\gamma\gamma}, \theta_{\rm cm}) = \int_0^1 [dy_i]\, \phi_H^*(x_i, Q)\, \phi_{\overline{H}}^*(y_i, Q)\, T_{\lambda\lambda'}(x, y; W_{\gamma\gamma}, \theta_{\rm cm})$$

where $T_{\lambda\lambda'}$ is the hard scattering helicity amplitude. To leading order $T \propto \alpha(\alpha_s/W_{\gamma\gamma}^2)^n$ and $d\sigma/dt \sim W_{\gamma\gamma}^{-(2n+2)} f(\theta_{\rm cm})$ where $n = 1$ for meson and $n = 2$ for baryon pairs.

Lowest order predictions for pseudo-scalar and vector-meson pairs for each helicity amplitude are given in Ref. 82. In each case the helicities of the hadron pairs are equal and opposite to leading order in $1/W^2$. The normalization and angular dependence of the leading order predictions for $\gamma\gamma$ annihilation into charged meson pairs are almost model independent; *i.e.* they are insensitive to the precise form of the meson distribution amplitude. If the meson distribution amplitudes is symmetric in x and $(1 - x)$, then the same quantity

$$\int_0^1 dx\, \frac{\phi_\pi(x, Q)}{(1 - x)}$$

controls the x-integration for both $F_\pi(Q^2)$ and to high accuracy $M(\gamma\gamma \to \pi^+\pi^-)$. Thus for charged pion pairs one obtains the relation:

$$\frac{\frac{d\sigma}{dt}(\gamma\gamma \to \pi^+\pi^-)}{\frac{d\sigma}{dt}(\gamma\gamma \to \mu^+\mu^-)} \cong \frac{4|F_\pi(s)|^2}{1 - \cos^4\theta_{\rm cm}} .$$

Note that in the case of charged kaon pairs, the asymmetry of the distribution amplitude may give a small correction to this relation.

The scaling behavior, angular behavior, and normalization of the $\gamma\gamma$ exclusive pair production reactions are nontrivial predictions of QCD. Recent Mark II meson pair data and PEP4/PEP9 data[85] for separated $\pi^+\pi^-$ and K^+K^- production in the range $1.6 < W_{\gamma\gamma} < 3.2$ GeV near 90° are in satisfactory agreement with the normalization and energy dependence predicted by QCD (see Fig. 31). In the case of $\pi^0\pi^0$ production, the $\cos\theta_{\rm cm}$ dependence of the cross section can be inverted to determine the x-dependence of the pion distribution amplitude.

The wavefunction of hadrons containing light and heavy quarks such as the K, D-meson are likely to be asymmetric due to the disparity of the quark masses. In a gauge theory one expects that the wavefunction is maximum when the quarks have zero relative velocity; this corresponds to $x_i \propto m_{i\perp}$ where $m_\perp^2 = k_\perp^2 + m^2$. An explicit model for the skewing of the meson distribution amplitudes based on QCD sum rules is given by Benyayoun and Chernyak.[86] These authors also apply their model to two-photon exclusive processes such as $\gamma\gamma \to K^+K^-$ and obtain some modification compared to the strictly symmetric distribution amplitudes. If the same conventions are used to label the quark lines, the calculations of Benyayoun and Chernyak are in complete agreement with those of Ref. 82.

The one-loop corrections to the hard scattering amplitude for meson pairs have been calculated by Nizic.[62] The QCD predictions for mesons containing admixtures of the $|gg\rangle$ Fock state is given by Atkinson, Sucher, and Tsokos.[56]

The perturbative QCD analysis has been extended to baryon-pair production in comprehensive analyses by Farrar *et al.*[60,56] and by Gunion *et al.*[61,56] Predictions are given for the "sideways" Compton process $\gamma\gamma \to p\overline{p}$, $\Delta\overline{\Delta}$ pair production, and the entire decuplet set of baryon pair states. The arduous calculation of 280 $\gamma\gamma \to qqq\overline{q}\overline{q}\overline{q}$ diagrams in T_H required for calculating $\gamma\gamma \to B\overline{B}$ is greatly simplified by using two-component spinor techniques. The doubly charged Δ pair is predicted to have a fairly small normalization. Experimentally such resonance pairs may be difficult to identify under the continuum background.

The normalization and angular distribution of the QCD predictions for proton-antiproton production shown in Fig. 32 depend in detail on the form of the nucleon distribution amplitude, and thus provide severe tests of the model form derived by Chernyak, Ogloblin, and Zhitnitsky[49] from QCD sum rules.

An important check of the QCD predictions can be obtained by combining data from $\gamma\gamma \to p\overline{p}$ and the annihilation reaction, $p\overline{p} \to \gamma\gamma$, with large angle Compton scattering $\gamma p \to \gamma p$. The available data[87] for large angle Compton scattering (see Fig. 33), for $5\ GeV^2 < s < 10\ GeV^2$ are consistent with the dimensional counting scaling prediction, $s^6 d\sigma/dt = f(\theta_{cm})$. In general, comparisons between channels related by crossing of the Mandelstam variables place a severe constraint on the angular dependence and analytic form of the underlying QCD exclusive amplitude. Furthermore in $p\overline{p}$ collisions one can study timelike photon production into e^+e^- and examine the virtual photon mass dependence of the Compton amplitude. Predictions for the q^2 dependence of the $p\overline{p} \to \gamma\gamma^*$ amplitude can be obtained by crossing the results of Gunion and Millers.[56]

The region of applicability of the leading power-law predictions for $\gamma\gamma \to$

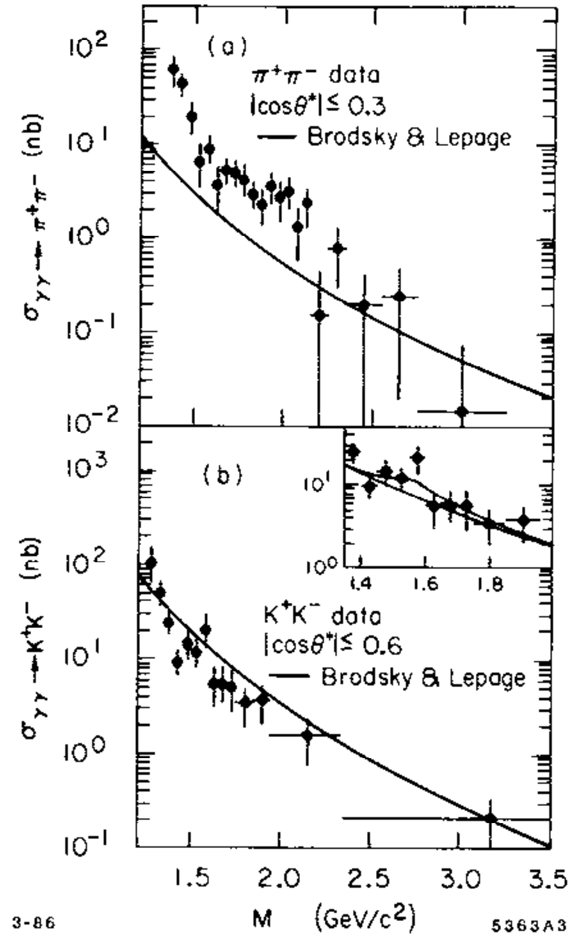

Figure 31. Comparison of $\gamma\gamma \to \pi^+\pi^-$ and $\gamma\gamma \to K^+K^-$ meson pair production data with the parameter-free perturbative QCD prediction of Ref. 82. The theory predicts the normalization and scaling of the cross sections. The data are from the TPC/$\gamma\gamma$ collaboration.[85]

$p\bar{p}$ requires that one be beyond resonance or threshold effects. It presumably is set by the scale where $Q^4 G_M(Q^2)$ is roughly constant, *i.e.* $Q^2 > 3$ GeV^2. Present measurements may thus be too close to threshold for meaningful tests.[88] It should be noted that unlike the case for charged meson pair production, the QCD predictions for baryons are sensitive to the form of the running coupling constant and the endpoint behavior of the wavefunctions.

The QCD predictions for $\gamma\gamma \to H\overline{H}$ can be extended to the case of one or two virtual photons, for measurements in which one or both electrons are tagged. Because of the direct coupling of the photons to the quarks, the Q_1^2 and Q_2^2 dependence of the $\gamma\gamma \to H\overline{H}$ amplitude for transversely polarized photons is minimal at W^2 large and fixed $\theta_{\rm cm}$, since the off-shell quark and gluon propagators

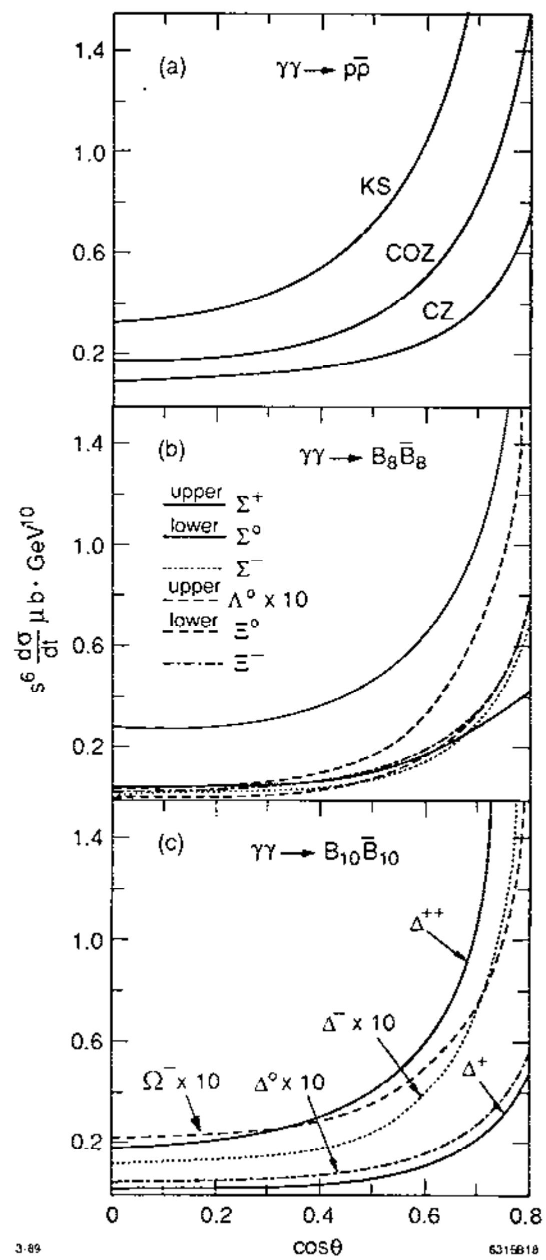

Figure 32. Perturbative QCD predictions by Farrar and Zhang for the $\cos(\theta_{cm})$ dependence of the $\gamma\gamma \to p\bar{p}$ cross section assuming the King-Sachrajda (KS), Chernyak, Ogloblin, and Zhitnitsky (COZ)[19], and original Chernyak and Zhitnitsky (CZ)[16] forms for the proton distribution amplitude, $\phi_p(x_i, Q)$.

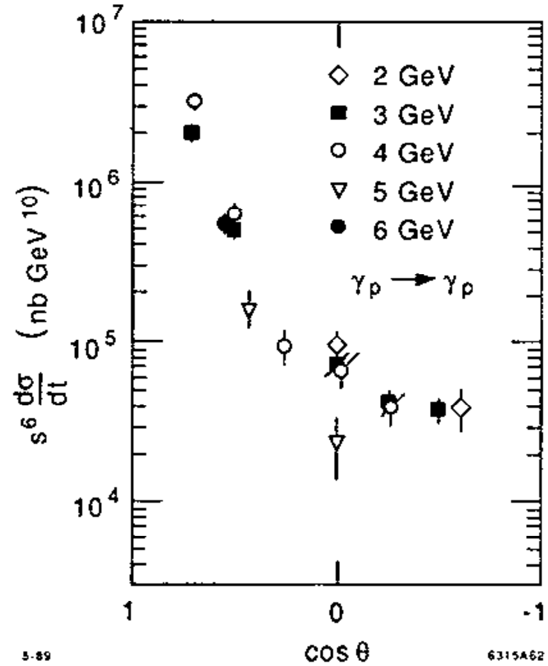

Figure 33. Test of dimensional counting for Compton scattering for $2 < E^{\gamma}_{lab} < 6\ GeV$.[87]

in T_H already transfer hard momenta; *i.e.* the 2γ coupling is effectively local for Q_1^2, $Q_2^2 \ll p_T^2$. The $\gamma^*\gamma^* \to \overline{B}B$ and $M\overline{M}$ amplitudes for off-shell photons have been calculated by Millers and Gunion.[56] In each case, the predictions show strong sensitivity to the form of the respective baryon and meson distribution amplitudes.

We also note that photon-photon collisions provide a way to measure the running coupling constant in an exclusive channel, independent of the form of hadronic distribution amplitudes.[82] The photon-meson transition form factors $F_{\gamma - M}(Q^2)$, $M = \pi^0, \eta^0, f$, etc., are measurable in tagged $e\gamma \to e'M$ reactions. QCD predicts

$$\alpha_s(Q^2) = \frac{1}{4\pi}\, \frac{F_\pi(Q^2)}{Q^2|F_{\pi\gamma}(Q^2)|^2}$$

where to leading order the pion distribution amplitude enters both numerator and denominator in the same manner.

The complete calculations of the tree-graph structure (see Figs. 34, 35, 36) of both $\gamma\gamma \to M\overline{M}$ and $\gamma\gamma \to B\overline{B}$ amplitudes has now been completed. One can use crossing to compute T_H for $p\overline{p} \to \gamma\gamma$ to leading order in $\alpha_s(p_T^2)$ from the calculations reported by Farrar, Maina and Neri[56] and Gunion and Millers.[56] Examples of the predicted angular distributions are shown in Figs. 37 and 38.

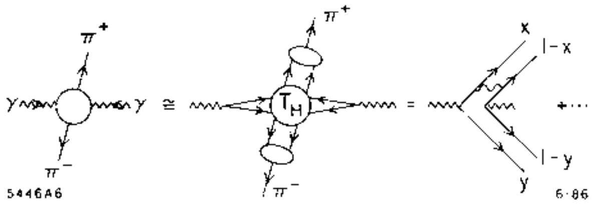

Figure 34. Application of QCD to two-photon production of meson pairs.[69]

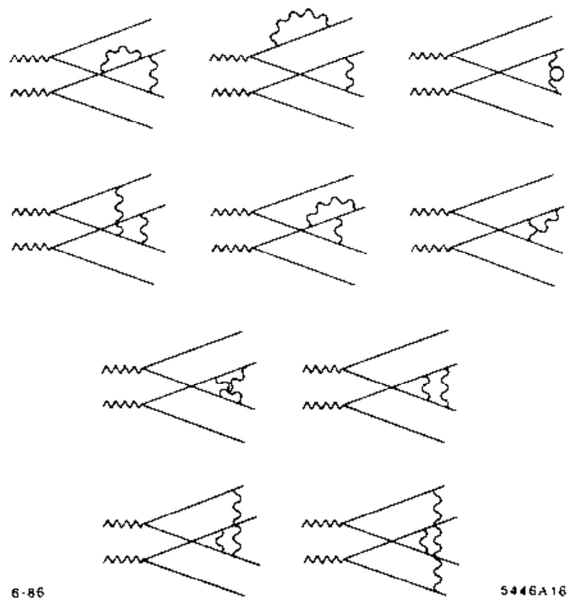

Figure 35. Next-to-leading perturbative contribution to T_H for the process $\gamma\gamma \rightarrow M\overline{M}$. The calculation has been done by Nizic.[69]

As discussed in Section 2, a model form for the proton distribution amplitude has been proposedby Chernyak and Zhitnitsky[16] based on QCD sum rules which leads to normalization and sign consistent with the measured proton form factor (see Fig. 21). The CZ sum rule analysis has been confirmed and extended by King and Sachrajda.[50] The CZ proton distribution amplitude yields predictions for $\gamma\gamma \rightarrow p\overline{p}$ in rough agreement with the experimental normalization, although the production energy is too low for a clear test. It should be noted that unlike

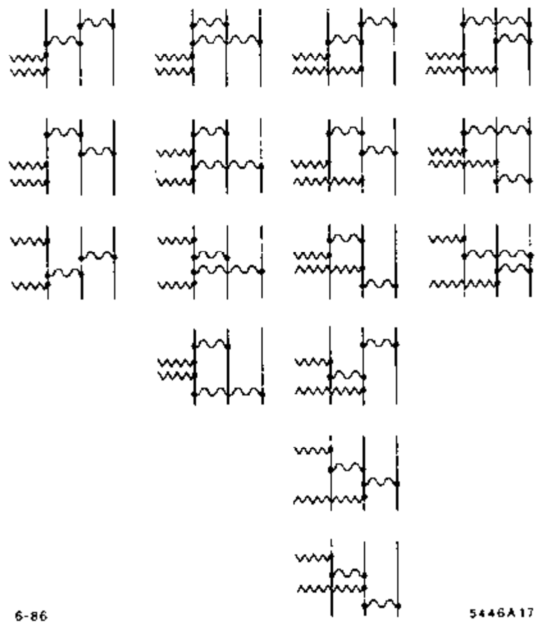

Figure 36. Leading diagrams for $\gamma + \gamma \to \bar{p} + p$ calculated in Ref. 56.

meson pair production[89] the QCD predictions for baryons are highly sensitive to the form of the running coupling constant and the endpoint behavior of the wavefunctions.

It is possible that data from $p\bar{p}$ collisions at energies up to 10 GeV could greatly clarify the question of whether the perturbative QCD predictions are reliable at moderate momentum transfer. As emphasized in Section 4, an important check of the QCD predictions can be obtained by combining data from $p\bar{p} \to \gamma\gamma$, $\gamma\gamma \to p\bar{p}$ with large angle Compton scattering $\gamma p \to \gamma p$. This comparison checks in detail the angular dependence and crossing behavior expected from the theory. Furthermore, in $p\bar{p}$ collisions one can even study time-like photon production into e^+e^- and examine the virtual photon mass dependence of the Compton amplitude. Predictions for the q^2 dependence of the $p\bar{p} \to \gamma\gamma^*$ amplitude can be obtained by crossing the results of Gunion and Millers.[56,61]

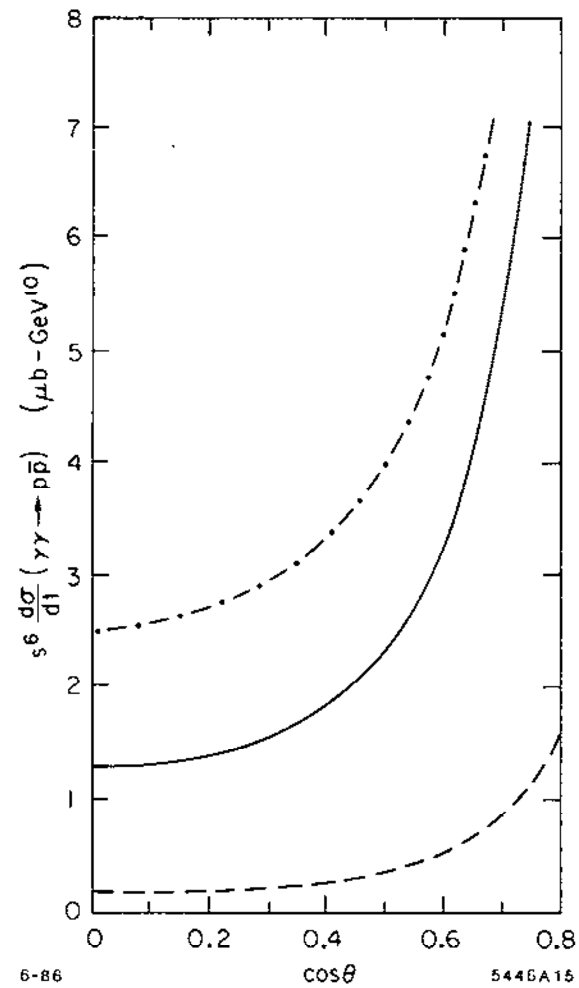

Figure 37. QCD prediction for the scaling and angular distribution for $\gamma + \gamma \to \bar{p} + p$ calculated by Farrar *et al.*[56] The dashed-dot curve corresponds to $4\Lambda^2/s = 0.0016$ and a maximum running coupling constant $\alpha_s^{max} = 0.8$. The solid curve corresponds to $4\Lambda^2/s = 0.016$ and a maximum running coupling constant $\alpha_s^{max} = 0.5$. The dashed curve corresponds to a fixed $\alpha_s = 0.3$. The results are very sensitive to the endpoint behavior of the proton distribution amplitude. The CZ form is assumed.

8. QCD PROCESSES IN NUCLEI

The least-understood process in QCD is *hadronization* — the mechanism which converts quark and gluon quanta to color-singlet integrally-charged hadrons. One way to study hadronization is to perturb the environment by introducing a nuclear medium surrounding the hard-scattering short distance reaction. This is obviously impractical in the theoretically simplest processes — e^+e^- or $\gamma\gamma$ annihilation. However, for large momentum transfer reactions occurring in a nuclear target, such as deep inelastic lepton scattering or massive lepton pair production,

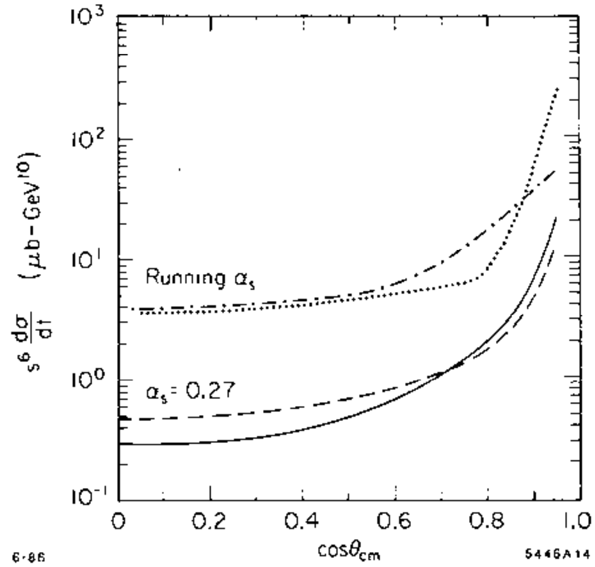

Figure 38. QCD prediction for the scaling and angular distribution for $\gamma + \gamma \rightarrow \bar{p} + p$ calculated by Gunion, Sparks and Millers.[56,61] CZ distribution amplitudes are assumed. The solid and running curves are for real photon annihilation. The dashed and dot-dashed curves correspond to one photon space-like, with $Q_i^2/s = 0.1$.

the nuclear medium provides a nontrivial perturbation to jet evolution through the influence of initial- and/or final-state interactions. In the case of large momentum transfer quasiexclusive reactions, one can use a nuclear target to filter and influence the evolution and structure of the hadron wavefunctions themselves. The physics of such nuclear reactions is surprisingly interesting and subtle — involving concepts and novel effects quite orthogonal to usual expectations.

The nucleus thus plays two complimentary roles in quantum chromodynamics:

1. A nuclear target can be used as a control medium or background field to modify or probe quark and gluon subprocesses. Some novel examples are *color transparency*, the predicted transparency of the nucleus to hadrons participating in high-momentum transfer exclusive reactions, and *formation zone phenomena*, the absence of hard, collinear, target-induced radiation by a quark or gluon interacting in a high-momentum transfer inclusive reaction if its energy is large compared to a scale proportional to the length of the target. (Soft radiation and elastic initial-state interactions in the nucleus still occur.) *Coalescence* with co-moving spectators[90] has been discussed as a mechanism which can lead to increased open charm hadroproduction, but which also suppresses forward charmonium production (relative to lepton pairs) in heavy ion collisions.[91] There are also interesting special features of nuclear diffractive amplitudes — high energy hadronic or electromagnetic

reactions which leave the entire nucleus intact and give nonadditive contributions to the nuclear structure function at low x_{Bj}. The Q^2 dependence of diffractive $\gamma^* p \to \rho^0 p$ is found to have a slope in the $t-$dependence $\exp bt$ where $b = b(Q^2)$ is of order $1 \sim 2\ GeV^{-2}$, much smaller than expected on the basis of vector meson dominance and $t-$channel factorization.

2. Conversely, the nucleus can be studied as a QCD structure. At short distances nuclear wavefunctions and nuclear interactions necessarily involve *hidden color*, degrees of freedom orthogonal to the channels described by the usual nucleon or isobar degrees of freedom. At asymptotic momentum transfer, the deuteron form factor and distribution amplitude are rigorously calculable. One can also derive new types of testable scaling laws for exclusive nuclear amplitudes in terms of the reduced amplitude formalism.

8.1. Exclusive Nuclear Reactions — Reduced Amplitudes

An ultimate goal of QCD phenomenology is to describe the nuclear force and the structure of nuclei in terms of quark and gluon degrees of freedom. Explicit signals of QCD in nuclei have been elusive, in part because of the fact that an effective Lagrangian containing meson and nucleon degrees of freedom must be in some sense equivalent to QCD if one is limited to low-energy probes. On the other hand, an effective local field theory of nucleon and meson fields cannot correctly describe the observed off-shell falloff of form factors, vertex amplitudes, Z-graph diagrams, etc. because hadron compositeness is not taken into account.

We have already mentioned the prediction $F_d(Q^2) \sim 1/Q^{10}$ which comes from simple quark counting rules, as well as perturbative QCD. One cannot expect this asymptotic prediction to become accurate until very large Q^2 is reached since the momentum transfer has to be shared by at least six constituents. However there is a simple way to isolate the QCD physics due to the compositeness of the nucleus, not the nucleons. The deuteron form factor is the probability amplitude for the deuteron to scatter from p to $p+q$ but remain intact. Note that for vanishing nuclear binding energy $\epsilon_d \to 0$, the deuteron can be regarded as two nucleons sharing the deuteron four-momentum (see Fig. 39). The momentum ℓ is limited by the binding and can thus be neglected. To first approximation the proton and neutron share the deuteron's momentum equally. Since the deuteron form factor contains the probability amplitudes for the proton and neutron to scatter from $p/2$ to $p/2 + q/2$; it is natural to define the reduced deuteron form factor[92,93]

$$f_d(Q^2) \equiv \frac{F_d(Q^2)}{F_{1N}\left(\frac{Q^2}{4}\right) F_{1N}\left(\frac{Q^2}{4}\right)}.$$

The effect of nucleon compositeness is removed from the reduced form factor. QCD then predicts the scaling

$$f_d(Q^2) \sim \frac{1}{Q^2}$$

i.e. the same scaling law as a meson form factor. Diagrammatically, the extra power of $1/Q^2$ comes from the propagator of the struck quark line, the one propagator not contained in the nucleon form factors. Because of hadron helicity conservation, the prediction is for the leading helicity-conserving deuteron form factor ($\lambda = \lambda' = 0$.) As shown in Fig. 40, this scaling is consistent with experiment for $Q = p_T \gtrsim 1$ GeV.[94]

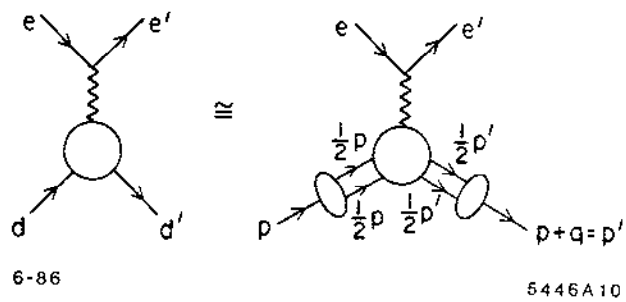

Figure 39. Application of the reduced amplitude formalism to the deuteron form factor at large momentum transfer.

The distinction between the QCD and other treatments of nuclear amplitudes is particularly clear in the reaction $\gamma d \to np$; *i.e.* photodisintegration of the deuteron at fixed center of mass angle. Using dimensional counting, the leading power-law prediction from QCD is simply $\frac{d\sigma}{dt}(\gamma d \to np) \sim \frac{1}{s^{11}} F(\theta_{cm})$. Again we note that the virtual momenta are partitioned among many quarks and gluons, so that finite mass corrections will be significant at low to medium energies. Nevertheless, one can test the basic QCD dynamics in these reactions taking into account much of the finite-mass, higher-twist corrections by using the "reduced amplitude" formalism.[92,93] Thus the photodisintegration amplitude contains the probability amplitude (*i.e.* nucleon form factors) for the proton and neutron to each remain intact after absorbing momentum transfers $p_p - 1/2p_d$ and $p_n - 1/2p_d$, respectively (see Fig. 41). After the form factors are removed, the remaining "reduced" amplitude should scale as $F(\theta_{\rm cm})/p_T$. The single inverse power of transverse momentum p_T is the slowest conceivable in any theory, but it is the unique power predicted by PQCD.

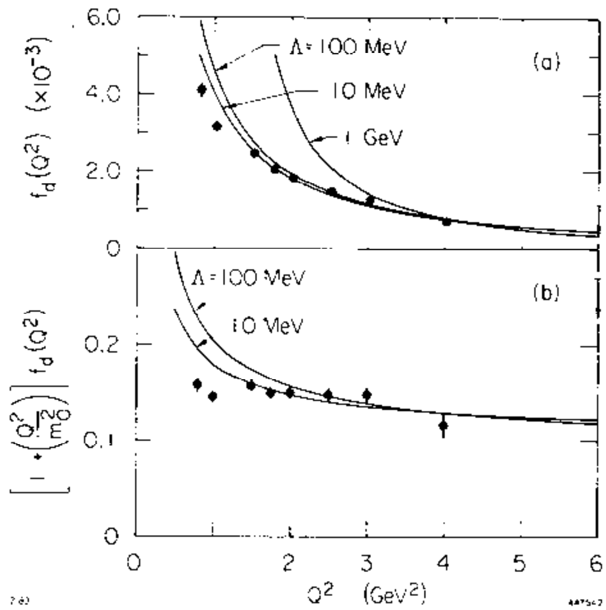

Figure 40. Scaling of the deuteron reduced form factor. The data are summarized in Ref. 92.

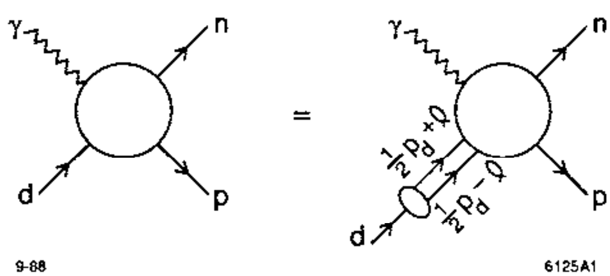

Figure 41. Construction of the reduced nuclear amplitude for two-body inelastic deuteron reactions.[92]

The prediction that $f(\theta_{\rm cm})$ is energy dependent at high-momentum transfer is compared with experiment in Fig. 42. It is particularly striking to see the QCD prediction verified at incident photon lab energies as low as 1 GeV. A comparison with a standard nuclear physics model with exchange currents is also shown for comparison as the solid curve in Fig. 42(a). The fact that this prediction falls less fast than the data suggests that meson and nucleon compositeness are not taken to into account correctly. An extension of these data to other angles and higher energy would clearly be very valuable.

An important question is whether the normalization of the $\gamma d \to pn$ amplitude is correctly predicted by perturbative QCD. A recent analysis by Fujita[98] shows that mass corrections to the leading QCD prediction are not significant in the region in which the data show scaling. However Fujita also finds that in a model based on simple one-gluon plus quark-interchange mechanism, normalized to the nucleon-nucleon scattering amplitude, gives a photo-disintegration amplitude with a normalization an order of magnitude below the data. However this model only allows for diagrams in which the photon insertion acts only on the quark lines which couple to the exchanged gluon. It is expected that including other diagrams in which the photon couples to the current of the other four quarks will increase the photo-disintegration amplitude by a large factor.

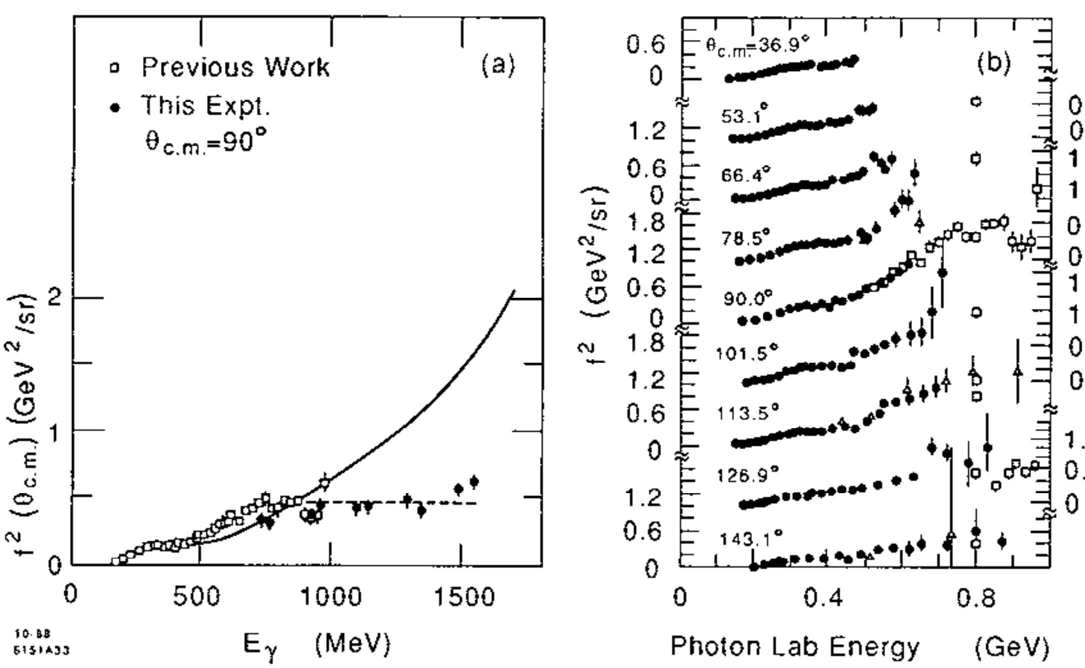

Figure 42. Comparison of deuteron photodisintegration data with the scaling prediction which requires $f^2(\theta_{cm})$ to be at most logarithmically dependent on energy at large momentum transfer. The data in (a) are from the recent experiment of Ref. 95. The nuclear physics prediction shown in (a) is from Ref. 96. The data in (b) are from Ref. 97.

The derivation of the evolution equation for the deuteron and other multi-quark states is given in Refs. 99 and 93. In the case of the deuteron, the evolution equation couples five different color singlet states composed of the six quarks. The leading anomalous dimension for the deuteron distribution amplitude and the helicity-conserving deuteron form factor at asymptotic Q^2 is given in Ref. 99.

There are a number of related tests of QCD and reduced amplitudes which require $\overline{p}$ beams[93] such as $\overline{p}d \to \gamma n$ and $\overline{p}d \to \pi^- p$ in the fixed $\theta_{\rm cm}$ region. These reactions are particularly interesting tests of QCD in nuclei. Dimensional counting rules predict the asymptotic behavior $\frac{d\sigma}{dt}\ (\overline{p}d \to \pi^- p) \sim \frac{1}{(p_T^2)^{12}}\ f(\theta_{\rm cm})$ since there are 14 initial and final quanta involved. Again one notes that the $\overline{p}d \to \pi^- p$ amplitude contains a factor representing the probability amplitude (*i.e.* form factor) for the proton to remain intact after absorbing momentum transfer squared $\hat{t} = (p - 1/2p_d)^2$ and the $\overline{N}N$ time-like form factor at $\hat{s} = (\overline{p} + 1/2p_d)^2$. Thus $\mathcal{M}_{\overline{p}d \to \pi^- p} \sim F_{1N}(\hat{t})\ F_{1N}(\hat{s})\, \mathcal{M}_r$, where $\mathcal{M}_r$ has the same QCD scaling properties as quark meson scattering. One thus predicts

$$\frac{\frac{d\sigma}{d\Omega}\ (\overline{p}d \to \pi^- p)}{F_{1N}^2(\hat{t})\, F_{1N}^2(\hat{s})} \sim \frac{f(\Omega)}{p_T^2}\ .$$

The reduced amplitude scaling for $\gamma d \to pn$ at large angles and $p_T \gtrsim 1$ GeV (see Fig. 42). One thus expects similar precocious scaling behavior to hold for $\overline{p}d \to \pi^- p$ and other $\overline{p}d$ exclusive reduced amplitudes. Recent analyses by Kondratyuk and Sapozhnikov[100] show that standard nuclear physics wavefunctions and interactions cannot explain the magnitude of the data for two-body anti-proton annihilation reactions such as $\overline{p}d \to \pi^- p$.

8.2. Color Transparency

A striking feature of the QCD description of exclusive processes is "color transparency:" The only part of the hadronic wavefunction that scatters at large momentum transfer is its valence Fock state where the quarks are at small relative impact separation. Such a fluctuation has a small color-dipole moment and thus has negligible interactions with other hadrons. Since such a state stays small over a distance proportional to its energy, this implies that quasi-elastic hadron-nucleon scattering at large momentum transfer as illustrated in Fig. 43 can occur additively on all of the nucleons in a nucleus with minimal attenuation due to elastic or inelastic final state interactions in the nucleus, *i.e.* the nucleus becomes "transparent." By contrast, in conventional Glauber scattering,

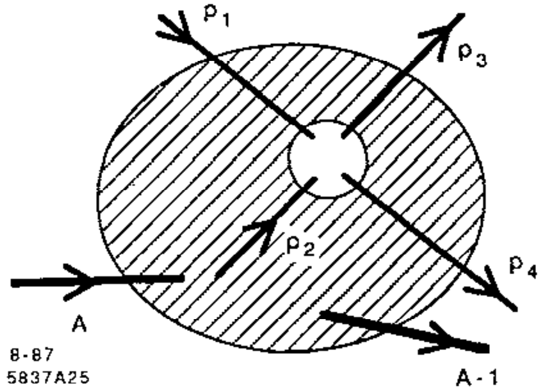

Figure 43. Quasi-elastic pp scattering inside a nuclear target. Normally one expects such processes to be attenuated by elastic and inelastic interactions of the incident proton and the final state interaction of the scattered proton. Perturbative QCD predicts minimal attenuation; *i.e.* "color transparency," at large momentum transfer.[7]

one predicts strong, nearly energy-independent initial and final state attenuation. A detailed discussion of the time and energy scales required for the validity of the PQCD prediction is given in by Farrar *et al.* and Mueller in Ref. 7.

A recent experiment[101] at BNL measuring quasi-elastic $pp \to pp$ scattering at $\theta_{\rm cm} = 90^\circ$ in various nuclei appears to confirm the color transparency prediction—at least for p_{lab} up to 10 GeV/c (see Fig. 44). Descriptions of elastic scattering which involve soft hadronic wavefunctions cannot account for the data. However, at higher energies, $p_{lab} \sim 12$ GeV/c, normal attenuation is observed in the BNL experiment. This is the same kinematical region $E_{\rm cm} \sim 5$ GeV where the large spin correlation in A_{NN} are observed.[102] Both features may be signaling new s-channel physics associated with the onset of charmed hadron production[103] or interference with Landshoff pinch singularity diagrams.[43] We will discuss these possible solutions in Section 9. Clearly, much more testing of the color transparency phenomena is required, particularly in quasi-elastic lepton-proton scattering, Compton scattering, antiproton-proton scattering, etc. The cleanest test of the PQCD prediction is to check for minimal attenuation in large momentum transfer lepton-proton scattering in nuclei since there are no complications from pinch singularities or resonance interference effects.

In Section 5.4 we emphasized the fact that soft initial-state interactions $\overline{p}p \to \bar{\ell}\ell$ are suppressed at high lepton pair mass. This is a remarkable consequence of gauge theory and is quite contrary to normal treatments of initial interactions based on Glauber theory. This novel effect can be studied in quasielastic $\overline{p}A \to \bar{\ell}\ell\ (A-1)$ reaction. in which there are no extra hadrons produced and the

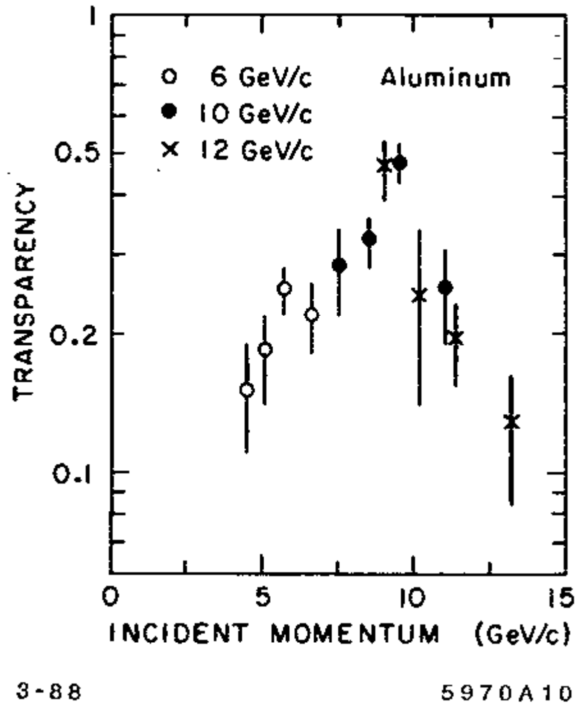

Figure 44. Measurements of the transparency ratio

$$T = \frac{Z_{eff}}{Z} = \frac{d\sigma}{dt}[pA \to p(A-1)]/\frac{d\sigma}{dt}[pA \to pp]$$

near 90° on Aluminum.[101] Conventional theory predicts that T should be small and roughly constant in energy. Perturbative QCD[7] predicts a monotonic rise to $T = 1$.

produced leptons are coplanar with the beam. (The nucleus $(A-1)$ can be left excited). Since PQCD predicts the absence of initial-state elastic and inelastic interactions, the number of such events should be strictly additive in the number Z of protons in the nucleus, every proton in the nucleus is equally available for short-distance annihilation. In traditional Glauber theory only the surface protons can participate because of the strong absorption of the $\overline{p}$ as it traverses the nucleus.

The above description is the ideal result for large s. QCD predicts that additivity is approached monotonically with increasing energy, corresponding to two effects: a) the effective transverse size of the $\overline{p}$ wavefunction is $b_\perp \sim 1/\sqrt{s}$, and b) the formation time for the $\overline{p}$ is sufficiently long, such that the Fock state stays small during transit of the nucleus.

The color transparency phenomena is also important to test in purely hadronic quasiexclusive antiproton-nuclear reactions. For large p_T one predicts

$$\frac{d\sigma}{dt\,dy}\ (\overline{p}A \to \pi^+\pi^- + (A-1)) \simeq \sum_{p\epsilon A} G_{p/A}(y)\ \frac{d\sigma}{dt}\ (\overline{p}p \to \pi^+\pi^-) \quad ,$$

where $G_{p/A}(y)$ is the probability distribution to find the proton in the nucleus with light-cone momentum fraction $y = (p^0 + p^z)/(p_A^0 + p_A^z)$, and

$$\frac{d\sigma}{dt}(\overline{p}p \to \pi^+\pi^-) \simeq \left(\frac{1}{p_T^2}\right)^8 f(\cos\theta_{\rm cm}) \ .$$

The distribution $G_{p/A}(y)$ can also be measured in $eA \to ep(A-1)$ quasiexclusive reactions. A remarkable feature of the above prediction is that there are no corrections required from initial-state absorption of the $\overline{p}$ as it traverses the nucleus, nor final-state interactions of the outgoing pions. Again the basic point is that the only part of hadron wavefunctions which is involved in the large p_T reaction is $\psi_H(b_\perp \sim \mathcal{O}(1/p_T))$. *i.e.* the amplitude where all the valence quarks are at small relative impact parameter. These configurations correspond to small color singlet states which, because of color cancellations, have negligible hadronic interactions in the target. Measurements of these reactions thus test a fundamental feature of the Fock state description of large p_T exclusive reactions.

Another interesting feature which can be probed in such reactions is the behavior of $G_{p/A}(y)$ for y well away from the Fermi distribution peak at $y \sim m_N/M_A$. For $y \to 1$ spectator counting rules[104] predict $G_{p/A}(y) \sim (1-y)^{2N_s-1} = (1-y)^{6A-7}$ where $N_s = 3(A-1)$ is the number of quark spectators required to "stop" ($y_i \to 0$) as $y \to 1$. This simple formula has been quite successful in accounting for distributions measured in the forward fragmentation of nuclei at the BEVALAC.[105] Color transparency can also be studied by measuring quasiexclusive J/ψ production by anti-protons in a nuclear target $\overline{p}A \to J/\psi(A-1)$ where the nucleus is left in a ground or excited state, but extra hadrons are not created (see Fig. 45). The cross section involves a convolution of the $\overline{p}p \to J/\psi$ subprocess cross section with the distribution $G_{p/A}(y)$ where $y = (p^0 + p^3)/(p_A^0 + p_A^3)$ is the boost-invariant light-cone fraction for protons in the nucleus. This distribution can be determined from quasiexclusive lepton-nucleon scattering $\ell A \to \ell p(A-1)$.

In first approximation $\overline{p}p \to J/\psi$ involves $qqq + \overline{qqq}$ annihilation into three charmed quarks. The transverse momentum integrations are controlled by the charm mass scale and thus only the Fock state of the incident antiproton which contains three antiquarks at small impact separation can annihilate. Again it follows that this state has a relatively small color dipole moment, and thus it

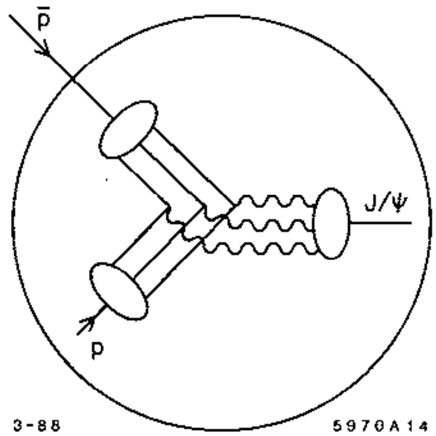

Figure 45. Schematic representation of quasielastic charmonium production in $\overline{p}A$ reactions.

should have a longer than usual mean-free path in nuclear matter; *i.e.* color transparency. Unlike traditional expectations, QCD predicts that the $\overline{p}p$ annihilation into charmonium is not restricted to the front surface of the nucleus. The exact nuclear dependence depends on the formation time for the physical $\overline{p}$ to couple to the small $\overline{qqq}$ configuration, $\tau_F \propto E_p$. It may be possible to study the effect of finite formation time by varying the beam energy, E_p, and using the Fermi-motion of the nucleon to stay at the J/ψ resonance. Since the J/ψ is produced at nonrelativistic velocities in this low energy experiment, it is formed inside the nucleus. The A-dependence of the quasiexclusive reaction can thus be used to determine the J/ψ-nucleon cross section at low energies. For a normal hadronic reaction $\overline{p}A \to HX$, we expect $A_{\rm eff} \sim A^{1/3}$, corresponding to absorption in the initial and final state. In the case of $\overline{p}A \to J/\psi\ X$ one expects $A_{\rm eff}$ much closer to A^1 if color transparency is fully effective and $\sigma(J/\psi\ N)$ is small.

9. SPIN CORRELATIONS IN PROTON-PROTON SCATTERING

One of the most serious challenges to quantum chromodynamics is the behavior of the spin-spin correlation asymmetry $A_{NN} = \frac{[d\sigma(\uparrow\uparrow) - d\sigma(\uparrow\downarrow)]}{[d\sigma(\uparrow\uparrow) + d\sigma(\uparrow\downarrow)]}$ measured in large momentum transfer pp elastic scattering (see Fig. 46). At $p_{lab} = 11.75$ GeV/c and $\theta_{\rm cm} = \pi/2$, A_{NN} rises to $\simeq 60\%$, corresponding to four times more probability for protons to scatter with their incident spins both normal to the scattering plane and parallel, rather than normal and opposite.

The polarized cross section shows a striking energy and angular dependence not expected from the slowly-changing perturbative QCD predictions. However,

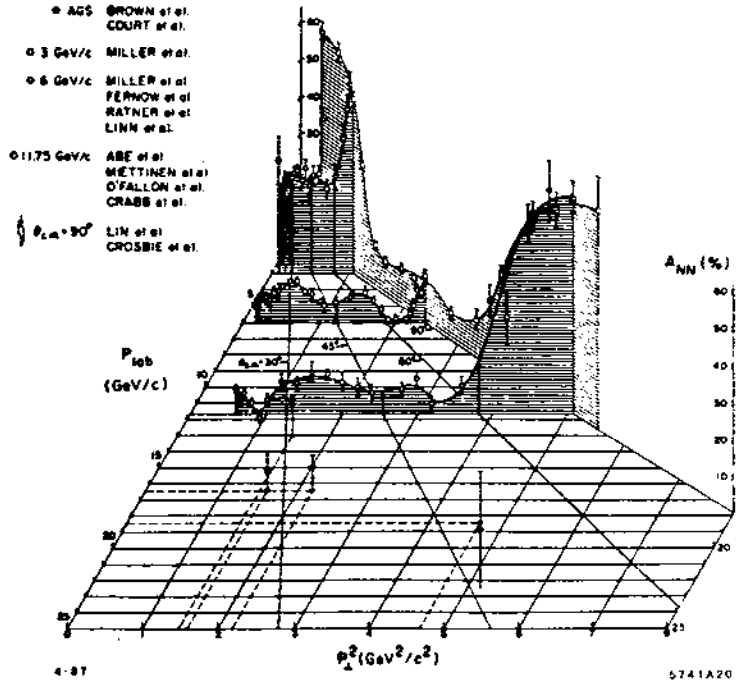

Figure 46. The spin-spin correlation A_{NN} for elastic pp scattering with beam and target protons polarized normal to the scattering plane.[106] $A_{NN} = 60\%$ implies that it is four times more probable for the protons to scatter with spins parallel rather than antiparallel.

the unpolarized data is in first approximation consistent with the fixed angle scaling law $s^{10}d\sigma/dt(pp \to pp) = f(\theta_{CM})$ expected from the perturbative analysis (see Fig. 23). The onset of new structure[107] at $s \simeq 23$ GeV^2 is a sign of new degrees of freedom in the two-baryon system. In this section, we will discuss a possible explanation[103] for (1) the observed spin correlations, (2) the deviations from fixed-angle scaling laws, and (3) the anomalous energy dependence of absorptive corrections to quasielastic pp scattering in nuclear targets, in terms of a simple model based on two $J = L = S = 1$ broad resonances (or threshold enhancements) interfering with a perturbative QCD quark-interchange background amplitude. The structures in the $pp \to pp$ amplitude may be associated with the onset of strange and charmed thresholds. If this view is correct, large angle pp elastic scattering would have been virtually featureless for $p_{lab} \geq 5$ GeV/c, had it not been for the onset of heavy flavor production. As a further illustration of the threshold effect, one can see the effect in A_{NN} due to a narrow $^3F_3$ pp resonance at $\sqrt{s} = 2.17$ GeV ($p_{lab} = 1.26$ GeV/c) associated with the $p\Delta$ threshold.

The perturbative QCD analysis[2] of exclusive amplitudes assumes that large momentum transfer exclusive scattering reactions are controlled by short distance quark-gluon subprocesses, and that corrections from quark masses and intrinsic transverse momenta can be ignored. The main predictions are fixed-angle scaling laws[5] (with small corrections due to evolution of the distribution amplitudes, the running coupling constant, and pinch singularities), hadron helicity conservation,[6] and the novel phenomenon, "color transparency."

As discussed in Section 8.2, a test of color transparency in large momentum transfer quasielastic pp scattering at $\theta_{\rm cm} \simeq \pi/2$ has recently been carried out at BNL using several nuclear targets (C, Al, Pb).[101] The attenuation at $p_{lab} = 10$ GeV/c in the various nuclear targets was observed to be in fact much less than that predicted by traditional Glauber theory (see Fig. 44). This appears to support the color transparency prediction.

The expectation from perturbative QCD is that the transparency effect should become even more apparent as the momentum transfer rises. Nevertheless, at $p_{lab} = 12$ GeV/c, normal attenuation was observed. One can explain this surprising result if the scattering at $p_{lab} = 12$ GeV/c ($\sqrt{s} = 4.93$ GeV), is dominated by an s-channel B=2 resonance (or resonance-like structure) with mass near 5 GeV, since unlike a hard-scattering reaction, a resonance couples to the fully-interacting large-scale structure of the proton. If the resonance has spin $S = 1$, this can also explain the large spin correlation A_{NN} measured nearly at the same momentum, $p_{lab} = 11.75$ GeV/c. Conversely, in the momentum range $p_{lab} = 5$ to 10 GeV/c one predicts that the perturbative hard-scattering amplitude is dominant at large angles. The experimental observation of diminished attenuation at $p_{lab} = 10$ GeV/c thus provides support for the QCD description of exclusive reactions and color transparency.

What could cause a resonance at $\sqrt{s} = 5$ GeV, more than 3 GeV beyond the pp threshold? There are a number of possibilities: (a) a multigluonic excitation such as $|qqqqqqggg\rangle$, (b) a "hidden color" color singlet $|qqqqqq\rangle$ excitation,[108] or (c) a "hidden flavor" $|qqqqqqQ\overline{Q}\rangle$ excitation, which is the most interesting possibility, since it is so predictive. As in QED, where final state interactions give large enhancement factors for attractive channels in which $Z\alpha/v_{rel}$ is large, one expects resonances or threshold enhancements in QCD in color-singlet channels at heavy quark production thresholds since all the produced quarks have similar velocities.[109] One thus can expect resonant behavior at $M^* = 2.55$ GeV and $M^* = 5.08$ GeV, corresponding to the threshold values for open strangeness: $pp \to \Lambda K^+ p$, and open charm: $pp \to \Lambda_c D^0 p$, respectively. In any case, the structure at 5 GeV is highly inelastic: its branching ratio to the proton-proton channel is $B^{pp} \simeq 1.5\%$.

A model for this phenomenon is given in Ref. 103 In order not to over complicate the phenomenology; the simplest Breit–Wigner parameterization of the resonances was used. There has not been an attempt to optimize the parameters of the model to obtain a best fit. It is possible that what is identified a single resonance is actually a cluster of resonances.

The background component of the model is the perturbative QCD amplitude. Although complete calculations are not yet available, many features of the QCD predictions are understood, including the approximate s^{-4} scaling of the $pp \to pp$ amplitude at fixed $\theta_{\rm cm}$ and the dominance of those amplitudes that conserve hadron helicity.[6] Furthermore, recent data comparing different exclusive two-body scattering channels from BNL[33] show that quark interchange amplitudes[110] dominate quark annihilation or gluon exchange contributions. Assuming the usual symmetries, there are five independent pp helicity amplitudes: $\phi_1 = M(++,++)$, $\phi_2 = M(--,++)$, $\phi_3 = M(+-,+-)$, $\phi_4 = M(-+,+-)$, $\phi_5 = M(++,+-)$. The helicity amplitudes for quark interchange have a definite relationship:[40]

$$\begin{aligned}\phi_1(\mathrm{PQCD}) &= 2\phi_3(\mathrm{PQCD}) = -2\phi_4(\mathrm{PQCD}) \\ &= 4\pi C F(t) F(u) [\frac{t - m_d^2}{u - m_d^2} + (u \leftrightarrow t)] e^{i\delta} \quad .\end{aligned}$$

The hadron helicity nonconserving amplitudes, $\phi_2(\mathrm{PQCD})$ and $\phi_5(\mathrm{PQCD})$ are zero. This form is consistent with the nominal power-law dependence predicted by perturbative QCD and also gives a good representation of the angular distribution over a broad range of energies.[111] Here $F(t)$ is the helicity conserving proton form factor, taken as the standard dipole form: $F(t) = (1 - t/m_d^2)^{-2}$, with $m_d^2 = 0.71\ \mathrm{GeV}^2$. As shown in Ref. 40, the PQCD-quark-interchange structure alone predicts $A_{NN} \simeq 1/3$, nearly independent of energy and angle.

Because of the rapid fixed-angle s^{-4} falloff of the perturbative QCD amplitude, even a very weakly-coupled resonance can have a sizeable effect at large momentum transfer. The large empirical values for A_{NN} suggest a resonant $pp \to pp$ amplitude with $J = L = S = 1$ since this gives $A_{NN} = 1$ (in absence of background) and a smooth angular distribution. Because of the Pauli principle, an $S = 1$ di-proton resonances must have odd parity and thus odd orbital angular momentum. The the two non-zero helicity amplitudes for a $J = L = S = 1$ resonance can be parameterized in Breit–Wigner form:

$$\phi_3(\mathrm{resonance}) = 12\pi \frac{\sqrt{s}}{p_{\rm cm}} d^1_{1,1}(\theta_{\rm cm}) \frac{\frac{1}{2}\Gamma^{pp}(s)}{M^* - E_{\rm cm} - \frac{i}{2}\Gamma} \quad ,$$

$$\phi_4(\text{resonance}) = -12\pi \frac{\sqrt{s}}{p_{\rm cm}} d^1_{-1,1}(\theta_{\rm cm}) \frac{\frac{1}{2}\Gamma^{pp}(s)}{M^* - E_{\rm cm} - \frac{i}{2}\Gamma} \quad .$$

(The ${}^3F_3$ resonance amplitudes have the same form with $d^3_{\pm1,1}$ replacing $d^1_{\pm1,1}$.) As in the case of a narrow resonance like the Z^0, the partial width into nucleon pairs is proportional to the square of the time-like proton form factor: $\Gamma^{pp}(s)/\Gamma = B^{pp}|F(s)|^2/|F(M^{*2})|^2$, corresponding to the formation of two protons at this invariant energy. The resonant amplitudes then die away by one inverse power of $(E_{\rm cm} - M^*)$ relative to the dominant PQCD amplitudes. (In this sense, they are higher twist contributions relative to the leading twist perturbative QCD amplitudes.) The model is thus very simple: each pp helicity amplitude ϕ_i is the coherent sum of PQCD plus resonance components: $\phi = \phi(\text{PQCD}) + \Sigma\phi(\text{resonance})$. Because of pinch singularities and higher-order corrections, the hard QCD amplitudes are expected to have a nontrivial phase;[43] the model allows for a constant phase δ in $\phi(\text{PQCD})$. Because of the absence of the ϕ_5 helicity-flip amplitude, the model predicts zero single spin asymmetry A_N. This is consistent with the large angle data at $p_{lab} = 11.75$ GeV/c.[112]

At low transverse momentum, $p_T \leq 1.5$ GeV, the power-law fall-off of $\phi(\text{PQCD})$ in s disagrees with the more slowly falling large-angle data, and one has little guidance from basic theory. The main interest in this low-energy region is to illustrate the effects of resonances and threshold effects on A_{NN}. In order to keep the model tractable, one can extend the background quark interchange and the resonance amplitudes at low energies using the same forms as above but replacing the dipole form factor by a phenomenological form $F(t) \propto e^{-1/2\beta\sqrt{|t|}}$. A kinematic factor of $\sqrt{s}/2p_{\rm cm}$ is included in the background amplitude. The value $\beta = 0.85$ GeV^{-1} then gives a good fit to $d\sigma/dt$ at $\theta_{\rm cm} = \pi/2$ for $p_{lab} \leq 5.5$ GeV/c.[113] The normalizations are chosen to maintain continuity of the amplitudes.

The predictions of the model and comparison with experiment are shown in Figs. 47-52. The following parameters are chosen: $C = 2.9 \times 10^3$, $\delta = -1$ for the normalization and phase of $\phi(\text{PQCD})$. The mass, width and pp branching ratio for the three resonances are $M_d^* = 2.17$ GeV, $\Gamma_d = 0.04$ GeV, $B_d^{pp} = 1$; $M_s^* = 2.55$ GeV, $\Gamma_s = 1.6$ GeV, $B_s^{pp} = 0.65$; and $M_c^* = 5.08$ GeV, $\Gamma_c = 1.0$ GeV, $B_c^{pp} = 0.0155$, respectively. As shown in Figs. 47 and 48, the deviations from the simple scaling predicted by the PQCD amplitudes are readily accounted for by the resonance structures. The cusp which appears in Fig. 48 marks the change in regime below $p_{lab} = 5.5$ GeV/c where PQCD becomes inapplicable. It is interesting to note that in this energy region normal attenuation of quasielastic pp scattering is observed.[101] The angular distribution (normalized to the data at $\theta_{cm} = \pi/2$) is predicted to broaden relative to the steeper perturbative QCD form, when the resonance dominates. As shown in Fig. 49 this is consistent with experiment, comparing data at $p_{lab} = 7.1$ and 12.1 GeV/c.

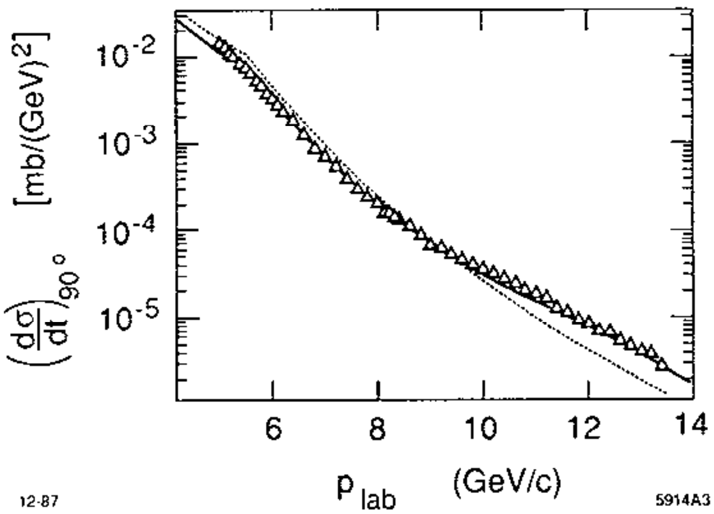

Figure 47. Prediction (solid curve) for $d\sigma/dt(pp \to pp)$ at $\theta_{cm} = \pi/2$ compared with the data of Akerlof *et al.*[113] The dotted line is the background PQCD prediction.

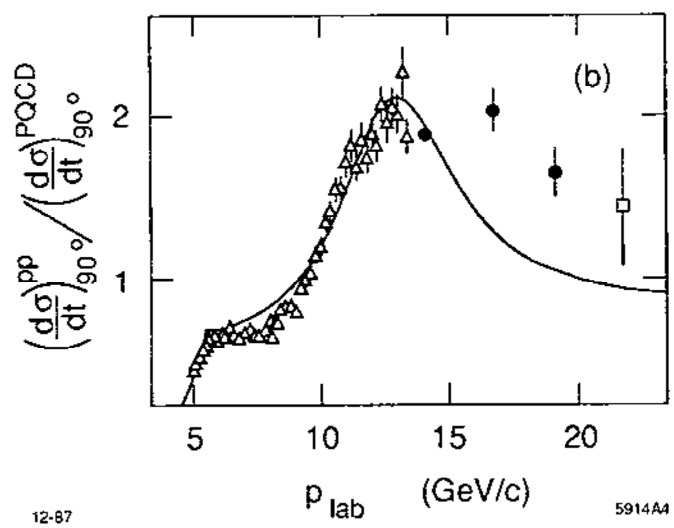

Figure 48. Ratio of $d\sigma/dt(pp \to pp)$ at $\theta_{cm} = \pi/2$ to the PQCD prediction. The data[113] are from Akerlof *et al.* (open triangles), Allaby *et al.* (solid dots) and Cocconi *et al.* (open square). The cusp at $p_{lab} = 5.5$ GeV/c indicates the change of regime from PQCD.

The most striking test of the model is its prediction for the spin correlation A_{NN} shown in Fig. 50. The rise of A_{NN} to $\simeq 60\%$ at $p_{lab} = 11.75$ GeV/c is correctly reproduced by the high energy J=1 resonance interfering with ϕ(PQCD). The narrow peak which appears in the data of Fig. 50 corresponds to the onset

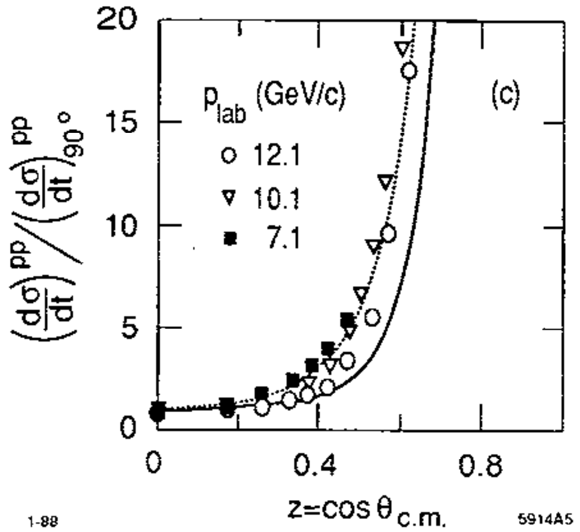

Figure 49. The $pp \to pp$ angular distribution normalized at $\theta_{cm} = \pi/2$. The data are from the compilation given in Sivers *et al.*, Ref. 32. The solid and dotted lines are predictions for $p_{lab} = 12.1$ and 7.1 GeV/c, respectively, showing the broadening near resonance.

of the $pp \to p\Delta(1232)$ channel which can be interpreted as a $uuuuddq\bar{q}$ resonant state. Because of spin-color statistics one expects in this case a higher orbital momentum state, such as a $pp\ ^3F_3$ resonance. The model is also consistent with the recent high-energy data point for A_{NN} at $p_{lab} = 18.5$ GeV/c and $p_T^2 = 4.7$ GeV^2 (see Fig. 51). The data show a dramatic decrease of A_{NN} to zero or negative values. This is explained in the model by the destructive interference effects above the resonance region. The same effect accounts for the depression of A_{NN} for $p_{lab} \approx 6$ GeV/c shown in Fig. 50. The comparison of the angular dependence of A_{NN} with data at $p_{lab} = 11.75$ GeV/c is shown in Fig. 52. The agreement with the data[114] for the longitudinal spin correlation A_{LL} at the same p_{lab} is somewhat worse.

The simple model discussed here shows that many features can be naturally explained with only a few ingredients: a perturbative QCD background plus resonant amplitudes associated with rapid changes of the inelastic pp cross section. The model provides a good description of the s and t dependence of the differential cross section, including its "oscillatory" dependence[115] in s at fixed θ_{cm}, and the broadening of the angular distribution near the resonances. Most important, it gives a consistent explanation for the striking behavior of both the spin-spin correlations and the anomalous energy dependence of the attenuation of quasielastic pp scattering in nuclei. It is predicted that color transparency should reappear at higher energies ($p_{lab} \geq 16$ GeV/c), and also at smaller angles ($\theta_{cm} \approx 60°$) at $p_{lab} = 12$ GeV/c where the perturbative QCD amplitude dominates. If the J=1 resonance structures in A_{NN} are indeed associated with heavy

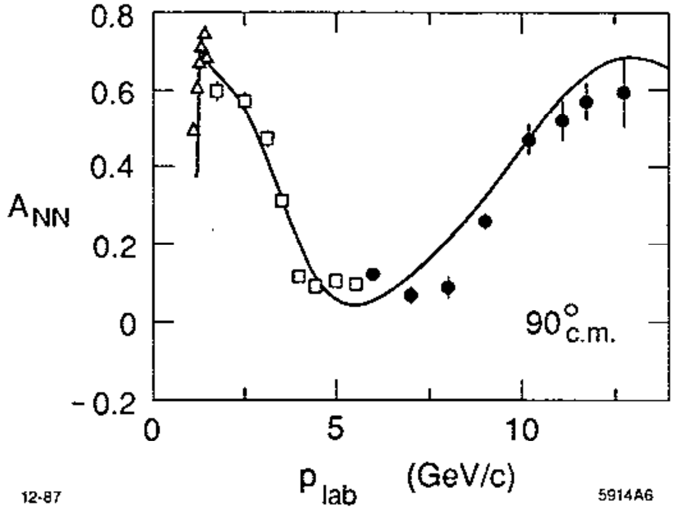

Figure 50. A_{NN} as a function of p_{lab} at $\theta_{cm} = \pi/2$. The data[113] are from Crosbie *et al.* (solid dots), Lin *et al.* (open squares) and Bhatia *et al.* (open triangles). The peak at $p_{lab} = 1.26$ GeV/c corresponds to the $p\Delta$ threshold. The data are well reproduced by the interference of the broad resonant structures at the strange ($p_{lab} = 2.35$ GeV/c) and charm ($p_{lab} = 12.8$ GeV/c) thresholds, interfering with a PQCD background. The value of A_{NN} from PQCD alone is 1/3.

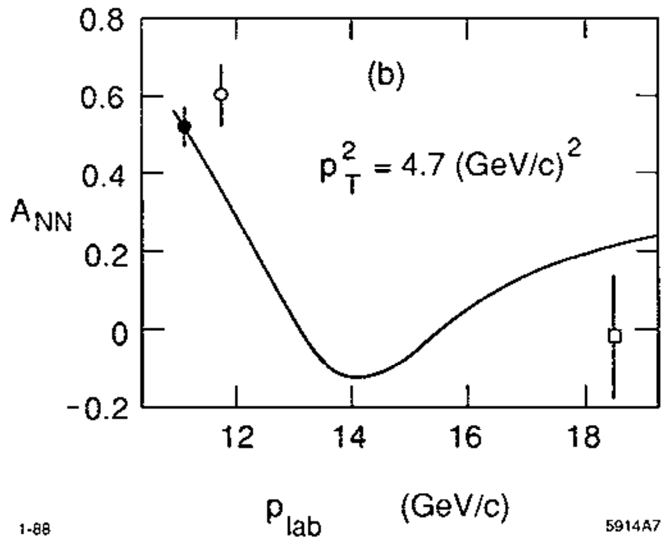

Figure 51. A_{NN} at fixed $p_T^2 = (4.7\ \mathrm{GeV/c})^2$. The data point[113] at $p_{lab} = 18.5$ GeV/c is from Court *et al.*

quark degrees of freedom, then the model predicts inelastic pp cross sections of the order of 1 mb and 1μb for the production of strange and charmed hadrons near their respective thresholds.[116] Thus a crucial test of the heavy quark hypothesis for explaining A_{NN}, rather than hidden color or gluonic excitations, is the observation of significant charm hadron production at $p_{lab} \gtrsim 12$ GeV/c.

Recently Ralston and Pire[43] have proposed that the oscillations of the pp elastic cross section and the apparent breakdown of color transparency are associated

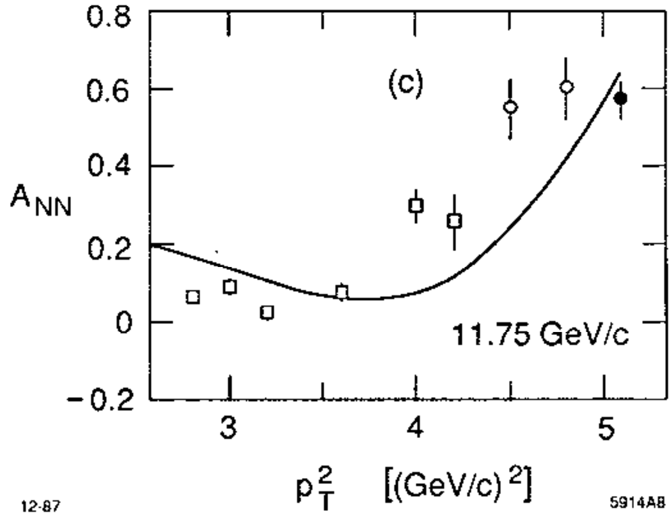

Figure 52. A_{NN} as a function of transverse momentum. The data[106] are from Crabb *et al.* (open circles) and O'Fallon *et al.* (open squares). Diffractive contributions should be included for $p_T^2 \leq 3$ GeV^2.

with the dominance of the Landshoff pinch contributions at $\sqrt{s} \sim 5\ GeV$. The oscillating behavior of $d\sigma/dt$ is due to the energy dependence of the relative phase between the pinch and hard-scattering contributions. Color transparency will disappear whenever the pinch contributions are dominant since such contributions could couple to wavefunctions of large transverse size. The large spin correlation in A_{NN} is not readily explained in the Ralston-Pire model. Clearly more data and analysis are needed to discriminate between the pinch and resonance models.

10. CONCLUSIONS

The understanding of exclusive processes is a crucial challenge to QCD. The analysis of these reactions is more complex than that of inclusive reactions since the detailed predictions necessarily depend on the form of the hadronic wavefunctions, the behavior of the running coupling constant, and analytically complex contributions from pinch and endpoint singularities. Unlike inclusive reactions, where the leading power contributions can be computed from an incoherent probabilistic form, exclusive reactions require the understanding of the phase and spin structure of hadronic amplitudes. These complications are also a virtue of exclusive reactions, since they allow a window on basic features of the theory which are extremely difficult to obtain in any other way. The perturbative QCD analysis is based on a factorization theorem so that only one distribution amplitude is required to describe the interaction of a given hadron in any large momentum transfer exclusive reaction. In some cases the predictions for exclusive processes in PQCD are completely rigorous in the sense that the results can be derived to all orders in perturbation theory. In particular the PQCD results for the pion form factor, the transition form factor $F_{\gamma\pi}(Q^2)$, and the $\gamma\gamma \to \pi\pi$ amplitudes are theorems of QCD and are as rigorous as the predictions for $R_{e^+e^-}(s)$, the evolution equations for the structure functions, etc. Although the perturbative QCD analysis is complex, it is hard to imagine that any other viable description would be simpler. At this point there is no other theoretical approach which provides as comprehensive a description of exclusive phenomena.

The application of perturbative QCD to exclusive processes has in fact been quite successful. The power laws predicted for form factors and fixed angle scattering amplitudes have been confirmed by experiment, ranging from the theoretically simplest reactions $\gamma^*\gamma \to \eta$ to the most complicated reactions such as $pp \to pp$. The application to nuclear exclusive amplitudes such as the deuteron form factor and $\gamma d \to np$ have also been surprisingly successful. Taken together with input from distribution amplitudes predicted by QCD sum rules, the sign and magnitude of the meson form factors, the $\gamma\gamma \to \pi^+\pi^-$, K^+K^-, the Compton amplitude $\gamma p \to \gamma p$ and the proton form factor are all apparent, though model dependent, successes of the theory.

The fact that PQCD scaling laws appear to hold even at momentum transfer as low as 1 GeV/c suggests that the QCD running coupling constant is rather slowly changing even at momentum transfers of order 200 MeV. Barring a conspiracy between non-perturbative and perturbative contributions, the evidence from exclusive reactions is that $\Lambda_{\overline{MS}}^{QCD}$ is of order 100 MeV or even smaller. Alternatively the running coupling constant may "freeze" at the low effective momenta characteristic of exclusive processes. Thus the analysis of exclusive reactions provides important information on the basic parameters of QCD.

As we discussed in Section 8.2, recent BNL data for pp quasi-elastic scattering in nuclei at $\theta_{cm} = \frac{\pi}{2}$ shows that the number of effective protons in the nucleus rises with the momentum transfer as predicted by color transparency at least up to $p_{lab} = 10$ GeV/c. This remarkable empirical result clearly rules out any description of exclusive reactions based on soft wavefunctions. The observation of the onset of color transparency in quasi-elastic $pp \to pp$ scattering appears to be an outstanding validation of a fundamental feature of perturbative QCD phenomenology. The tests of color transparency address directly the central dynamical assumption of the perturbative analysis, that exclusive reactions at high momentum transfer are controlled by Fock components of the hadron wavefunction with small transverse size.

However, in direct contradiction to PQCD expectations, the BNL data at higher momentum, $p_{lab} = 12$ GeV/c, indicates normal Glauber attenuation. Because of the importance of this and other anomalies and the challenges they pose to the theory, we have devoted several sections of this article to these topics and their possible resolution.

The successes of fixed-angle scaling laws could of course be illusory, perhaps due to soft hadronic mechanisms which temporarily simulate the dimensional counting rules at a range of intermediate momentum transfer. If such a description is correct, then the perturbative contributions become dominant only at very large momentum transfer. Quantities such as $Q^2 F_\pi(Q^2)$ would drop from the present plateau to the PQCD prediction, but at a high value of Q^2, much higher than the natural scales of the theory. An important question is whether a soft hadronic model can also account for the normalization of the cross sections for other exclusive processes besides form factor measurements. For example, consider hadronic Compton amplitudes such as $\gamma p \to \gamma p$ or $\gamma\gamma \to \pi^+\pi^-$. As we have shown in Section 7, the data appear to scale in momentum transfer according to the perturbative QCD predictions. One can consider a simple model where the hadronic Compton amplitude is given by the product of a point-like Compton amplitude multiplied by the corresponding hadronic form factor. This model predicts $d\sigma/dt(\gamma p \to \gamma p) \simeq 5\ pb/GeV^2$ at $s = 8\ GeV^2$, $\theta_{cm} = \pi/2$ compared to the experimental value of 300 pb/GeV^2 (see Fig. 33). The same simple model predicts $\sigma(\gamma\gamma \to \pi^+\pi^-) \simeq 0.1\ nb$ at $s = 5\ GeV^2$ compared to the experimental value of 2 nb (see Fig. 31).

The above estimates are also characteristic of the soft-scattering models in which the end-point large x regime dominates so that the Compton amplitude is given by the sum of coherent point-like quark Compton amplitudes with $x_q \simeq 1$ multiplied by the electromagnetic form factor. Again one has the problem that the normalization of data for large angle Compton scattering is one to two orders of magnitude larger than predicted. In contrast, in the perturbative QCD description there are many more contributing coherent hard scattering amplitudes for Compton scattering than lepton-proton scattering, so the large relative magnitude of the proton Compton cross section can be accounted for. In the case of large angle pp scattering, the large normalization of the data relative to that obtained by simply multiplying form factors can be understood as a consequence of the many coherent contributions to T_H for this process. We also emphasize that the observation of color transparency in the BNL experiment implies minimal attenuation of the incident and outgoing protons and thus appears to exclude any model in which the full size of the hadron participates in the hard scattering reaction.

Questions have been raised recently[24] on a number of questions concerning the application of perturbative QCD to exclusive reactions in the momentum transfer range presently accessible to experiment. The issues involved are very important for understanding the basis of virtually all perturbative QCD predictions. The debate is not on the validity of the predictions but on the appropriate range of their applicability because of possible complications such as nonperturbative effects. The questions raised highlight the importance of further experimental tests of exclusive processes.

As we have discussed in this article, there are, in addition to the numerous successes of the theory, a number of major conflicts between perturbative QCD predictions for exclusive processes and experiment which can not be readily blamed on higher contributions in $\alpha_s(Q^2)$. For example, the helicity selection rule appears to be broken in $\pi p \to \rho^0 p$ scattering at large angles, the $J/\psi \to \pi\rho$ and $J/\psi \to KK^*$ decays. The strong spin correlations seen in large angle pp scattering at $\sqrt{s} = 5\ GeV$ are not explained by PQCD mechanisms. Color transparency appears to fail at the same energy. Small but systematic deviations or oscillations are observed relative to the PQCD power-law behavior. In each case, the data seems to indicate the intrusion of soft non-perturbative QCD mechanisms such as resonances perhaps due to gluonic or color excitations or heavy quark threshold effects. The presence of contributions from Landshoff pinch singularities may also be indicated.

Thus exclusive reactions still remain a challenge to theory. A crucial requirement for future progress is the computation of hadron light-cone wavefunctions directly from QCD. Unfortunately it appears very difficult to obtain much more than the leading moments of the distribution amplitude from either lattice gauge theory or QCD sum rules. The discretized light-cone quantization method reviewed in Appendix III shows promise, but so far solutions have been limited to QCD in one space and one time dimension. The computation of hadronic structure functions, magnetic moments, and electroweak decay amplitudes also require this non-perturbative input. The detailed understanding of the relative role of perturbative and non-perturbative contributions to exclusive amplitudes will unquestionably require a fuller understanding of the hadronic wavefunctions.

Much more theoretical work is also required to compute the hard scattering amplitudes for experimentally accessible exclusive processes, and to understand in detail how to integrate over the pinch and endpoint singularities, taking into account Sudakov suppression in the non-Abelian theory. The computerized algebraic methods now available can be used to compute the hard-scattering quark-gluon amplitude T_H for processes as complicated as $pp \to pp$ and the deuteron form factor. Each Feynman diagram which contributes to T_H represents a particular overlap of the participating hadron wavefunctions. Considering the uncertainties in the wavefunctions and the myriad number of diagrams contributing to pp scattering, even getting the correct order of magnitude of the large angle cross section would be a triumph of the theory. Computations of the higher order corrections to high momentum transfer exclusive reactions will eventually also be needed.

More precise predictions for color transparency is needed, particularly ep quasi-elastic scattering in nuclei. The analysis requires computing the detailed parameters which control the color transparency effect due to smallness of the participating Fock state amplitude, and by uncertainties involving the role of formation zone physics, which controls the length of time the hadron can stay small as it traverses the nucleus.

The experimental study of exclusive reactions is also in its infancy. Much more experimental input is required particularly from ep, γp, $\overline{p}p$, and $\gamma\gamma$ initial states. Ratios of processes such as $\gamma\gamma \to p\overline{p}$ and $\Delta^{++}\overline{\Delta}^{++}$ can isolate important features of the baryon wavefunctions. The ratio of the square transition form factor for $\gamma^*\gamma \to \pi^0$ to the pion form factor provides a wave-function independent determination of $\alpha_s(Q^2)$. It is important to confirm the color transparency phenomena, particularly in the simplest channels such as ep quasi-elastic scattering. It is important to verify that both elastic and inelastic initial and final state interactions are suppressed in the nucleus. Once this phenomena is validated it can be used as a "color filter" to separate soft and hard contributions to a large range of exclusive reactions.

We have emphasized in this article that the correctness of the PQCD description of exclusive processes is by no means settled. There is now a strong challenge to design decisive experimental and theoretical tests of the theory. If the theory survives, the reward is high: through exclusive reactions we can explore both the behavior of QCD and the structure of hadrons.

APPENDIX I
BARYON FORM FACTORS AND EVOLUTION EQUATIONS

The meson form factor analysis given in Section 3 is the prototype for the calculation of the QCD hard scattering contribution for the whole range of exclusive processes at large momentum transfer. Away from possible special points in the x_i integrations a general hadronic amplitude can be written to leading order in $1/Q^2$ as a convolution of a connected hard-scattering amplitude T_H convoluted with the meson and baryon distribution amplitudes:

$$\phi_M(x,Q) = \int^{|\mathcal{E}|<Q^2} \frac{d^2k_\perp}{16\pi^2} \psi^Q_{q\overline{q}}(x,\vec{k}_\perp) \quad ,$$

and

$$\phi_B(x_i, Q) = \int^{|\mathcal{E}|<Q^2} [d^2k_\perp]\psi_{qqq}(x_i, \vec{k}_{\perp i}) \ .$$

The hard scattering amplitude T_H is computed by replacing each external hadron line by massless valence quarks each collinear with the hadron's momentum $p_i^\mu \cong x_i p_H^\mu$. For example the baryon form factor at large Q^2 has the form[4,6]

$$G_M(Q^2) = \int [dx][dy]\phi^*(y_i, \overline{Q})T_H(x, y; Q^2)\phi(x, \overline{Q})$$

where T_H is the $3q + \gamma \to 3q'$ amplitude. For the proton and neutron we have to leading order $[C_B = 2/3]$

$$T_p = \frac{128\pi^2 C_B^2}{(Q^2 + M_0^2)^2}\, T_1$$
$$T_n = \frac{128\pi^2 C_B^2}{3(Q^2 + M_0^2)^2}\, [T_1 - T_2]$$

where

$$\begin{aligned} T_1 = &- \frac{\alpha_s(x_3 y_3 Q^2)\ \alpha_s(1 - x_1)(1 - y_1)Q^2)}{x_3(1 - x_1)^2\ y_3(1 - y_1)^2} \\ &+ \frac{\alpha_s(x_2 y_2 Q^2)\ \alpha_s\left((1 - x_1)(1 - y_1)Q^2\right)}{x_2(1 - x_1)^2\ y_2(1 - y_1)^2} \\ &- \frac{\alpha_s(x_2 y_2 Q^2)\ \alpha_s(x_3 y_3 Q^2)}{x_2 x_3(1 - x_3)\ y_2 y_3(1 - y_1)} \end{aligned} \quad ,$$

and

$$T_2 = -\frac{\alpha_s(x_1 y_1 Q^2)\ \alpha_s(x_3 y_3 Q^2)}{x_1 x_3(1 - x_1)\ y_1 y_3(1 - y_3)} \quad .$$

T_1 corresponds to the amplitude where the photon interacts with the quarks (1) and (2) which have helicity parallel to the nucleon helicity, and T_2 corresponds to the amplitude where the quark with opposite helicity is struck. The running coupling constants have arguments $\hat{Q}^2$ corresponding to the gluon momentum transfer of each diagram. Only the large Q^2 behavior is predicted by the theory; we utilize the parameter M_0 to represent the effect of power-law suppressed terms from mass insertions, higher Fock states, etc.

The Q^2-evolution of the baryon distribution amplitude can be derived from the operator product expansion of three quark fields or from the gluon exchange kernel, in parallel with derivation of Eq. (90). The baryon evolution equation to leading order in α_s is[6]

$$x_1x_2x_3\left\{\frac{\partial}{\partial\zeta}\tilde{\phi}(x_i,Q)+\frac{3}{2}\frac{C_F}{\beta_0}\tilde{\phi}(x_i,Q)\right\}=\frac{C_B}{\beta_0}\int_0^1[dy]V(x_i,y_i)\tilde{\phi}(y_i,Q).$$

Here $\phi = x_1x_2x_3\tilde{\phi}, \zeta = \log(\log Q^2/\Lambda^2)$, $C_F = (n_c^2-1)/2n_c = 4/3$, $C_B = (n_c + 1)/2n_c = 2/3$, $\beta = 11-(2/3)n_f$, and $V(x_i,y_i)$ is computed to leading order in α_s from the single-gluon-exchange kernel [see Fig. 19(b)]:

$$\begin{aligned} V(x_i,y_i) &= 2x_ix_2x_3\sum_{i\neq j}\theta(y_i-x_i)\delta(x_k-y_k)\frac{y_j}{x_j}\left(\frac{\delta_{h_i\bar{h}_j}}{x_i+x_j}+\frac{\Delta}{y_i-x_i}\right)\\ &= V(y_i,x_i) \quad . \end{aligned}$$

The infrared singularity at $x_i = y_i$ is cancelled because the baryon is a color singlet.

The evolution equation automatically sums to leading order in $\alpha_s(Q^2)$ all of the contributions from multiple gluon exchange which determine the tail of the valence wavefunction and thus the Q^2-dependence of the distribution amplitude. The general solution of this equation is

$$\phi(x_i,Q) = x_1x_2x_3\sum_{n=0}^{\infty}a_n\left(\ell n\,\frac{Q^2}{\Lambda^2}\right)^{-\gamma_n}\quad\tilde{\phi}_n(x_i)\quad ,$$

where the anomalous dimensions γ_n and the eigenfunctions $\tilde{\phi}_n(x_i)$ satisfy the characteristic equation:

$$x_1x_2x_3\left(-\gamma_n+\frac{3C_F}{2\beta}\right)\tilde{\phi}_n(x_i)=\frac{C_B}{\beta}\int_0^1[dy]\;V(x_i,y_i)\,\tilde{\phi}_n(y_i)\quad .$$

A useful technique for obtaining the solution to the evolution equations is to construct completely antisymmetric representations as a polynomial orthonormal basis for the distribution amplitude of multiquark bound states. In this way one obtain a distinctive classification of nucleon (N) and delta (Δ) wave functions and the corresponding Q^2 dependence which discriminates N and Δ form factors. This technique is developed in detail in Ref. 117.

Taking into account the evolution of the baryon distribution amplitude, the nucleon magnetic form factors at large Q^2, has the form[4,6]

$$G_M(Q^2) \to \frac{\alpha_s^2(Q^2)}{Q^4} \sum_{n,m} b_{nm} \left(\log \frac{Q^2}{\Lambda^2}\right)^{\gamma_n^B - \gamma_n^B} \left[1 + \mathcal{O}\left(\alpha_s(Q^2), \frac{m^2}{Q^2}\right)\right] \quad .$$

where the γ_n are computable anomalous dimensions of the baryon three-quark wave function at short distance and the b_{mn} are determined from the value of the distribution amplitude $\phi_B(x, Q_0^2)$ at a given point Q_0^2 and the normalization of T_H. Asymptotically, the dominant term has the minimum anomalous dimension. The dominant part of the form factor comes from the region of the x_i integration where each quark has a finite fraction of the light cone momentum. The integrations over x_i and y_i have potential endpoint singularities. However, it is easily seen that any anomalous contribution [*e.g.* from the region $x_2, x_3 \sim \mathcal{O}(m/Q), x_1 \sim 1 - \mathcal{O}(m/Q)$] is asymptotically suppressed at large Q^2 by a Sudakov form factor arising from the virtual correction to the $\bar{q}\gamma q$ vertex when the quark legs are near-on-shell [$p^2 \sim \mathcal{O}(mQ)$].[6,19] This Sudakov suppression of the endpoint region requires an all orders resummation of perturbative contributions, and thus the derivation of the baryon form factors is not as rigorous as for the meson form factor, which has no such endpoint singularity.[19]

One can also use PQCD to predict ratios of various baryon and isobar form factors assuming isospin or $SU(3)$-flavor symmetry for the basic wave function structure. Results for the neutral weak and charged weak form factors assuming standard $SU(2) \times U(1)$ symmetry are given in Ref. 47.

APPENDIX II
LIGHT CONE QUANTIZATION AND PERTURBATION THEORY

In this Appendix, we outline the canonical quantization of QCD in $A^+ = 0$ gauge. The discussion follows that given in Refs. 4 and 51. This proceeds in several steps. First we identify the independent dynamical degrees of freedom in the Lagrangian. The theory is quantized by defining commutation relations for these dynamical fields at a given light-cone time $\tau = t + z$ (we choose $\tau = 0$). These commutation relations lead immediately to the definition of the Fock state basis. Expressing dependent fields in terms of the independent fields, we then derive a light-cone Hamiltonian, which determines the evolution of the state space with changing τ. Finally we derive the rules for τ-ordered perturbation theory.

The major purpose of this exercise is to illustrate the origins and nature of the Fock state expansion, and of light-cone perturbation theory. We will ignore subtleties due to the large scale structure of non-Abelian gauge fields (*e.g.* 'instantons'), chiral symmetry breaking, and the like. Although these have a profound effect on the structure of the vacuum, the theory can still be described with a Fock state basis and some sort of effective Hamiltonian. Furthermore, the short distance interactions of the theory are unaffected by this structure, or at least this is the central ansatz of perturbative QCD.

Quantization

The Lagrangian (density) for QCD can be written

$$\mathcal{L} = -\frac{1}{2}\,\mathrm{Tr}\,(F^{\mu\nu}\,F_{\mu\nu}) + \overline{\psi}\,(i\,\not{D} - m)\,\psi$$

where $F^{\mu\nu} = \partial^\mu A^\nu - \partial^\nu A^\mu + ig[A^\mu, A^\nu]$ and $iD^\mu = i\partial^\mu - gA^\mu$. Here the gauge field A^μ is a traceless 3×3 color matrix ($A^\mu \equiv \sum_a A^{a\mu}T^a$, $\mathrm{Tr}(T^aT^b) = 1/2\delta^{ab}$, $[T^a, T^b] = ic^{abc}T^c, \ldots$), and the quark field ψ is a color triplet spinor (for simplicity, we include only one flavor). At a given light-cone time, say $\tau = 0$, the independent dynamical fields are $\psi_\pm \equiv \Lambda_\pm\psi$ and $A^i_\perp$ with conjugate fields $i\psi^\dagger_+$ and $\partial^+ A^i_\perp$, where $\Lambda_\pm = \gamma^o\gamma^\pm/2$ are projection operators ($\Lambda_+\Lambda_- = 0$, $\Lambda^2_\pm = \Lambda_\pm$, $\Lambda_+ + \Lambda_- = 1$) and $\partial^\pm = \partial^0 \pm \partial^3$. Using the equations of motion, the remaining fields in $\mathcal{L}$ can be expressed in terms of ψ_+, $A^i_\perp$:

$$\begin{aligned}
\psi_- \equiv \Lambda_-\psi &= \frac{1}{i\partial^+}\left[i\vec{D}_\perp\cdot\vec{\alpha}_\perp + \beta m\right]\psi_+ \\
&= \widetilde{\psi}_- - \frac{1}{i\partial^+}\,g\vec{A}_\perp\cdot\vec{\alpha}_\perp\,\psi_+\ , \\
A^+ &= 0\ , \\
A^- &= \frac{2}{i\partial^+}\,i\vec{\partial}_\perp\cdot\vec{A}_\perp + \frac{2g}{(i\partial^+)^2}\left\{\left[i\partial^+ A^i_\perp, A^i_\perp\right] + 2\psi^\dagger_+\,T^a\,\psi_+\,T^a\right\} \\
&\equiv \widetilde{A}^- + \frac{2g}{(i\partial^+)^2}\left\{\left[i\partial^+ A^i_\perp, A^i_\perp\right] + 2\psi^\dagger_+\,T^a\,\psi_+\,T^a\right\}\ ,
\end{aligned}$$

with $\beta = \gamma^o$ and $\vec{\alpha}_\perp = \gamma^o\vec{\gamma}$.

To quantize, we expand the fields at $\tau = 0$ in terms of creation and annihilation operators,

$$\psi_+(x) = \int\limits_{k^+>0} \frac{dk^+\, d^2k_\perp}{k^+\, 16\pi^3} \sum_\lambda \Big\{ b(\underline{k},\lambda)\; u_+(\underline{k},\lambda)\; e^{-ik\cdot x}$$

$$+\, d^\dagger(\underline{k},\lambda)\; v_+(\underline{k},\lambda)\; e^{ik\cdot x} \Big\} \ , \quad \tau = x^+ = 0$$

$$A^i_\perp(x) = \int\limits_{k^+>0} \frac{dk^+\, d^2k_\perp}{k^+\, 16\pi^3} \sum_\lambda \Big\{ a(\underline{k},\lambda)\; \epsilon^i_\perp(\lambda)\; e^{-ik\cdot x} + c\, c \Big\} \ , \quad \tau = x^+ = 0 \ ,$$

with commutation relations ($\underline{k} = (k^+, \vec{k}_\perp)$):

$$\begin{aligned}
\Big\{ b(\underline{k},\lambda),\ b^\dagger(\underline{p},\lambda) \Big\} &= \Big\{ d(\underline{k},\lambda),\ d^\dagger(\underline{p},\lambda') \Big\} \\
&= \Big[a(\underline{k},\lambda),\ a^\dagger(\underline{p},\lambda') \Big] \\
&= 16\pi^3\, k^+\, \delta^3(\underline{k}-\underline{p})\, \delta_{\lambda\lambda'} \ , \\
\{b,b\} = \{d,d\} &= \ldots = 0 \ ,
\end{aligned}$$

where λ is the quark or gluon helicity. These definitions imply canonical commutation relations for the fields with their conjugates ($\tau = x^+ = y^+ = 0$, $\underline{x} = (x^-, x_\perp), \ldots$):

$$\Big\{ \psi_+(\underline{x}),\ \psi_+^\dagger(\underline{y}) \Big\} = \Lambda_+\, \delta^3(\underline{x}-\underline{y}) \ ,$$

$$\Big[A^i(\underline{x}),\ \partial^+ A^j_\perp(\underline{y}) \Big] = i\delta^{ij}\, \delta^3(\underline{x}-\underline{y}) \ .$$

The creation and annihilation operators define the Fock state basis for the theory at $\tau = 0$, with a vacuum $|0\rangle$ defined such that $b\,|0\rangle = d\,|0\rangle = a\,|0\rangle = 0$. The evolution of these states with τ is governed by the light-cone Hamiltonian, $H_{LC} = P^-$, conjugate to τ. The Hamiltonian can be readily expressed in terms of ψ_+ and $A^i_\perp$:

$$H_{LC} = H_0 + V \ ,$$

where

$$H_0 = \int d^3x \left\{ \mathrm{Tr}\left(\partial_\perp^i A_\perp^j \partial_\perp^i A_\perp^j\right) + \psi_+^\dagger \left(i\partial_\perp \cdot \alpha_\perp + \beta m\right) \frac{1}{i\partial^+} \left(i\partial_\perp \cdot \alpha_\perp + \beta m\right) \psi_+ \right\}$$

$$= \sum_{\substack{\lambda \\ \text{colors}}} \int \frac{dk^+ \, d^2k_\perp}{16\pi^3 \, k^+} \left\{ a^\dagger(\underline{k}, \lambda)\, a(\underline{k}, \lambda) \frac{k_\perp^2}{k^+} + b^\dagger(\underline{k}, \lambda)\, b(\underline{k}, \lambda) \right.$$

$$\left. \times \frac{k_\perp^2 + m^2}{k^+} + d^\dagger(\underline{k}, \lambda)\, b(\underline{k}, \lambda) \frac{k_\perp^2 + m^2}{k^+} \right\} + \text{constant}$$

is the free Hamiltonian and V the interaction:

$$V = \int d^3x \left\{ 2g \, \mathrm{Tr}\left(i\partial^\mu \widetilde{A}^\nu \left[\widetilde{A}_\mu, \widetilde{A}_\nu\right]\right) - \frac{g^2}{2} \mathrm{Tr}\left(\left[\widetilde{A}^\mu, \widetilde{A}^\nu\right]\left[\widetilde{A}_\mu, \widetilde{A}_\nu\right]\right) \right.$$

$$+ g\overline{\widetilde{\psi}} \, \not{A} \, \widetilde{\psi} + g^2 \, \mathrm{Tr}\left(\left[i\partial^+ \widetilde{A}^\mu, \widetilde{A}_\mu\right] \frac{1}{(i\partial^+)^2} \left[i\partial^+ \widetilde{A}^\nu, \widetilde{A}_\nu\right]\right)$$

$$+ g^2 \overline{\widetilde{\psi}} \, \not{A} \frac{\gamma^+}{2i\partial^+} \, \not{A} \, \widetilde{\psi} - g^2 \overline{\widetilde{\psi}} \gamma^+ \left(\frac{1}{(i\partial^+)^2} \left[i\partial^+ \widetilde{A}^\nu, \widetilde{A}_\nu\right]\right) \widetilde{\psi}$$

$$\left. + \frac{g^2}{2} \, \overline{\psi}\gamma^+ \, T^a \psi \, \frac{1}{(i\partial^+)^2} \, \overline{\psi}\gamma^+ \, T^a \psi \right\} ,$$

with $\widetilde{\psi} = \widetilde{\psi}_- + \psi_+$ ($\rightarrow \psi$ as $g \rightarrow 0$) and $\widetilde{A}^\mu = (0, \widetilde{A}^-, A_\perp^i)$ ($\rightarrow A^\mu$ as $g \rightarrow 0$). The Fock states are obviously eigenstates of H_0 with

$$H_0 \left| n : k_i^+, k_{\perp i} \right\rangle = \sum_i \left(\frac{k_\perp^2 + m^2}{k^+}\right)_i \left| n : k_i^+, k_{\perp i} \right\rangle .$$

It is equally obvious that they are not eigenstates of V, though any matrix element of V between Fock states is trivially evaluated. The first three terms in V correspond to the familiar three and four gluon vertices, and the gluon-quark vertex [Fig. 53(a)]. The remaining terms represent new four-quanta interactions containing instantaneous fermion and gluon propagators [Fig. 53(b)]. All terms conserve total three-momentum $\underline{k} = (k^+, \vec{k}_\perp)$, because of the integral over $\underline{x}$ in V. Furthermore, all Fock states other than the vacuum have total $k^+ > 0$, since each individual bare quantum has $k^+ > 0$. Consequently the Fock state vacuum

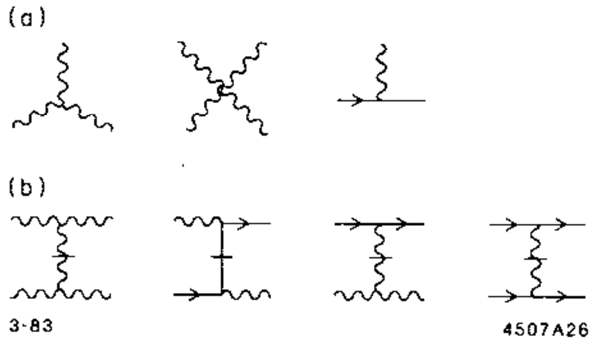

Figure 53. Diagrams which appear in the interaction Hamiltonian for QCD on the light cone. The propagators with horizontal bars represent "instantaneous" gluon and quark exchange which arise from reduction of the dependent fields in $A^+ = 0$ gauge. (a) Basic interaction vertices in QCD. (b) "Instantaneous" contributions.

must be an eigenstate of V and therefore an eigenstate of the full light-cone Hamiltonian.

Light-Cone Perturbation Theory

We define light-cone Green's functions to be the probability amplitudes that a state starting in Fock state $|i\rangle$ ends up in Fock state $|f\rangle$ a (light-cone) time τ later

$$\begin{aligned}\langle f|i\rangle\ G(f,i;\tau) &\equiv \langle f|e^{-iH_{LC}\tau/2}|i\rangle \\ &= i\int \frac{d\epsilon}{2\pi}\ e^{-i\epsilon\tau/2}\ G(f,i;\epsilon)\,\langle f|i\rangle\ ,\end{aligned}$$

where Fourier transform $G(f,i;\epsilon)$ can be written

$$\begin{aligned}\langle f|i\rangle\ G(f,i;\epsilon) &= \left\langle f\left|\frac{1}{\epsilon - H_{LC} + i0_+}\right|i\right\rangle \\ &= \left\langle f\left|\frac{1}{\epsilon - H_{LC} + i0_+} + \frac{1}{\epsilon - H_0 + i0_+}\,V\,\frac{1}{\epsilon - H_0 + i0_+}\right.\right. \\ &\quad \left.\left. + \frac{1}{\epsilon - H_0 + i0_+}\,V\,\frac{1}{\epsilon - H_0 + i0_+}\,V\,\frac{1}{\epsilon - H_0 + i0_+} + \dots\right|i\right\rangle .\end{aligned}$$

The rules for τ-ordered perturbation theory follow immediately when $(\epsilon - H_0)^{-1}$ is replaced by its spectral decomposition.

$$\frac{1}{\epsilon - H_0 + i0_+} = \sum_{n,\lambda_i}\int \widetilde{\prod}\ \frac{dk_i^+\,d^2k_{\perp i}}{16\pi^3\,k_i^+}\ \frac{|n:\underline{k}_i,\lambda_i\rangle\ \langle n:\underline{k}_i,\lambda_i|}{\epsilon - \sum\limits_i (k^2+m^2)_i/k_i^+ + i0_+}$$

The sum becomes a sum over all states n intermediate between two interactions.

To calculate $G(f,i;\epsilon)$ perturbatively then, all τ-ordered diagrams must be considered, the contribution from each graph computed according to the following rules:

1. Assign a momentum k^μ to each line such that the total $k^+, k_\perp$ are conserved at each vertex, and such that $k^2 = m^2$, *i.e.* $k^- = (k^2 + m^2)/k^+$. With fermions associate an on-shell spinor.

$$u(\underline{k},\lambda) = \frac{1}{\sqrt{k^+}}\left(k^+ + \beta m + \vec{\alpha}_\perp \cdot \vec{k}_\perp\right) \begin{cases} \chi(\uparrow) & \lambda = \uparrow \\ \chi(\downarrow) & \lambda = \downarrow \end{cases}$$

or

$$v(\underline{k},\lambda) = \frac{1}{\sqrt{k^+}}\left(k^+ - \beta m + \vec{\alpha}_\perp \cdot \vec{k}_\perp\right) \begin{cases} \chi(\downarrow) & \lambda = \uparrow \\ \chi(\uparrow) & \lambda = \downarrow \end{cases}$$

where $\chi(\uparrow) = 1/\sqrt{2}\,(1,0,1,0)$ and $\chi(\downarrow) = 1/\sqrt{2}\,(0,1,0,-1)^T$. For gluon lines, assign a polarization vector $\epsilon^\mu = (0,\ 2\vec{\epsilon}_\perp \cdot \vec{k}_\perp/k^+,\ \vec{\epsilon}_\perp)$ where $\vec{\epsilon}_\perp(\uparrow) = -1/\sqrt{2}\,(1,i)$ and $\vec{\epsilon}_\perp(\downarrow) = 1/\sqrt{2}\,(1,-i)$.

2. Include a factor $\theta(k^+)/k^+$ for each internal line.

3. For each vertex include factors as illustrated in Fig. 54. To convert incoming into outgoing lines or vice versa replace

$$u \leftrightarrow v\ , \qquad \overline{u} \leftrightarrow -\overline{v}\ , \qquad \epsilon \leftrightarrow \epsilon^*$$

in any of these vertices.

4. For each intermediate state there is a factor

$$\frac{1}{\epsilon - \sum\limits_{\text{interm}} k^- + i0_+}$$

where ϵ is the incident P^-, and the sum is over all particles in the intermediate state.

5. Integrate $\int dk^+ d^2k_\perp/16\pi^3$ over each independent k, and sum over internal helicities and colors.

6. Include a factor -1 for each closed fermion loop, for each fermion line that both begins and ends in the initial state (*i.e.* $\overline{v}\ldots u$), and for each diagram in which fermion lines are interchanged in either of the initial or final states.

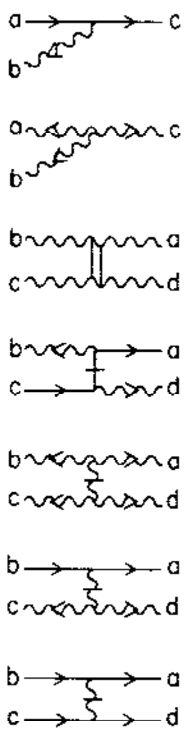

Vertex Factor	Color Factor
$g\bar{u}(c)\,\not{\epsilon}_b\,u(a)$	T^b
$g\{(p_a - p_b)\cdot\epsilon_c^*\epsilon_a\cdot\epsilon_b$ + cyclic permutations$\}$	iC^{abc}
$g^2\left\{\epsilon_b\cdot\epsilon_c\epsilon_a^*\cdot\epsilon_d^* + \epsilon_a^*\cdot\epsilon_c\epsilon_b\cdot\epsilon_d^*\right\}$	$iC^{abe}\,iC^{cde}$
$g^2\,\bar{u}(a)\,\not{\epsilon}_b\,\dfrac{\gamma^+}{2(p_c^+ - p_d^+)}\,\not{\epsilon}_c^*\,u(c)$	$T^b\,T^d$
$g^2\epsilon_a^*\cdot\epsilon_b\,\dfrac{(p_a^+ - p_b^+)(p_c^+ - p_d^+)}{(p_c^+ + p_b^+)}\,\epsilon_d^*\cdot\epsilon_c$	$iC^{abe}\,iC^{cde}$
$g^2\,\bar{u}(a)\,\gamma^+u(b)\,\dfrac{(p_c^+ - p_d^+)}{(p_c^+ + p_d^+)^2}\,\epsilon_d^*\cdot\epsilon_c$	$iC^{cde}\,T^e$
$g^2\,\dfrac{\bar{u}(a)\,\gamma^+u(b)\,\bar{u}(d)\,\gamma^+u(c)}{(p_c^+ - p_d^+)^2}$	$T^e\,T^e$

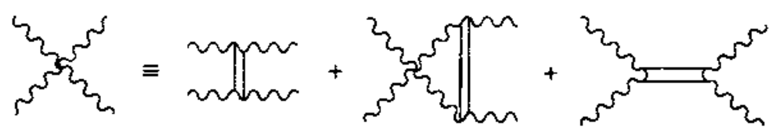

3-83 4507A25

Figure 54. Graphical rules for QCD in light-cone perturbation theory.

As an illustration, the second diagram in Fig. 54 contributes

$$\frac{1}{\epsilon - \sum\limits_{i=b,d}\left(\frac{k_\perp^2+m^2}{k^+}\right)_i}\cdot\frac{\theta(k_a^+ - k_b^+)}{k_a^+ - k_b^+}$$

$$\times\frac{g^2\sum\limits_\lambda \overline{u}(b)\,\epsilon^*(\underline{k}_a - \underline{k}_b,\lambda)\,u(a)\,\overline{u}(d)\,\not{\epsilon}(\underline{k}_a - \underline{k}_b,\lambda)\,u(c)}{\epsilon - \sum\limits_{i=b,c}\left(\frac{k_\perp^2+m^2}{k^+}\right)_i - \frac{(k_{\perp a}-k_{\perp b})^2}{k_a^+ - k_b^+}}\cdot\frac{1}{\epsilon - \sum\limits_{i=a,c}\left(\frac{k_\perp^2+m^2}{k^+}\right)_i}$$

(times a color factor) to the $q\overline{q}\to q\overline{q}$ Green's function. (The vertices for quarks and gluons of definite helicity have very simple expressions in terms of the momenta of the particles.) The same rules apply for scattering amplitudes, but with propagators omitted for external lines, and with $\epsilon = P^-$ of the initial (and final) states.

Finally, notice that this quantization procedure and perturbation theory (graph by graph) are manifestly invariant under a large class of Lorentz transformations:

1. boosts along the 3-direction — *i.e.* $p^+ \to Kp^+$, $p^- \to K^{-1}p^-$, $p_\perp \to p_\perp$ for each momentum;
2. transverse boosts — *i.e.* $p^+ \to p^+$, $p^- \to p^- + 2p_\perp \cdot Q_\perp + p^+ Q_\perp^2$, $p_\perp \to p_\perp + p^+ Q_\perp$ for each momentum ($Q_\perp$ like K is dimensionless);
3. rotations about the 3-direction.

It is these invariances which lead to the frame independence of the Fock state wave functions.

APPENDIX III
A NONPERTURBATIVE ANALYSIS OF EXCLUSIVE REACTIONS–DISCRETIZED LIGHT-CONE QUANTIZATION

Only a small fraction of exclusive processes can be addressed by perturbative QCD analyses. Despite the simplicity of the e^+e^- and $\gamma\gamma$ initial state, the full complexity of hadron dynamics is involved in understanding resonance production, exclusive channels near threshold, jet hadronization, the hadronic contribution to the photon structure function, and the total e^+e^- or $\gamma\gamma$ annihilation cross section. A primary question is whether we can ever hope to confront QCD directly in its nonperturbative domain. Lattice gauge theory and effective Lagrangian methods such as the Skyrme model offer some hope in understanding the low-lying hadron spectrum but dynamical computations relevant to $\gamma\gamma$ annihilation appear intractable. Considerable information[16] on the spectrum and the moments of hadron valence wavefunctions has been obtained using the ITEP QCD sum rule method, but the region of applicability of this method to dynamical problems appears limited.

Recently a new method for analysing QCD in the nonperturbative domain has been developed: discretized light-cone quantization (DLCQ).[118] The method has the potential for providing detailed information on all the hadron's Fock light-cone components. DLCQ has been used to obtain the complete spectrum of neutral states in QED[8] and QCD[119] in one space and one time for any mass and coupling constant. The QED results agree with the Schwinger solution at infinite coupling. We will review the QCD[1+1] results below. Studies of QED in 3+1 dimensions are now underway.[120] Thus one can envision a nonperturbative

TABLE III

Table III. Comparison Between Time-Ordered and τ-Ordered Perturbation Theory

Equal t	Equal $\tau = t + z$
$k^o = \sqrt{\vec{k}^2 + m^2}$ (particle mass shell)	$k^- = \dfrac{k_\perp^2 + m^2}{k^+}$ (particle mass shell)
$\sum \vec{k}$ conserved	$\sum \vec{k}_\perp,\ k^+$ conserved
$\mathcal{M}_{ab} = V_{ab} + \sum_c V_{ac} \dfrac{1}{\sum_a k^o - \sum_c k^o + i\epsilon} V_{ac}$	$\mathcal{M}_{ab} = V_{ab} + \sum_c V_{ac} \dfrac{1}{\sum_a k^- - \sum_c k^- + i\epsilon} V_{cb}$
$n!$ time-ordered contributions	$k^+ > 0$ only
Fock states $\psi_n(\vec{k}_i)$	Fock states $\psi_n(\vec{k}_{\perp i}, x_i)$
$\sum_{i=1}^{n} \vec{k}_i = \vec{P} = 0$	$x = \dfrac{k^+}{P^+}\ ,\ \sum_{i=1}^{n} x_i = 1\ ,\ \sum_{i=1}^{n} \vec{k}_{\perp i} = 0$ $(0 < x_i < 1)$
$\mathcal{E} = P^o - \sum_{i=1}^{n} k_i^o$	$\mathcal{E} = P^+ \left(P^- - \sum_{i=1}^{n} k_i^-\right)$
$= M - \sum_{i=1}^{n} \sqrt{k_i^2 + m_i^2}$	$= M^2 - \sum_{i=1}^{n} \left(\dfrac{k_\perp^2 + m^2}{x}\right)_i$

method which in principle could allow a quantitative confrontation of QCD with the data even at low energies and momentum transfer.

The basic idea of DLCQ is as follows: QCD dynamics takes a rather simple form when quantized at equal light-cone "time" $\tau = t + z/c$. In light-cone gauge $A^+ = A^0 + A^z = 0$, the QCD light-cone Hamiltonian

$$H_{\mathrm{QCD}} = H_0 + gH_1 + g^2 H_2$$

contains the usual 3-point and 4-point interactions plus induced terms from instantaneous gluon exchange and instantaneous quark exchange diagrams. The perturbative vacuum is an eigenstate of H_{QCD} and serves as the lowest state in constructing a complete basis set of color singlet Fock states of H_0 in momentum space. Solving QCD is then equivalent to solving the eigenvalue problem:

$$H_{\mathrm{QCD}}|\Psi>= M^2|\Psi>$$

as a matrix equation on the free Fock basis. The set of eigenvalues $\{M^2\}$ represents the spectrum of the color-singlet states in QCD. The Fock projections of the eigenfunction corresponding to each hadron eigenvalue gives the quark and gluon Fock state wavefunctions $\psi_n(x_i, k_{\perp i}, \lambda_i)$ required to compute structure functions, distribution amplitudes, decay amplitudes, etc. For example, as shown by Drell and Yan,[10] the form-factor of a hadron can be computed at any momentum transfer Q from an overlap integral of the ψ_n summed over particle number n. The e^+e^- annihilation cross section into a given $J = 1$ hadronic channel can be computed directly from its $\psi_{q\bar{q}}$ Fock state wavefunction.

The light-cone momentum space Fock basis becomes discrete and amenable to computer representation if one chooses (anti-)periodic boundary conditions for the quark and gluon fields along the $z^- = z - ct$ and $z_\perp$ directions. In the case of renormalizable theories, a covariant ultraviolet cutoff Λ is introduced which limits the maximum invariant mass of the particles in any Fock state. One thus obtains a finite matrix representation of $H^{(\Lambda)}_{\mathrm{QCD}}$ which has a straightforward continuum limit. The entire analysis is frame independent, and fermions present no special difficulties.

Since H_{LC}, P^+, $\vec{P}_\perp$, and the conserved charges all commute, H_{LC} is block diagonal. By choosing periodic (or antiperiodic) boundary conditions for the basis states along the negative light-cone $\psi(z^- = +L) = \pm\psi(z^- = -L)$, the Fock basis becomes restricted to finite dimensional representations. The eigenvalue problem thus reduces to the diagonalization of a finite Hermitian matrix. To see this, note that periodicity in z^- requires $P^+ = \frac{2\pi}{L}K$, $k_i^+ = \frac{2\pi}{L}\, n_i$, $\sum_{i=1}^{n} n_i = K$. The dimension of the representation corresponds to the number of partitions of the integer K as a sum of positive integers n. For a finite resolution K, the wavefunction is sampled at the discrete points

$$x_i = \frac{k_i^+}{P^+} = \frac{n_i}{K} = \left\{ \frac{1}{K}, \quad \frac{2}{K}, \quad \ldots \frac{K-1}{K} \right\} \quad .$$

The continuum limit is clearly $K \to \infty$.

One can easily show that P^- scales as L. One thus defines $P^- \equiv \frac{L}{2\pi} H$. The eigenstates with $P^2 = M^2$ at fixed P^+ and $\vec{P}_\perp = 0$ thus satisfy $H_{LC} |\Psi\rangle = KH |\Psi\rangle = M^2 |\Psi\rangle$, independent of L (which corresponds to a Lorentz boost factor).

The basis of the DLCQ method is thus conceptually simple: one quantizes the independent fields at equal light-cone time τ and requires them to be periodic or antiperiodic in light-cone space with period $2L$. The commuting operators, the light-cone momentum $P^+ = \frac{2\pi}{L}K$ and the light cone energy $P^- = \frac{L}{2\pi}H$ are constructed explicitly in a Fock space representation and diagonalized simultaneously. The eigenvalues give the physical spectrum: the invariant mass squared $M^2 = P^\nu P_\nu$. The eigenfunctions give the wavefunctions at equal τ and allow one to compute the current matrix elements, structure functions, and distribution amplitudes required for physical processes. All of these quantities are manifestly independent of L, since $M^2 = P^+P^- = HK$. Lorentz-invariance is violated by periodicity, but re-established at the end of the calculation by going to the continuum limit: $L \to \infty, K \to \infty$ with P^+ finite. In the case of gauge theory, the use of the light-cone gauge $A^+ = 0$ eliminates negative metric states in both Abelian and non–Abelian theories.

Since continuum as well as single hadron color singlet hadronic wavefunctions are obtained by the diagonalization of H_{LC}, one can also calculate scattering amplitudes as well as decay rates from overlap matrix elements of the interaction Hamiltonian for the weak or electromagnetic interactions. An important point is that all higher Fock amplitudes including spectator gluons are kept in the light-cone quantization approach; such contributions cannot generally be neglected in decay amplitudes involving light quarks.

The simplest application of DLCQ to local gauge theory is QED in one-space and one-time dimensions. Since $A^+ = 0$ is a physical gauge there are no photon degrees of freedom. Explicit forms for the matrix representation of H_{QED} are given in Ref. 8.

The basic interactions which occur in H_{LC}(QCD) are illustrated in Fig. 53. Recently Hornbostel[119] has used DLCQ to obtain the complete color-singlet spectrum of QCD in one space and one time dimension for $N_C = 2, 3, 4$. The hadronic spectra are obtained as a function of quark mass and QCD coupling constant (see Fig. 55). Where they are available, the spectra agree with results obtained earlier;

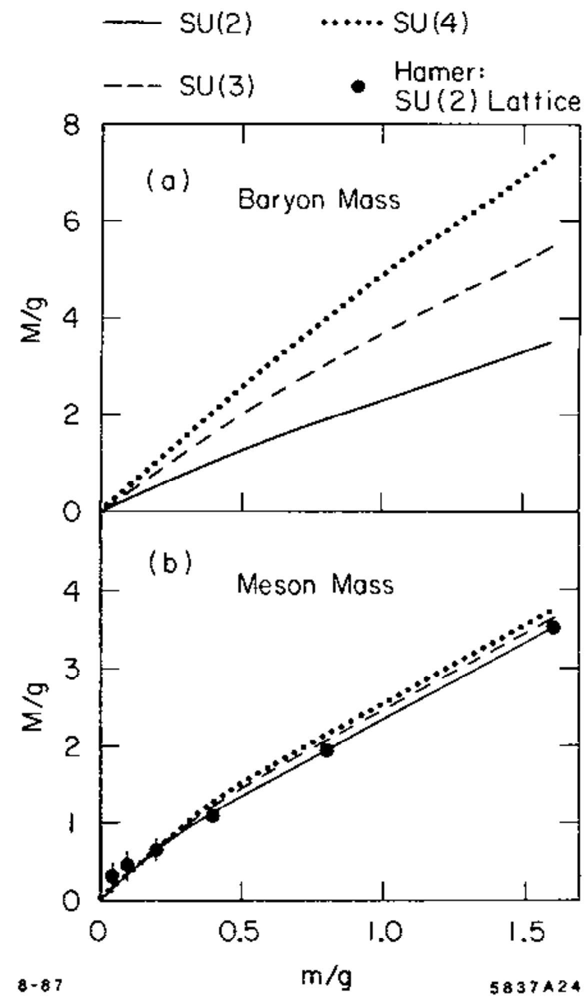

Figure 55. The baryon and meson spectrum in QCD [1+1] computed in DLCQ for $N_C = 2, 3, 4$ as a function of quark mass and coupling constant.[119]

in particular, the lowest meson mass in SU(2) agrees within errors with lattice Hamiltonian results.[121] The meson mass at $N_C = 4$ is close to the value obtained in the large N_C limit. The method also provides the first results for the baryon spectrum in a non-Abelian gauge theory. The lowest baryon mass is shown in

Fig. 55 as a function of coupling constant. The ratio of meson to baryon mass as a function of N_C also agrees at strong coupling with results obtained by Frishman and Sonnenschein.[122] Precise values for the mass eigenvalue can be obtained by extrapolation to large K since the functional dependence in $1/K$ is understood.

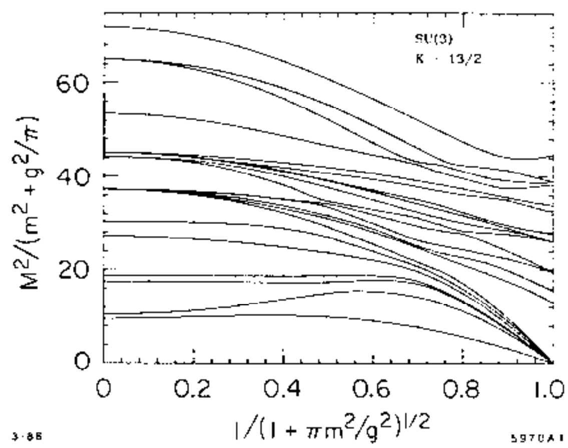

Figure 56. Representative baryon spectrum for QCD in one-space and one-time dimension.[119]

As emphasized above, when the light-cone Hamiltonian is diagonalized for a finite resolution K, one gets a complete set of eigenvalues corresponding to the total dimension of the Fock state basis. A representative example of the spectrum is shown in Fig. 56 for baryon states ($B = 1$) as a function of the dimensionless variable $\lambda = 1/(1 + \pi m^2/g^2)$. Antiperiodic boundary conditions are used. Note that spectrum automatically includes continuum states with $B = 1$.

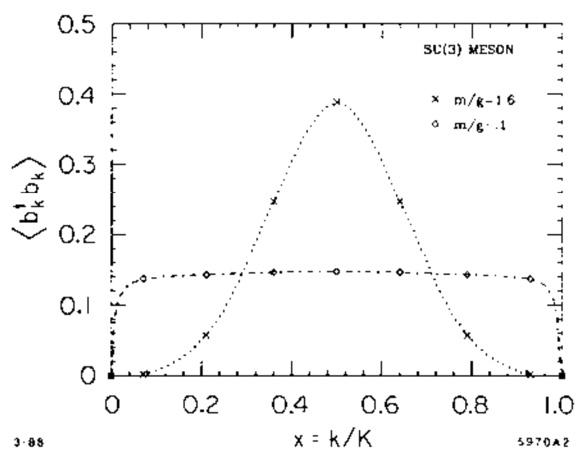

Figure 57. The meson quark momentum distribution in QCD[1+1] computed using DLCQ.[119]

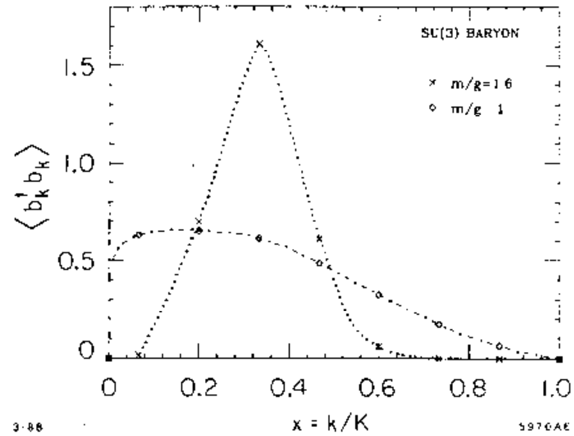

Figure 58. The baryon quark momentum distribution in QCD[1+1] computed using DLCQ.[119]

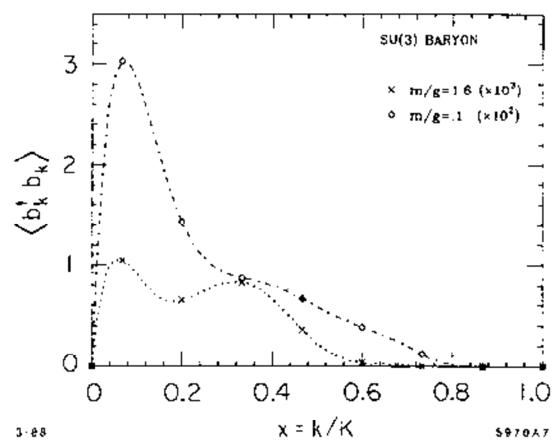

Figure 59. Contribution to the baryon quark momentum distribution from $qqq\overline{q}\overline{q}$ states for QCD[1+1].[119]

The structure functions for the lowest meson and baryon states in SU(3) at two different coupling strengths $m/g = 1.6$ and $m/g = 0.1$ are shown in Figs. 57 and 58. Higher Fock states have a very small probability; representative contributions to the baryon structure functions are shown in Figs. 59 and 60. For comparison, the valence wavefunction of a higher mass state which can be identified as a composite of meson pairs (analogous to a nucleus) is shown in Fig. 61. The interactions of the quarks in the pair state produce Fermi motion beyond $x = 0.5$. Although these results are for one time one space theory they do suggest that the sea quark distributions in physical hadrons may be highly structured.

In the case of gauge theory in 3+1 dimensions, one also takes the $k_\perp^i$ =

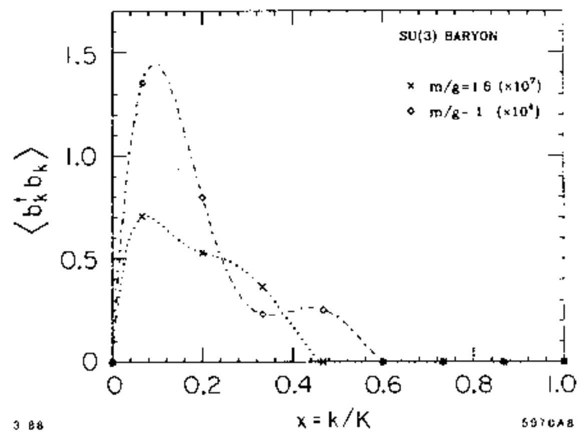

Figure 60. Contribution to the baryon quark momentum distribution from $qqq\overline{qqq}$ states for QCD[1+1].[119]

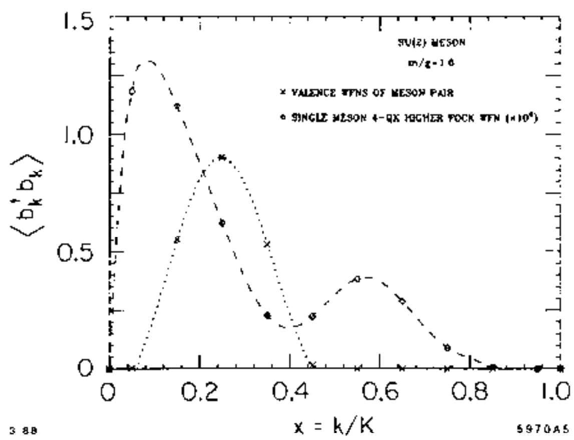

Figure 61. Comparison of the meson quark distributions in the $qq\overline{qq}$ Fock sate with that of a continuum meson pair state. The structure in the former may be due to the fact that these four-particle wavefunctions are orthogonal.[119]

$(2\pi/L_\perp)n^i_\perp$ as discrete variables on a finite cartesian basis. The theory is covariantly regulated if one restricts states by the condition

$$\sum_i \frac{k^2_{\perp i} + m^2_i}{x_i} \leq \Lambda^2 \quad ,$$

where Λ is the ultraviolet cutoff. In effect, states with total light-cone kinetic energy beyond Λ^2 are cut off. In a renormalizable theory physical quantities are independent of physics beyond the ultraviolet regulator; the only dependence on Λ appears in the coupling constant and mass parameters of the Hamiltonian.

consistent with the renormalization group.[123] The resolution parameters need to be taken sufficiently large such that the theory is controlled by the continuum regulator Λ, rather than the discrete scales of the momentum space basis.

There are a number of important advantages of the DLCQ method which have emerged from this study of two-dimensional field theories. They are as follows:

1. The Fock space is denumerable and finite in particle number for any fixed resolution K. In the case of gauge theory in 3+1 dimensions, one expects that photon or gluon quanta with zero four-momentum decouple from neutral or color-singlet bound states, and thus need not be included in the Fock basis.
2. Because one is using a discrete momentum space representation, rather than a space-time lattice, there are no special difficulties with fermions: *e.g.* no fermion doubling, fermion determinants, or necessity for a quenched approximation. Furthermore, the discretized theory has basically the same ultraviolet structure as the continuum theory. It should be emphasized that unlike lattice calculations, there is no constraint or relationship between the physical size of the bound state and the length scale L.
3. The DLCQ method has the remarkable feature of generating the complete spectrum of the theory; bound states and continuum states alike. These can be separated by tracing their minimum Fock state content down to small coupling constant since the continuum states have higher particle number content. In lattice gauge theory it appears intractable to obtain information on excited or scattering states or their correlations. The wavefunctions generated at equal light cone time have the immediate form required for relativistic scattering problems. In particular one can calculate the relativistic form factor from the matrix element of currents.
4. DLCQ is basically a relativistic many-body theory, including particle number creation and destruction, and is thus a basis for relativistic nuclear and atomic problems. In the nonrelativistic limit the theory is equivalent to the many-body Schrödinger theory.

Whether QCD can be solved using DLCQ — considering its large number of degrees of freedom is unclear. The studies for Abelian and non-Abelian gauge theory carried out so far in 1+1 dimensions give grounds for optimism.

ACKNOWLEDGEMENTS

We wish to thank the following: G. de Teramond, J. F. Gunion, J. R. Hiller, K. Hornbostel, C. R. Ji, A. H. Mueller, H. C. Pauli, D. E. Soper, A. Tang and S. F. Tuan.

REFERENCES

1. For general reviews of QCD see J. C. Collins and D. E. Soper, Ann. Rev. Nucl. Part. Sci., 37, 383 (1987); E. Reya, Phys. Rept. 69, 195 (1981); and A. H. Mueller, Lectures on Perturbative QCD given at the Theoretical Advanced Study Institute, New Haven, 1985.

2. General QCD analyses of exclusive processes are given in Ref. 4, S. J. Brodsky and G. P. Lepage, SLAC-PUB-2294, presented at the Workshop on Current Topics in High Energy Physics, Cal Tech (Feb. 1979), S. J. Brodsky, in the Proc. of the La Jolla Inst. Summer Workshop on QCD, La Jolla (1978), A. V. Efremov and A. V. Radyushkin, Phys. Lett. B94, 245 (1980), V. L. Chernyak, V. G. Serbo, and A. R. Zhitnitskii, Yad. Fiz. 31, 1069 (1980), S. J. Brodsky, Y. Frishman, G. P. Lepage, and C. Sachrajda, Phys. Lett. 91B, 239 (1980), and A. Duncan and A. H. Mueller, Phys. Rev. D21, 1636 (1980).

3. QCD predictions for the pion form factor at asymptotic Q^2 were first obtained by V. L. Chernyak, A. R. Zhitnitskii, and V. G. Serbo, JETP Lett. 26, 594 (1977), D. R. Jackson, Ph.D. Thesis, Cal Tech (1977), and G. Farrar and D. Jackson, Phys. Rev. Lett. 43, 246 (1979). See also A. M. Polyakov, Proc. of the Int. Symp. on Lepton and Photon Interactions at High Energies, Stanford (1975), and G. Parisi, Phys. Lett. 84B, 225 (1979). See also S. J. Brodsky and G. P. Lepage, in *High Energy Physics–1980*, proceedings of the XXth International Conference, Madison, Wisconsin, edited by L. Durand and L. G. Pondrom (AIP, New York, 1981); p. 568. A. V. Efremov and A. V. Radyushkin, Rev. Nuovo Cimento 3, 1 (1980); Phys. Lett. 94B, 245 (1980). V. L. Chernyak and A. R. Zhitnitsky, JETP Lett. 25, 11 (1977); G. Parisi, Phys. Lett. 43, 246 (1979); M. K. Chase, Nucl. Phys. B167, 125 (1980).

4. G. P. Lepage and S. J. Brodsky, Phys. Rev. D22, 2157 (1980); Phys. Lett. 87B, 359 (1979); Phys. Rev. Lett. 43, 545, 1625(E) (1979).

5. S. J. Brodsky and G. R. Farrar, Phys. Rev. Lett. 31, 1153 (1973), and Phys. Rev. D11, 1309 (1975); See also V. A. Matveev, R. M. Muradyan and A. V. Tavkheldize, Lett. Nuovo Cimento 7, 719 (1973).

6. S. J. Brodsky and G. P. Lepage, Phys. Rev. D24, 2848 (1981).

7. A. H. Mueller, Proc. XVII Recontre de Moriond (1982); S. J. Brodsky, Proc. XIII Int. Symp. on Multiparticle Dynamics, Volendam (1982). See also G. Bertsch, A. S. Goldhaber, and J. F. Gunion, Phys. Rev. Lett. 47, 297 (1981); G. R. Farrar, H. Liu, L. L. Frankfurt, M. J. Strikmann, Phys. Rev. Lett. 61, 686 (1988); A. H. Mueller, CU-TP-415, talk given at

the DPF meeting, Stoors, Conn (1988), and CU-TP-412 talk given at the Workshop on Nuclear and Particle Physics on the Light-Cone, Los Alamos, (1988).

8. T. Eller, H. C. Pauli and S. J. Brodsky, Phys. Rev. D35, 1493 (1987).
9. P. A. M. Dirac, Rev. Mod. Phys. 21, 392 (1949). Further references to light-cone quantization are given in Ref. 8.
10. S. D. Drell and T. M. Yan, Phys. Rev. Lett. 24, 181 (1970).
11. S. J. Brodsky, Y. Frishman, G. P. Lepage and C. Sachrajda, Phys. Lett. 91B, 239 (1980).
12. M. Peskin, Phys. Lett. 88B, 128 (1979); A. Duncan and A. H. Mueller. Phys. Lett. 90B, 159 (1980); Phys. Rev. D 21, 1636 (1980).
13. S. J. Brodsky, Y. Frishman, G. Peter Lepage Phys. Lett. 167B, 347, (1986); S. J. Brodsky, P. Damgaard, Y. Frishman, G. Peter Lepage Phys. Rev. D33, 1881, (1986).
14. S. Gottlieb and A. S. Kronfeld, Phys. Rev. D33, 227–233 (1986); CLNS-85/646, June 1985.
15. G. Martinelli and C. T. Sachrajda, Phys. Lett. 190B, 151, 196B, 184, (1987); Phys. Lett. B217, 319, (1989).
16. V. L. Chernyak and I. R. Zhitnitskii, Phys. Rept. 112, 1783 (1984). Xiao-Duang Xiang, Wang Xin-Nian and Huang Tao, BIHEP–TH–84, 23 and 29, 1984.
17. F. del Aguila and M. K. Chase, Nucl. Phys. B193, 517 (1982). E. Braaten, Phys. Rev. D28, 524 (1982). R. D. Field, R. Gupta, S. Ottos, and L. Chang, Nucl. Phys. B186, 429 (1981). F.-M. Dittes and A. V. Radyushkin, Sov. J. Phys. 34, 293 (1981), Phys. Lett. 134B, 359 (1984). M. H. Sarmadi, University of Pittsburgh Ph. D. thesis (1982), Phys. Lett. 143B, 471 (1984). G. R. Katz, Phys. Rev D31, 652 (1985).
18. E. Braaten and S.-M. Tse, Phys. Rev. D35, 2255 (1987).
19. A. Duncan and A. Mueller, Phys. Rev. D21, 636 (1980); Phys. Lett. 98B, 159 (1980); A. Mueller, Ref. 1.
20. P. V. Landshoff, Phys. Rev. D10, 1024 (1974). See also P. Cvitanovic, *ibid.* 10, 338 (1974); S. J. Brodsky and G. Farrar, *ibid.* 11, 1309 (1975).
21. A.H. Mueller, Phys. Rept. 73, 237 (1981). See also S. S. Kanwal, Phys. Lett. 294, 1984).
22. P. V. Landshoff and D. J. Pritchard, Z. Phys. C6, 9 (1980)
23. J. Botts and G. Sterman, Stony Brook preprint ITP-SB-89-7.

24. N. Isgur and C.H. Llewellyn Smith, Phys. Rev. Lett. 52, 1080 (1984). G. P. Korchemskii, A. V. Radyushkin, Sov. J. Nucl. Phys. 45, 910 (1987) and refs. therein.

25. C. Carlson and F. Gross, Phys. Rev. Lett. 53, 127 (1984); Phys. Rev. D36 2060 (1987).

26. O. C. Jacob and L. S. Kisslinger, Phys. Rev. Lett. 56, 225 (1986).

27. Z. Dziembowski and L. Mankiewicz, Phys. Rev. Lett. 58, 2175 (1987); Z. Dziembowski, Phys. Rev. D37, 768, 778, 2030 (1988)

28. J. Ashman *et al.*, Phys. Lett. 206B, 384 (1988).

29. See *e.g.* S. J. Brodsky, J. Ellis and M. Karliner, Phys. Lett. 206B, 309 (1988).

30. S. J. Brodsky, SLAC–PUB–4342 and in the *Proceedings of the VIIIth Nuclear and Particle Physics Summer School*, Launceston, Australia, 1987.

31. Arguments for the conservation of baryon chirality in large-momentum transfer processes have been given by B. L. Ioffe, Phys. Lett. 63B, 425 (1976). For some processes this rule leads to predictions which differ from the QCD results given here. The QCD helicity conservation rule also differs from the electroproduction helicity rules given in O. Nachtmann, Nucl. Phys. B115, 61 (1976).

32. D. Sivers, S. J. Brodsky, and R. Blankenbecler, Phys. Rep. 23C, 1, (1976).

33. G. C. Blazey *et al.*, Phys. Rev. Lett. 55, 1820 (1985); G. C. Blazey, Ph.D. Thesis, University of Minnesota (1987); B. R. Baller, Ph.D. Thesis, University of Minnesota (1987); D. S. Barton, *et al.*, J. de Phys. 46, C2, Supp. 2 (1985). For a review, see D. Sivers, Ref. 32.

34. V. D. Burkert, CEBAF-PR-87-006.

35. M. D. Mestayer, SLAC-Report 214 (1978) F. Martin, *et al.*, Phys. Rev. Lett. 38, 1320 (1977); W. P. Schultz, *et al.*, Phys. Rev. Lett. 38, 259 (1977); R. G. Arnold, *et al.*, Phys. Rev. Lett. 40, 1429 (1978); SLAC-PUB-2373 (1979); B. T. Chertok, Phys. Lett. 41, 1155 (1978); D. Day, *et al.*, Phys. Rev. Lett. 43, 1143 (1979). Summaries of the data for nucleon and nuclear form factors at large Q^2 are given in B. T. Chertok, in Progress in Particle and Nuclear Physics, Proceeding of the International School of Nuclear Physics, 5th Course, Erice (1978), and Proceedings of the XVI Rencontre de Moriond, Les Arcs, Savoie, France, 1981.

36. R. G. Arnold *et al.*, Phys. Rev. Lett. 57, 174 (1986).

37. R. L. Anderson *et al.*, Phys. Rev. Lett. 30, 627 (1973).

38. A. W. Hendry, Phys. Rev. D10, 2300 (1974).

39. G. R. Court *et al.*, UM–HE–86–03, April 1986, 14 pp.

40. S. J. Brodsky, C. E. Carlson and H. J. Lipkin, Phys. Rev. D20, 2278 (1979); G. R. Farrar, S. Gottlieb, D. Sivers and G. Thomas, Phys. Rev. D20, 202 (1979).

41. G. R. Farrar, RU–85–46, 1986.

42. S. J. Brodsky, C. E. Carlson and H. J. Lipkin, Ref. 40; H. J. Lipkin, (private communication).

43. J. P. Ralston and B. Pire, Phys. Rev. Lett. 57, 2330 (1986); Phys. Lett. 117B, 233 (1982).

44. S. Gupta, Phys. Rev. D24, 1169 (1981).

45. P. H. Damgaard, Nucl. Phys. B211, 435,(1983).

46. G. R. Farrar, G. Sterman, and H. Zhang, Rutgers Preprint 89-07 (1989).

47. S. J. Brodsky, G. P. Lepage, and S. A. A. Zaidi, Phys. Rev. D23, 1152 (1981).

48. A. Yokosawa, contributed to the 1980 International Symposium on High Energy Physics with Polarized Targets, Lausanne, Switzerland, 1980 (unpublished). For the review of the model calculations for the *pp* spin asymmetries, see S. J. Brodsky and G. P. Lepage in *High Energy Physics with Polarized Beams and Polarized Targets*; J. Szwed, Jagellonian University Report No. TPJU-13/80, 1980 (unpublished) and references therein. A review of the nucleon-nucleon scattering experiments is given by A. Yokosawa, Phys. Rep. 64, 47 (1980).

49. V. L. Chernyak, A. A. Ogloblin and I. R. Zhitnitsky, Novosibirsk preprints INP 87–135,136, and references therein. See also Xiao-Duang Xiang, Wang Xin-Nian, and Huang Tao, BIHEP-TH-84, 23 and 29, 1984, and M. J. Lavelle, ICTP-84-85-12; Nucl. Phys. B260, 323 (1985).

50. I. D. King and C. T. Sachrajda, Nucl. Phys. B279, 785 (1987).

51. G. P. Lepage, S. J. Brodsky, Tao Huang and P. B. Mackenzie, published in the *Proceedings of the Banff Summer Institute*, 1981.

52. S.J. Brodsky and B.T. Chertok, Phys. Rev. Lett. 37, 269 (1976); Phys. Rev. D114, 3003 (1976).

53. M. Gari and N. Stefanis, Phys. Lett. B175, 462 (1986), M. Gari and N. Stefanis, Phys. Lett. 187B, 401 (1987).

54. C-R Ji, A. F. Sill and R. M. Lombard-Nelsen, Phys. Rev. D36, 165 (1987).

55. See also G. R. Farrar, presented to the Workshop on Quantum Chromodynamics at Santa Barbara, 1988.

56. G. W. Atkinson, J. Sucher, and K. Tsokos, Phys. Lett. 137B, 407 (1984); G. R. Farrar, E. Maina, and F. Neri, Nucl. Phys. B259, 702 (1985) Err.-ibid. B263, 746 (1986).; E. Maina, Rutgers Ph.D. Thesis (1985); J. F. Gunion, D. Millers, and K. Sparks, Phys. Rev. D33, 689 (1986); P. H. Damgaard, Nucl. Phys. B211, 435 (1983); B. Nezic, Ph.D. Thesis, Cornell University (1985); D. Millers and J. F. Gunion, Phys. Rev. D34, 2657 (1986).

57. Z. Dziembowski, G. R. Farrar, H. Zhang, and L. Mankiewicz, contribution to the 12th Int. Conf. on Few Body Problems in Physics, Vancouver, 1989.

58. Z. Dziembowski and J. Franklin contribution to the 12th Int. Conf. on Few Body Problems in Physics, Vancouver, 1989.

59. J. D. Bjorken and M. C. Chen Phys. Rev. 154, 1335 (1966).

60. G. R. Farrar RU-88-47, Invited talk given at Workshop on Particle and Nuclear Physics on the Light Cone, Los Alamos, New Mexico, 1988; G. R. Farrar, H. Zhang, A. A. Globlin and I. R. Zhitnitsky, Nucl. Phys. B311, 585 (1989); G. R. Farrar, E. Maina, and F. Neri, Phys. Rev. Lett. 53, 28 and, 742 (1984).

61. J. F. Gunion, D. Millers, and K. Sparks, Phys. Rev. D33, 689 (1986); D. Millers and J. F. Gunion, Phys. Rev. D34, 2657 (1986).

62. B. Nizic Phys. Rev. D35, 80 (1987)

63. S. J. Brodsky, G. P. Lepage, P. B. Mackenzie, Phys. Rev. D28, 228 (1983.)

64. The connection of the parton model to QCD is discussed in G. Altarelli, Phys. Rep. 81, No. 1, 1982.

65. V. N. Gribov and L. V. Lipatov, Sov. Jour. Nucl Phys. 15, 438, 675 (1972).

66. R. P. Feynman, Photon-Hadron Interactions, (W. A. Benjamin, Reading, Mass. 1972).

67. J. F. Gunion, S. J. Brodsky and R. Blankenbecler, Phys. Rev. D8, 287 (1973); Phys. Lett. 39B, 649 (1972); see also Ref. 32. References to fixed angle scattering are given in this review.

68. P. V. Landshoff, J. C. Polkinghorne Phys. Rev. D10, 891 (1974).

69. B. R. Baller, et al., Phys. Rev. Lett. 60, 1118 (1988).

70. See also A. I. Vainshtein and V. I. Zakharov, Phys. Lett. 72B, 368 (1978); G. R. Farrar and D. R. Jackson, Phys. Rev. Lett. 35, 1416 (1975); B. Ioffe, Ref. 31).

71. For other applications, see A. Duncan and A. H. Mueller, Phys. Lett. 93B, 119 (1980); see also S. Gupta, Ref. 44.

72. Unless otherwise noted, the data used here is from the compilation of the Particle Data Group, Rev. Mod. Phys. 52, S1 (1980).

73. I. Peruzzi *et al.*, Phys. Rev. D17, 2901 (1978).

74. M. E. B. Franklin, Ph.D Thesis (1982), SLAC–254, UC–34d; M. E. B. Franklin *et al.*, Phys. Rev. Lett. 51, 963 (1983); G. Trilling, in *Proceedings of the Twenty-First International Conference on High Energy Physics*, Paris, July 26–31, 1982; E. Bloom, ibid.

75. S. J. Brodsky, G. P. Lepage and San Fu Tuan, Phys. Rev. Lett. 59, 621 (1987).

76. M. Chaichian, N. A. Tornqvist HU-TFT-88-11 (1988).

77. Wei-Shou Hou and A. Soni, Phys. Rev. Lett. 50, 569 (1983).

78. P. G. O. Freund and Y. Nambu, Phys. Rev. Lett. 34, 1645 (1975).

79. S. J. Brodsky and C. R. Ji, Phys. Rev. Lett. 55, 2257 (1985).

80. For general discussions of $\gamma\gamma$ annihilation in $e^+e^- \rightarrow e^+e^-X$ reactions, see S. J. Brodsky, T. Kinoshita, and H. Terazawa, Phys. Rev. Lett. 25, 972 (1970), Phys. Rev. D4, 1532 (1971), V. E. Balakin, V. M. Budnev, and I. F. Ginzburg, JETP Lett. 11, 388 (1970), N. Arteaga-Romero, A. Jaccarini, and P. Kessler, Phys. Rev. D3, 1569 (1971), R. W. Brown and I. J. Muzinich, Phys. Rev. D4, 1496 (1971), and C. E. Carlson and W.-K. Tung, Phys. Rev. D4, 2873 (1971). Reviews and further references are given in H. Kolanoski and P. M. Zerwas, DESY 87-175 (1987), H. Kolanoski, *Two-Photon Physics in e^+e^- Storage Rings,* Springer–Verlag (1984), and Ch. Berger and W. Wagner, Phys. Rep. 136 (1987); J. H. Field, University of Paris Preprint LPNHE 84-04 (1984).

81. G. Köpp, T. F. Walsh, and P. Zerwas, Nucl. Phys. B70, 461 (1974). F. M. Renard, Proc. of the Vth International Workshop on $\gamma\gamma$ Interactions, and Nuovo Cim. 80, 1 (1984). Backgrounds to the $C = +$, $J = 1$ signal can occur from tagged $e^+e^- \rightarrow e^+e^-X$ events which produce $C = -$ resonances.

82. S. J. Brodsky and G. P. Lepage, Phys. Rev. D24, 1808 (1981).

83. H. Aihara *et al.*, Phys. Rev. Lett. 57, 51, 404 (1986). Mark II data for combined charged meson pair production are also in good agreement with the PQCD predictions. See J. Boyer *et al.*, Phys. Rev. Lett. 56, 207 (1986).

84. H. Suura, T. F. Walsh, and B. L. Young, Lett. Nuovo Cimento 4, 505 (1972). See also M. K. Chase, Nucl. Phys. B167, 125 (1980).

85. J. Boyer *et al.*, Ref. 83; TPC/Two Gamma Collaboration (H. Aihara *et al.*), Phys. Rev. Lett. 57, 404 (1986).

86. M. Benyayoun and V. L. Chernyak, College de France preprint LPC 89 10 (1989).

87. M. A. Shupe, et al., Phys. Rev. D19, 1921 (1979).

88. A simple method for estimating hadron pair production cross sections near threshold in $\gamma\gamma$ collisions is given in S. J. Brodsky, G. Köpp, and P. M. Zerwas, Phys. Rev. Lett. 58, 443 (1987).

89. See Ref. 82. The next-to-leading order evaluation of T_H for these processes is given by B. Nezic, Ph.D. Thesis, Cornell University (1985).

90. S. J. Brodsky, J. F. Gunion and D. E. Soper, Phys. Rev. D36, 2710 (1987).

91. S.J. Brodsky and A. H. Mueller

92. See Ref. 52 and S. J. Brodsky and J. R. Hiller, Phys. Rev. C28, 475 (1983).

93. C. R. Ji and S. J. Brodsky, Phys. Rev. D34, 1460 (1986); D33, 1951, 1406, 2653, (1986). For a review of multi-quark evolution, see S. J. Brodsky, C.-R. Ji, SLAC-PUB-3747, (1985).

94. The data are compiled in Brodsky and Hiller, Ref. 92.

95. J. Napolitano *et al.*, ANL preprint PHY-5265-ME-88 (1988).

96. T. S.-H. Lee, ANL preprint (1988).

97. H. Myers *et al.*, Phys. Rev. 121, 630 (1961); R. Ching and C. Schaerf. Phys. Rev. 141, 1320 (1966); P. Dougan *et al.*, Z. Phys. A 276, 55 (1976).

98. T. Fujita, MPI-Heidelberg preprint, 1989.

99. S. J. Brodsky, C.-R. Ji, G. P. Lepage, Phys. Rev. Lett. 51, 83 (1983).

100. L.A. Kondratyuk and M. G. Sapozhnikov, Dubna preprint E4-88-808.

101. A. S. Carroll, *et al.*, Phys. Rev. Lett. 61, 1698 (1988).

102. G. R. Court *et al.*, Phys. Rev. Lett. 57, 507 (1986).

103. S. J. Brodsky and G. de Teramond, Phys. Rev. Lett. 60, 1924 (1988).

104. R. Blankenbecler and S. J. Brodsky, Phys. Rev. D10, 2973 (1974).

105. I. A. Schmidt and R. Blankenbecler, Phys. Rev. D15, 3321 (1977).

106. See Ref. 102; T. S. Bhatia *et al.*, Phys. Rev. Lett. 49, 1135 (1982); E. A. Crosbie *et al.*, Phys. Rev. D23, 600 (1981); A. Lin *et al.*, Phys. Lett. 74B, 273 (1978); D. G. Crabb *et al.*, Phys. Rev. Lett. 41, 1257 (1978); J. R. O'Fallon *et al.*, Phys. Rev. Lett. 39, 733 (1977); For a review, see A. D. Krisch, UM-HE-86-39 (1987).

107. For other attempts to explain the spin correlation data, see C. Avilez. G. Cocho and M. Moreno, Phys. Rev. D24, 634 (1981); G. R. Farrar, Phys. Rev. Lett. 56, 1643 (1986), Err-ibid. 56, 2771 (1986); H. J. Lipkin, Nature 324, 14 (1986); S. M. Troshin and N. E. Tyurin, JETP Lett. 44, 149 (1986) [Pisma Zh. Eksp. Teor. Fiz. 44, 117 (1986)]; G. Preparata and J. Soffer, Phys. Lett. 180B, 281 (1986); S. V. Goloskokov, S. P. Kuleshov

and O. V. Seljugin, *Proceedings of the VII International Symposium on High Energy Spin Physics*, Protvino (1986); C. Bourrely and J. Soffer, Phys. Rev. D35, 145 (1987).

108. There are five different combinations of six quarks which yield a color singlet B=2 state. It is expected that these QCD degrees of freedom should be expressed as B=2 resonances. See, *e.g.* S. J. Brodsky and C. R. Ji, Ref. 93.

109. For other examples of threshold enhancements in QCD, see S. J. Brodsky, J. F. Gunion and D. E. Soper, Ref. 90 and also Ref. 88. Resonances are often associated with the onset of a new threshold. For a discussion, see D. Bugg, Presented at the IV LEAR Workshop, Villars-Sur-Ollon, Switzerland, September 6–13, 1987.

110. J. F. Gunion, R. Blankenbecler and S. J. Brodsky, Phys. Rev. D6, 2652 (1972).

111. With the above normalization, the unpolarized pp elastic cross section is $d\sigma/dt = \Sigma_{i=1,2,...5} \mid \phi_i^2 \mid /(128\pi s p_{\rm cm}^2)$.

112. At low momentum transfers one expects the presence of both helicity-conserving and helicity nonconserving pomeron amplitudes. It is possible that the data for A_N at $p_{lab} = 11.75$ GeV/c can be understood over the full angular range in these terms. The large value of $A_N = 24 \pm 8\%$ at $p_{lab} = 28$ GeV/c and $p_T^2 = 6.5$ GeV^2 remains an open problem. See P. R. Cameron *et al.*, Phys. Rev. D32, 3070 (1985).

113. K. Abe *et al.*, Phys. Rev. D12, 1 (1975), and references therein. The high energy data for $d\sigma/dt$ at $\theta_{\rm cm} = \pi/2$ are from C. W. Akerlof *et al.*, Phys. Rev. 159, 1138 (1967); G. Cocconi *et al.*, Phys. Rev. Lett. 11, 499 (1963); J. V. Allaby *et al.*, Phys. Lett. 23, 389 (1966).

114. I. P. Auer *et al.*, Phys. Rev. Lett. 52, 808 (1984). Comparison with the low energy data for A_{LL} at $\theta_{\rm cm} = \pi/2$ suggests that the resonant amplitude below $p_{lab} = 5.5$ GeV/c has more structure than the single resonance form adopted here. See I. P. Auer *et al.*, Phys. Rev. Lett. 48, 1150 (1982).

115. See Ref. 38 and N. Jahren and J. Hiller, University of Minnesota preprint, 1987.

116. The neutral strange inclusive pp cross section measured at $p_{lab} = 5.5$ GeV/c is 0.45 ± 0.04 mb; see G. Alexander *et al.*, Phys. Rev. 154, 1284 (1967).

117. Phys. Rev. D33, 1951 (1986).

118. H. C. Pauli and S. J. Brodsky, Phys. Rev. D32, 1993, 2001 (1985) and Ref. 8.

119. K. Hornbostel, SLAC-0333, Dec 1988; K. Hornbostel, S. J. Brodsky, and H. C. Pauli, SLAC-PUB-4678, Talk presented to Workshop on Relativistic Many Body Physics, Columbus, Ohio, June, 1988.

120. S. J. Brodsky, H. C. Pauli, and A. Tang, in preparation.

121. C. J. Burden and C. J. Hamer, Phys. Rev. D37, 479 (1988), and references therein.

122. Y. Frishman and J. Sonnenschein, Nucl. Phys. B294, 801 (1987), and Nucl. Phys. B301, 346 (1988).

123. For a discussion of renormalization in light-cone perturbation theory, see S. J. Brodsky, R. Roskies and R. Suaya, Phys. Rev. D8, 4574 (1974), and also Ref. 4.